Experimental data-driven design of sustainable bulk moulding compounds

Aditya Babu

Experimental Data Driven Design of Sustainable Bulk Moulding Compounds

by

Aditya Babu

to obtain the degree of Master of Science
at the Delft University of Technology,
to be defended publicly on Wednesday May 25, 2022 at 3:00 PM.

Student number:	5002303	
Project duration:	February, 2021 – May, 2022	
Thesis Supervisors:	Prof.dr. S. J. Picken,	TU Delft, AS faculty
	Dr. ir. M.A. Bessa,	TU Delft, 3ME faculty
	Dr. ir. Z. Zarafshani,	NPSP B.V.
PhD mentor:	Ir. M.P. van der Schelling,	TU Delft, 3ME faculty
Thesis Committee:	Dr.ir. O.K. Bergsma	TU Delft, AE faculty

Cover: Natural Materials & Biocomposites Research Group "Flax Linen fabric macro image."
Retrieved from: https://www.canterbury.ac.nz/engineering/schools/mechanical/research/naturalfibres/

An electronic version of this thesis is available at https://repository.tudelft.nl/.

Summary

Bio-based composites have been a viable material choice in aerospace, automobile and construction industries over the past few decades. From day-to-day products like spoons and chairs to the construction of rocket parts, bio-based composites find their applications due to their mechanically enhanced, cost-effective and lightweight structures, with a reduced carbon footprint. This study collaborates with NPSP, one of the companies leading the way towards a circular economy.

However, the manufacturing and testing of bio-based composites is time and resource expensive. Moreover, exploring all natural fillers and fibres ratios is not feasible experimentally. Optimization and analytical models are two potential approaches that accelerate the search towards an optimal bio-based composite recipe when combined with bio-based materials research. A data-scarce Bayesian optimization model was already developed to research the composition of bio-based composites. The proof-of-concept program adjusts the natural materials' weight ratios to optimize toward user-defined mechanical properties. The objective of this study is to experimentally investigate if the Bayesian Optimization model works by varying the objective functions and adapting the model according to the clients' needs. By exploiting the machine learning model at an initial stage, the purpose is to test how the model reacts to different objective functions defined at high weight values and observe if the model can generate optimized recipes with better mechanical properties than the defined training set. For this study, four different fillers (calcite, lignocellulosic filler 1, lignocellulosic filler 2, waste based filler) and two different fibres (flax, bamboo) are used, with calcite as the reference filler. A primary goal to be achieved by NPSP is to reduce or eliminate calcite as the primary filler due to its high density and brittle nature. Promising results have been obtained within two iterations of using the model for the different filler/fibre systems used.

Additionally, the thesis also investigates the rules of mixing for multi-component systems to develop analytical models that predict the mechanical properties of the composite. The Lewis-Nielsen model and the Cox -Krenchel theory have been used to compare theoretical values with experimental data points. The initial binary phase curve fitting followed by applying cascading to obtain ternary and quaternary phase mechanical properties provides approximate results for most recipes made. Finally, recommendations to improve both models have been covered, and a potential to combine both approaches has been shown.

Contents

List of Figures

List of Tables

Chapter 1

Introduction

With an increase in sustainable and bio-based composites in almost every major industry like automotive, aerospace, biomedical and electronics, the building and construction industry has also seen a rise in bio-composites research and development, providing mechanically enhanced, cost-effective, and lightweight structures with the reduced carbon footprint.

The building and construction industry has seen a tremendous increase in the application of thermoset composites owing to their superior flexural modulus and strength compared to thermoplastics, making them appropriate to be used in large and integral structures. Polymer composites (thermoset composites in particular) are gaining attention as they contribute to the high specific modulus and strength. A highly cross-linked polymer structure increases rigidity, adhesion, heat and fire resistance [1]. They also offer cost-effective solutions and low-density structures compared to thermoplastics. Out of the current types of thermoset composites, Bulk Moulding Compounds (BMC) and Sheet Moulding Compounds (SMC) are becoming increasingly popular due to their reduced density and improved mechanical properties. Both BMC and SMC produce a polymeric composite material consisting primarily of a thermosetting resin, mineral/bio fillers, and fibre reinforcement.

Bulk Moulding Compounds can mould into a complex geometry due to less fibre content and short fibres but compromise a bit on their flexural properties, hence being used for non-critical structures. On the other hand, Sheet Moulding Compounds have higher flexural properties due to long continuous fibres and are better for high-end critical parts with structural requirements. For several years now, the attempt to replace synthetic fillers with natural fillers has become increasingly popular in composites. With promising and constantly improving results in economic and environmental factors and mechanical properties and density, these lignocellulosic fillers are gaining quite a lot of attention from the scientific community as a potential circular economy approach. Although it comes with its own set of challenges like moisture retention, UV sensitivity, and high deviation in properties, these challenges need to be analysed and solved to develop bio-based composites with improved and stable mechanical properties. NPSP B.V, a research-based company in Amsterdam, has been actively involved in researching and developing bio-composites involving natural fillers and fibres. The fillers and fibres are products/ by-products of biomass, agriculture and waste-water streams. The products produced are currently being used in various industries, including automotive and transportation, construction, and food and beverage to basic household applications. Some of the products are shown in Figure 1.1.

Figure 1.1 (a) shows a park bench made of NABASCO 8010 made out of reed fibres, which is the

(a) Park bench

(b) Bike bridge

(c) Van Eko scooter body

(d) NS train nose

Figure 1.1: A wide variety of biobased composite products by NPSP B.V [2]

patented NPSP product. Figure 1.1 (b) shows the first ever biocomposite based bicycle bridge made of flax and hemp fibres constructed on TU Eindhoven campus by NPSP, TU Delft and TU Eindhoven. Figure 1.1 (c) shows a single part biocomposite body of a Van Eko scooter which also uses biomass as for power in batteries. Figure 1.1 (d) shows the nose of the newer intercity NS trains which is made up of biocomposite materials. Products shown above are Bulk Moulding (BMC) and Sheet Moulding Compounds (SMC), which are a major part of research and development conducted at NPSP.

Bulk Moulding Compound (BMC): Bulk Moulding Compound is a class of composites that incorporate shorter chopped fibres (usually up to 6-12 mm) [3]. However, the impact strength of BMCs remains constant on increasing the fibre length above 12.7mm, with an ideal length of about 6mm. BMCs have shorter fibres, which are randomly oriented, unlike SMCs, which have long continuous fibres with a well-defined orientation. The continuous fibres and the high fibre content provide SMCs with more strength compared to BMCs [4]. BMCs usually have a higher filler weight percentage than SMCs (higher fibre weight percentage). They typically consist of resin, fillers, fibres and additional additives. After mixing all the ingredients uniformly, the dough is heated as part of the final step by compression moulding, injection moulding, or transfer moulding. Transfer moulding involves placing the dough in a heating chamber next to the pre-heated closed mould. The dough is first heated to decrease its viscosity and then pushed by a plunger into the closed mould where curing takes place [5].

Injection Moulding involves the dough being manually pushed into the machine's feed. The plasticating screw/ 3 zones screw (Feed zone, Transition zone and Metering zone) of the injection moulding facility rotates about its axis. It moves inside the pre-heated barrel simultaneously and, in doing so, pulls the dough into the barrel. Heating elements around the barrel and the shear heating due to mixing and plastication reduce the dough's viscosity as it moves into the closed pre-heated cavity. The uniformly mixed BMC dough is injected into a closed mould cavity that is preheated to the curing temperature by the plasticating screw. The important thing to be noted is that the dough should not gel before reaching the mould. This can lead to solidified regions that must be removed from the barrel or the sprue. Thus, an optimized temperature has to be applied [5].

The compression moulding technique involves the dough being placed in the lower fixed mould of the machine. This mould is preheated to an optimum temperature at which the dough cures. The upper movable mould then compresses the dough under high pressure and temperature as a function of time till the BMC dough is cured.

Sheet Moulding Compound (SMC): Sheet Moulding Compound is another type of thermoset composite that can be used for structural applications requiring high stiffness and strength. They have long, continuous fibres that can be stacked together in parallel directions to form a single sheet layer or lamina. Multiple layers can be stacked together depending on the required density and thickness to form a laminate. The SMC, like BMC, consists of a thermosetting resin, additives, fillers and fibres. Except for the fibre laminas, the other ingredients can be mixed (which forms the wet mixture in this case), applied to the lamina and passed through a series of calendering rollers, making it stiffer. A plastic film is used to separate the layers to allow coiling and prevent external contamination, interlayer stacking and monomer evaporation [6]. This can then be compression moulded into the desired shape. Unlike BMC, the filler weight percentage is less than that in BMCs. Also, the complexity of the SMC plate geometry reduces with increasing reinforcements which is not the case in BMCs [7]. Dominick et al. also state the necessity of a maturation period before the SMC is moulded. This is needed to increase the viscosity of the wet mixture applied to the fibre layers and thicken it to improve the adhesion between the wet mix and the fibre layer. The ideal maturation time is expected to be approximately 3-5 days. The use of different additives is to improve the flow behaviour of the resin in the fibre layers, the curing behaviour, viscosity etc. depending on the requirements.

The scope of this thesis is defined as working with natural fibre, and filler reinforced Bulk Moulding Compounds. However, higher deviations/noise in the results of the mechanical tests is expected in the case of composites with natural fibres/fillers. This can pose a serious challenge in applying bio-composites for structural purposes. In addition, repeated manufacturing of composites by trial and error to test the best BMC/SMC recipe for its mechanical properties consumes unnecessary time and resources. Thus, to speed up obtaining an optimal bio-composite recipe, two of the solutions are to apply an analytical and data-driven approach to determine the best BMC ratio. The BMC Optimizer is a data-scarce Bayesian optimization model developed by Martin Van der Schelling at NPSP and TU Delft. Bayesian optimization is an important strategy for global optimization of black-box functions [8]. The model does not assume any functional forms and is an important tool for optimising expensive-to-evaluate functions. The BMC optimization model initially cannot predict an accurate BMC recipe for the desired properties due to insufficient data inputs. These data inputs or parameters are a complete set of information about the BMC (fibre and filler weight fraction, flexural modulus and strength, impact modulus and strength) produced, which are then stored in a database. Sufficient data inputs in the database aid in better predictions of the desired output. Updating the database with the newer outputs stored as inputs further improves the accuracy of the next prediction.

On the other hand, theoretical models are based on micromechanics and the general rule of mixtures. Unlike data-driven models, theoretical models provide prediction trend lines of mechanical properties like modulus, strength, thermal conductivity and electrical conductivity, based on material properties like fibre/matrix modulus, fibre length and orientation, packing fraction etc. Multiple models such as Halpin Tsai, Hashin Shtrikman, Mori-Tanaka and Einstein's rule of mixtures have been tested on polymer composites which have provided more than approximate predictions of Young's modulus, strength and conductivity. Although such models have not been used or studied extensively in bio-based composites, they can be considered a potential method for predicting mechanical properties with much less utilization of time and resources than quasi-random or data-driven methods.

Chapter 2

Literature Review

This thesis has two main objectives. The first one is to experimentally validate the BMC optimizer model created by Martin Van Der Schelling [9]. The design of experiments will be carried out using different ratios of 2-3 other natural fillers and fibres. Experimentally confirming this model will ultimately provide an optimized composite with the desired stiffness, strength and density. The second objective is to provide an analytical model in parallel by dwelling on the rules of mixtures that provide approximately accurate predictions of the mechanical properties of the desired composite. Combining the analytical and the BMC Optimization model can aid predict an optimized recipe followed by the mechanical properties provided by that recipe.

2.1 Bio Based Composites

Natural fibre composites have caught the attention of many researchers and industries in the past decades due to their higher specific mechanical properties and environmental impact than synthetic fibres. These fibres derived from plants such as hemp, flax, bamboo etc., have a high cellulose content which gives them good mechanical properties and, when reinforced with thermoset or thermoplastic polymers, improves the mechanical properties of the polymers [10]. Filler reinforcements reduce the cost of the composites, improve the overall stiffness to a certain extent and provide a higher packing fraction by utilizing the voids between the polymer and the fibres. As a result, fillers, in comparison to fibres, are less expensive. Furthermore, if the ratio of filler to fibre in the polymer is optimized such that the mechanical properties are comparable, then the cost and environmental impact can be brought down, further improving the Life Cycle Assessment factor (LCA).

2.1.1 Natural Fillers

For several years now, the attempt to replace synthetic fillers with natural and waste stream derived fillers has become increasingly popular in the field of composites. With promising and constantly improving results not only in economic and environmental factors but also in mechanical properties and density, natural fillers are gaining quite a lot of attention from the scientific community.

Calcite
The application of wastewater streams materials as fillers in composites is becoming increasingly popular due to its recyclability and cost-efficiency. Inorganic wastes from these waste streams and the PP matrix have shown improved mechanical properties compared to the pure matrix. In addition,

cost analysis of the chemical constituents shows that the wastewater filler reinforced PP composites significantly reduce the impact on climate than pure PP[11]. Calcium carbonate (calcite) is found to be a potential bio-filler when incorporated with epoxy resin, improves its flexural properties as well contributes to the circular economy [12]. Unsaturated polyester resin, when incorporated with calcium carbonate, found an increase in the flexural properties [13]. The calcite filler used in NPSP composites is mainly gained from wastewater treatment. However, a significant disadvantage of calcite is its high density and brittle nature. These are the primary reasons why NPSP seeks to replace it and look for alternative natural solutions like lignocellulosic materials, biocarbon, etc., that are lightweight, sustainable and offer better specific properties than calcite. One of the major challenges while replacing calcite is the increase in viscosity of the composite dough. Lower viscosity helps flow the composite dough into more uniform and complex shapes. Further research and studies are being conducted on plasticizers and additives to improve the viscosity of the dough [14].

Natural fillers added to polymer composites improve sustainability and reduce the carbon footprint. An optimal percentage of fillers relative to total dough ingredients has to be determined for different lignocellulosic fillers, as an increase in filler content above a certain threshold can lead to a decrease in mechanical properties [15].

The challenges that arise when replacing calcite with lignocellulosic and other organic fillers like an grinded fuit pits and shells, are a decrease in absolute stiffness, increased viscosity and decreasing flow behaviour of the dough. The lower viscosity of calcite based composite doughs provides a better dough flow when cured by compression moulding. The internal porosity of lignocellulosic fillers allows them to absorb more resin, which is the main reason why the dough dries up at lower concentrations of the lignocellulosic filler compared to that of the calcite filler.

Lignocellulosic Fillers

Lignocellulosic fillers comprise three main components:

1) Lignin: Lignin is the second most abundant organic polymer. It plays a crucial role in rigidity and the hydrophobic nature of secondary plant cells. They comprise phenylpropane units linked by ether bonds [16]. An important function of lignin is being a UV absorber and a flame retardant. Hence, lignin-based fillers in composites have potential applications in the aerospace, automotive, and building industry [17].

2) Cellulose: Cellulose is the most abundant organic polymer and one of the most abundant biomaterials present. They comprise glucose units linked by -(1–4)-glycosidic bonds [18]. The periodic arrangement of hydroxyl groups along cellulose chains forms H- bridges and provides an overall crystalline fibrillar structure. Its tough and fibrous structure plays a crucial role to keep plant cell walls stable [19].

3) Hemicellulose: Hemicellulose is considered the second most abundant biopolymer of lignocellulosic biomass present after cellulose. They comprise multiple different monosaccharide units, namely different pentose and hexose monosaccharides. They are considered to be polysaccharides but not classified under cellulose or pectin. The monosaccharides present are glucose, xylose, mannose, arabinose etc., in varying compositions. Along with lignin, hemicellulose acts as a solidified base for cellulose in the plant cell wall [20].
Figure 2.1 shows the lignin, cellulose and hemicellulose content of different types of filler.
The chemical composition and structure of a plant cell wall composed of these three components are shown in Figure 2.1.

Filler	Lignocellulose type	Content Range (%)	References
Olive Stone	Lignin Cellulose Hemicellulose	20-30 30-40 20-30	[21, 22]
Almond Shell	Lignin Cellulose Hemicellulose	20-30 30-40 20-30	[23, 24]
Pistachio Shell	Lignin Cellulose Hemicellulose	12-38 30-55 20-32	[23, 25]
Rice Husk	Lignin Cellulose Hemicellulose	20-25 35-40 15-20	[26, 27]
Chestnut Shell	Lignin Cellulose Hemicellulose	35-40 20-25 15-20	[23, 28]
Coconut Shell	Lignin Cellulose Hemicellulose	28-46 21-34 17-22	[23, 29]
Cocoa Husk	Lignin Cellulose Hemicellulose	14-28 20-26 9-13	[30]
Poplar	Lignin Cellulose Hemicellulose	21-29 42-49 16-23	[23, 31]
Walnut Shell	Lignin Cellulose Hemicellulose	> 48 23-25 20-23	[23, 32, 33]

Table 2.1: Lignin, Cellulose and Hemicellulose content in Lignocellulosic Fillers

The past decade has seen an increase in bio-fillers as reinforcements for the reasons stated earlier. Almond shell, olive stone, coconut choir, cocoa powder, wood ash etc., are among the few examples of natural fillers. The incorporation of fillers helps in improving the cost aspect of the FRPs. The task is to optimize the ratio of fillers to fibres such that the mechanical properties are comparable and density and cost are reduced. Dhawan et al., tested the influence of bio-fillers like coconut coir and rice husk in FRPs and concluded that the mechanical properties of glass fibre reinforced thermoset composites are comparable to those with coconut or rice husk fillers incorporated thermoset composites [35]. Similarly, in other studies, the use of apricot, almond, coir, and argan shells in thermoplastic composites has increased tensile modulus and strength. These studies have also suggested an optimal use of different compatibilizers, additives, dispersing agents etc., to improve the flow of props in the resin [36].

A study also revealed the potential of using bio-based polyesters in fibre and filler reinforced composites. The results obtained are positive in mechanical properties, increasing the value-added potential of agricultural and forest wastes and contributing to the circular economy. The challenges faced are interfacial adhesion between the matrix and filler and the fragmentation of composites (increased

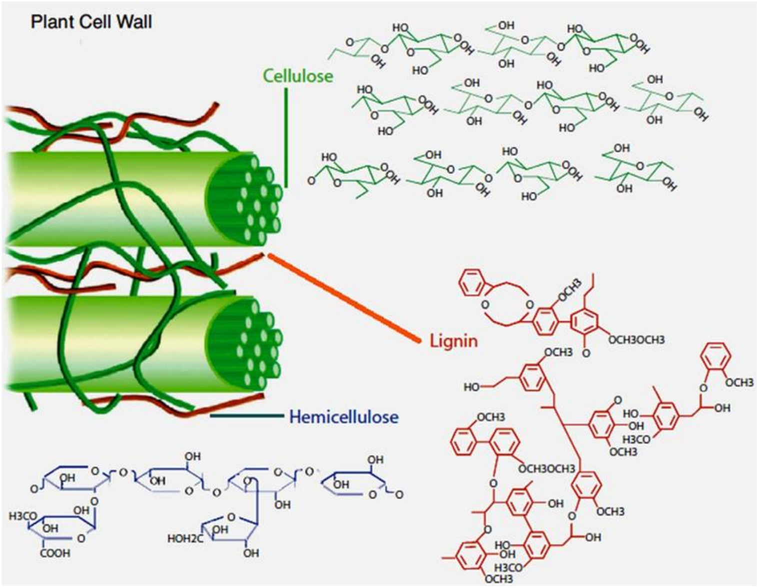

Figure 2.1: Chemical Composition and Structure [34]

viscosity, drying up of dough into fragments), limiting the addition of fillers. Adding different compatibilizers and additives improve the flow of reinforcements in the resin and helps in adding more filler [37]. Similar research on temperate regions depicts the importance of utilizing agricultural waste in composites, giving an almond shell example. Almond shell constitutes about 35-75% weight of an almond, which leaves about 0.8-1.7 million tonnes of the almond shell as unused waste products. These wastes are either dumped or incinerated, causing air, soil and water pollution. For this study, Polypropylene (PP) has been used as a matrix with almond shell filler. The results show an improvement in mechanical properties compared to the pure PP matrix. The screw extruder machine provides good dispersion and distribution of the particles in the polymer. The addition of coupling agents forms strong ester bonds between particles and the PP matrix, leading to good wettability of particles. The results are proven to improve by adding different compatibilizers [38].

Studies have also shown olive stone powder as a potential filler due to its abundance and simple extraction. The European Union is considered the leading producer, consumer and exporter of olive oil, with an average production of about 16-17 million tonnes. Studies estimate an average of 0.6 tons of solid olive waste from 1 ton of olives. Converting these wastes into value-added products requires both high expenses and accessibility. The complex nature of lignocellulosic materials is also the reason for a difficult breakdown of its components into simpler and profitable value-added products. Utilizing these lignocellulosic materials as fillers have proven to be amongst the better solutions [39]. Similar studies have shown the growing popularity of chemically modified olive stone powder in polymer composites. The addition of olive nut filler in unsaturated polyester resin (UPR) showed an increase in the modulus of the composite, as well as its strength [40]. Comparison in properties between the almond and olive nuts in the same matrix have been done, and the following results have been determined:

Although there is an increase in modulus in both almond shell and olive nuts, the mechanical prop-

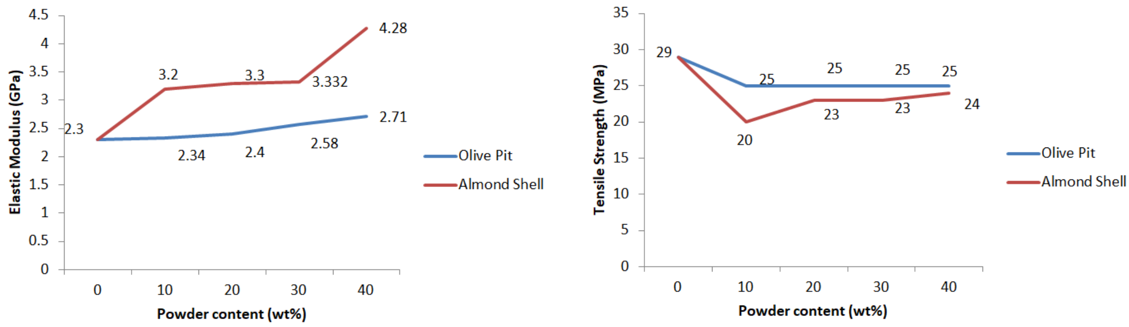

(a) Elastic Modulus vs Filler content

(b) Tensile Strength vs Filler content

Figure 2.2: Comparison Mechanical Properties of Olive Stone and Almond Shell Powders [41]

erties of the almond shell are higher than that of olive nuts, as it can be observed in Figure 2.2.

Another study reinforces the PP matrix with the cocoa pod husk and determines its results. Young's modulus of the PP matrix increases with the increase in cocoa filler concentration. However, the strength decreases with the increase of the filler concentration in the matrix. The reasons for this have been discussed as irregular shape, low aspect ratio and poor interfacial adhesion, which reduces the efficiency of stress transfer from matrix to filler [42]. Another study with PLA matrix showed an increase in the matrixs' strength up to 10 wt% loadings, followed by a decrease in strength. This was discussed as better dispersion of the filler in the PLA matrix. As the concentration goes beyond 10%, the decrease is due to poor interfacial adhesion between the matrix and the filler and filler agglomeration. An increase in the modulus was also recorded in this study with the increase in filler concentration. The reason for this can be attributed to the better dispersion of the filler in the matrix [43]. A study on wood apple and coconut shell applications as fillers showed positive flexural and tensile strength results. The addition of fillers up to 15% improved the strength of the polymer matrix in comparison to the pure epoxy matrix. Additionally, the density and void content decrease with the increase in the filler content [44].

Biochar

Biochar is the by-product of burning agricultural/forest wastes at high temperatures at around 450-500°C or even more in an anaerobic environment. They have become an interesting topic of research in the agriculture industry as a source of soil fertility enhancement due to their ability to reduce soil erosion and replace soil carbon [45]. The properties of biochar (both physical and chemical) change if the biochar source or the pyrolysis conditions are changed. The functional groups that bind the cations are similar only when you use similar temperatures. Major chemical components of the wastes like lignin, starch, cellulose and hemicellulose are broken down thermally, and pores are formed, which vary in size due to processing conditions and feedstock. Also, the chemical composition of the feedstock plays an important role in the size of the pores. Lignin-rich and cellulose-rich feedstock result in macro-level pores under pyrolysis, while cellulose-rich biochar forms micro-level pores [46].

Multiple studies have concluded that the higher the pyrolysis temperature, the higher the content of fixed carbon is, which is expected to be stable aromatic carbon or graphitic carbon and also higher thermal stability compared to lignocellulosic filler [47, 48]. It also helps catalyse the formation of a porous structure with a high specific surface area. An increase in pyrolysis temperature also increases the carbon content in the biochar whilst reducing hydrogen and oxygen content. A higher pyrolysis temperature reduces functional groups present in the biochar and enhances the degree of aromaticity in them [49]. The shape of the biocarbon also depends on its source of origin. The method of preparation of biochar (pyrolysis conditions) plays a significant role in the shape and aspect ratio of the biochar. This, along with its size, plays an important role in its flow behaviour concerning resin and fibres.

The source of origin (chemical composition and properties of the agricultural/forest waste which is pyrolysed) is an important aspect of the composites' mechanical properties. Temperature plays the most important role among other pyrolysis conditions in the stability of biochar. There is an increase in the strength of biochar as the temperature increases [50]. The temperature also affects the hydrophilicity/hydrophobicity of the biocarbon. Temperatures less than 550°C allow water retention in the biocarbon (hydrophilic) as lignin is not yet converted into a hydrophobic polycyclic aromatic hydrocarbon (PAH) matrix. When the pyrolysis temperature increases to 650°C, the biochar becomes thermally stable and counts as hydrophobic[51]. Biochar is considered to have better humidity stability than natural fibres like flax, jute, hemp etc., as it is hydrophobic compared to natural fibres, which absorb moisture from the atmosphere[52]. Particle size ranges above 300µm show decreasing flexural properties, and so does the size range below 20µm. The particle size distribution between 300µm - 20µm does not show much difference in flexural or impact strength[53]. Some studies also states particle size does not affect the flexural properties much, and even if they do, they do it to a small extent[54]. A suitable manufacturing method can help modify the morphology of materials and their rheological and mechanical properties. This allows for the replacement of inorganic fillers with biochar. Low production costs owing to the derivation of the biochar from different waste sources contribute to the circular economy approach and provide a sustainable approach[55].

A study comparing the mechanical properties of both powder and biochar of rice husk reinforced High-density polyethylene (HDPE) has shown positive results favouring the biochar reinforced HDPE. The flexural and tensile strength of biochar reinforced HDPE has been shown to increase with the increase in the biochar filler content, whereas opposite trends have been observed in the case of powder filler content. The biochar restricts the movement of HDPE linear chains and decreases the deformation capacity at higher filler loading. The powder, on the other hand, agglomerates at higher loading capacities and forms stress concentrations and defects, which reduces their strength[56].

Another study involving biochar with glass fibre in an epoxy matrix showed improved mechanical properties compared to a pure matrix with glass fibre. The addition of higher concentrations of biochar (up to 10 wt %) showed improved stiffness, lower damping and improved fire-retardant properties. The storage modulus was found to be more than 30% for biochar reinforced matrix as compared to only glass fibre reinforced polymer[57].

A different study on cashew nutshell waste biochar reinforced polyester resin at different filler loading (0-15 wt %) was tested for flexural, tensile and impact properties. The flexural strength increased as the filler loading increased, while the tensile strength increased initially till 10 wt% loadings, followed by a decrease in strength. A similar trend was found in the impact strength results[58]. A study involving date palm biochar (BC) reinforced polypropylene (PP) matrix shows improved tensile modulus compared to neat PP. However, rheological studies showed poor interfacial adhesion between BC/PP. Few ways to improve adhesion are by enhancing porosity, surface treatments and removal of ash[59].

2.1.2 Natural Fibres

Fibres provide strength to the filler reinforced composite. Lignocellulosic fibres derived from plants and trees are considered as potential alternatives for synthetic fibres due to both environmental and (specific) mechanical aspects.

Mechanical Aspects:
1) Low Density
2) Non-Abrasive
3) Better Specific Strength
4) Better Corrosion and Fatigue resistance

Environmental Aspects:
1) Biodegradability and circularity
2) Reduced environmental Impact
3) Lower Carbon footprint
4) Availability and cost
5) Better Life Cycle Assessment (LCA) results

Fibre	Density(g/cc)	Elongation(%)	Tensile Strength (MPa)	Young's Modulus (GPa)	Cost (Eur/kg)	References
			Natural Fibres			
Jute	1.4	1.7-2	400-700	50-80	0.1-0.3	[60]
Hemp	1.5	1.6	690	55-70	0.5-1.5	[61, 62]
Ramie	1.45	2.7	627	31.8	1.2-2.1	[63, 62]
Flax	1.2	2.7–3.2	1500-1800	60-80	0.5-3	[64]
Viscose	1.5	11.4	593	11	0.75-1	[65, 62]
Coir	1.2	15-20	125-200	4-6	0.1-0.3	[66, 62]
Bamboo	0.6-0.8	2.8-3.5	160-280	8-15	1.1-1.7	[67]
			Synthetic Fibres			
Carbon	1.8	1.7-2	3500-4000	228-245	21-30	[68, 62]
Glass	2.54	2-2.5	1700-3500	69-72	1.5-1.6	[69]
Aramid	1.47	2.2-4.5	2400-3000	60-120	25-40	[70]

Table 2.2: Mechanical properties and Cost in Eur/Kg of different Natural Fibres in comparison With Synthetic Fibres

Table 2.2 makes it clear that natural fibres have lower density and cost as compared to synthetic fibres. The mechanical properties of flax can be comparable to that of glass fibres, and the specific properties derived are better due to its low density. Although natural fibres have become a topic of interest in the past few years, industries still rely heavily on synthetic fibres, mainly due to better and consistent mechanical properties. However, there are certain drawbacks associated with them, such as high costs, low recyclability and higher environmental impacts[71]. Although having comparable properties, natural fibres have severe drawbacks such as inconsistency in mechanical properties, poor matrix-fibre interfacial adhesion, sensitivity to severe environmental conditions, etc. The interfacial adhesion can be improved by chemically treating the fibres, while the consistency in mechanical properties depends on maintaining the chemical composition and geometry of the fibres and fillers[72].

Flax is grown extensively in countries like Canada, Belgium, the Netherlands and France. The EU has produced about 145,000 tonnes of flax fibres in 2019/2020, and the annual flax production has increased by 7% compared to the previous year. Perfect climatic conditions in these regions for flax cultivation and the shorter cultivation cycle of about 100 days make them a potential reinforcement for bio-based composites. The primary constituent of the fibre is cellulose which makes up about 70 per cent of the fibres, thus making it stiffer and stronger [73].

A study comparing flax and glass fibre-based epoxy composites increases both fibres' tensile modulus with volume fraction. Arctic flax-based composites used in this study have been found to have slightly better stiffness than glass fibre based composites [74]. Flax reinforced with polypropylene matrix improves elastic modulus as the fibre volume fraction increases. 40 volume percent of flax improves the elastic modulus by about 300 percent, which is a significant increase in its properties [75]. Similar studies have shown the influence of natural fibres like flax in the improvement of mechanical properties of thermoset resins like epoxy resin [76]. Flax/PLA composites, in comparison with Jute/PLA and pure PLA, have significantly higher tensile properties [77]. NPSP's patent product NABASCO also shows improvement of flexural properties of UP resin on the addition of loading flax fibres.

Studies on bamboo fibre reinforced composites showed improvements in flexural modulus of the epoxy matrix at increased fibre loading percentages. Chemical treatment of the fibres showed improved mechanical properties like flexural strength. Common chemical treatment of the fibres can be using chemicals like NaOH, silane etc. [78]. Bamboo reinforced polypropylene improves the tensile modulus and strength up to 40 wt% loading and decreases. Adding coupling agents like MAPP (methylacetylene-propadiene propane) improves the tensile properties up to 60 percent when loaded with 60 wt% [79]. Other studies show improvement in tensile properties of natural rubber on the addition of bamboo fibres with or without coupling agents[80]. Studies also show the comparison in mechanical properties of different thermoset resins like epoxy,unsaturated polyester and vinyl ester resins on loading of bamboo fibres as shown in Figure 2.3. The flexural properties of all the resins increase significantly on addition of bamboo fibres [81] .

Similar results were observed in kenaf fibre reinforced epoxy polymers. The modulus and strength of epoxy polymers increased with the addition of kenaf fibres (either treated or untreated). The treatment of kenaf fibres improves the flexural properties of the epoxy polymers by 36 percent as compared to untreated fibres, which offers about 20 percent improvement in properties [82]. Viscose reinforced unsaturated polyester resin and epoxy resin, tested for flexural properties, proved that incorporating 40 wt% of viscose is achievable. The modulus and the strength increased significantly (about 70% and 40% respectively). Chemical treatment of the fibres, however, did not improve the modulus of the composites and water absorption capacity, although strength was improved to a significant level [83]. Hemp fibre reinforced UP resin has improved flexural modulus as the fibre content increases. However, the flexural strength decreases as the fibre loading increases. This trend is present even with the treatment of fibres, which makes it not a suitable composite for higher strength applications [84]. Studies on other natural fibres have been done, such as jute. Jute reinforced unsaturated polyester resin has been compared with glass fibre and carbon fibre-based composites for turbine applications. Jute based composites and Jute/glass fibre hybrid composites have a good balance of flexural and damping properties. However, higher content of jute in the recipe is avoided as it increases the overall density of the composite [85]. Similarly, snake grass fibre reinforced unsaturated UP resin show maximum flexural strength and modulus at about 25 vol% loadings.

Bamboo has an unbelievable average growth rate of 1.5 inches per hour, and the average cultivation time is around three months. This ensures an abundance of bamboo throughout the year and can be utilized even by countries with a scarcity of forest resources. Moreover, due to their high strength

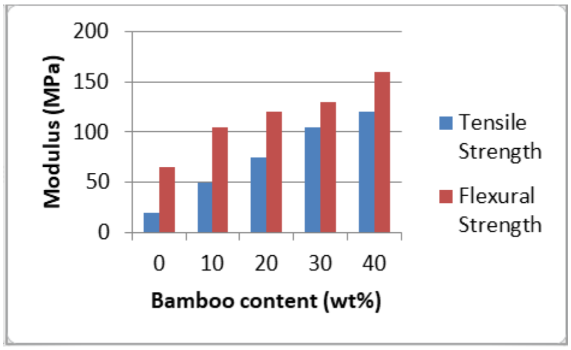

(a) Bamboo reinforced Epoxy Composite (BFRC)

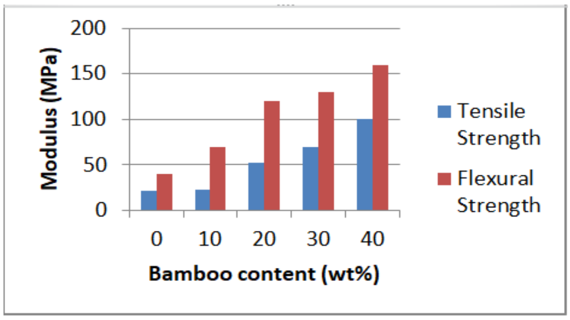

(b) Bamboo reinforced Unsaturated Polyester Composite (BFRPC)

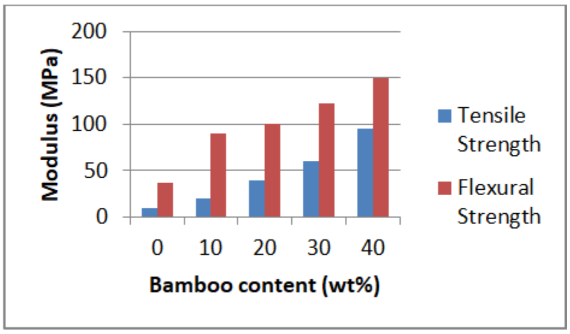

(c) Bamboo reinforced Vinyl Ester Composite (BFRVC)

Figure 2.3:
Tensile and Flexural Strength of Bamboo reinforced Epoxy, Unsaturated Polyester and Vinyl Ester Resin

to weight ratio, structural variation (dense fibre distribution on the outer surface and sparse on the inner surface), chemical modification and thermal properties, they are becoming a potential fibre in the polymer composite industry. Its high cellulose and lignin content provide it with higher mechanical properties. With a maturity period of over three years, its tensile strength is comparable to or even greater than that of mild and conventional steels [86].

Chemical Treatment of Fibres

Natural fibres are usually hydrophilic in nature as opposed to the matrix which is hydrophobic. This leads to improper mixing of the fibre and the matrix, debonding, cracks, fibre pull out due to poor interfacial adhesion. Chemical treatment of the fibres ensures penetration of the resin into the fibres ensuring strong interlocking/interfacial adhesion [82]. This improves the flexural properties of the treated natural fibre reinforced composite as compared to the untreated fibre composite. As seen in most of the literature in this and the previous subsection, the natural fibres tend to increase their properties on chemical treatment of the fibres.

Fibre	Resin	Remarks
Jute	UPR	High specific modulus, low cost, low strength [87]
	PP	High tensile strength and modulus, High flexural modulus [88]
Flax	Epoxy	High tensile properties, Comparable to traditional GFRPs [74]
	PP	High Elastic modulus and strength, low density [75]
Viscose	Epoxy	High Flexural modulus and strength, chemical treatment not potentially effective and needs further research [83]
	UPR	High Flexural modulus and strength, chemical treatment not potentially effective and needs further research [83]
Bamboo	PP	High tensile modulus and strength [79]
	Epoxy	High impact, tensile and flexural strength, low density [89]
	UPR	Moderate flexural and tensile properties, low density [80]
Kenaf	Epoxy	MModerate flexural properties, low density and cost [82]
Reed	PP	High flexural modulus, high tensile strength [90]
	UPR	High flexural and tensile modulus, moderate flexural strength, low impact strength [2]
	Bio-epoxy	High tensile properties, little influence of plasma treatment on mechanical properties [91].

Table 2.3: Influence in mechanical properties on reinforcing natural fibres to polymers

Fibre	Resin	Treatment	Remarks
Pineapple	PP	Alkali/Silane	Improved flexural modulus and strength in both cases, silane treated composites comparatively stronger [92]
Reed	Bio based Epoxy	Plasma	Improved flexural modulus and strength in both cases [91]
Coir	Epoxy	Alkali	Improved flexural strength by 16.7% [93]
Abaca	PP	Benzenediazonium chloride	Improved flexural strength by 65% [94]
Flax	PP	Maleic anhydride	Improves tensile and flexural strength [95]
Seaweed	PP	Bioethanol/biodiesel/ biomethane	No significant improvements in the mechanical properties [96]
Bamboo	UPR	NaOH	Improves flexural strength (by 25%) to a greater extent as compared to flexural modulus (by 6%) [97]
Viscose	Epoxy	Silane	Improves flexural strength [83]

Table 2.4: Influence in mechanical properties on reinforcing natural fibres to polymers

2.1.3 Matrix

The polymer matrix acts as the medium to transfer the load to the reinforcements (filler+fibre). The choice of the matrix for combination with natural fibres is dependent on a lot of parameters. An important factor is the curing/softening the thermosetting/thermoplastic resin below the temperature at which natural fibres degrade. This temperature is usually 200°C for natural fibres [10]. To improve the sustainability factor and the LCA of composites, there is an increase in the research on bio-based resins. Several natural thermoplastic resins like poly(3-hydroxybutyrate-co-3-hydroxyvalerate) (PHBV), polyhydroxybutyrate (PHB), polylactic acid (PLA) etc., used in composites contribute to the total green composite. As stated in the previous sections, they are easily recyclable and have higher toughness than thermosets. PLA has been observed to have optimized strength and stiffness compared to the other bio-thermoplastics, making it a promising biopolymer. There are, however, drawbacks to using bio-resins. They are expensive, making them less affordable for large scale industrial production. Another factor is the inability to be used for long life applications due to the decomposition of bio-degradable resins[98]. However, bulk moulding compounds (BMCs) use thermoset resins (unsaturated polyester, epoxy or vinyl ester), and NPSP primarily works with partially bio-based unsaturated polyester resins owing to lower cost and structural applications. Epoxy resins provide low viscosity (at room temperature), low shrinkage and good bonding. But they are expensive. Unsaturated polyester resin offers good mechanical properties and easy processing whilst being cheaper[99]. Bamboo fibre reinforced polyester, epoxy and vinyl ester resins were tested for tensile and flexural strength. The epoxy-based composite had the highest tensile and flexural strength, followed by polyester and vinyl ester composites. The flexural properties between epoxy-based and polyester-based were comparable according to the study [81]. The NPSP product NABASCO 8010 uses unsaturated polyester resin, providing a flexural stiffness of 8 GPa and a strength of 30 MPa.

The scope of the thesis is to study different natural fillers and their interactions with unsaturated polyester resin and compare their properties with mechanical properties with composites made with standard calcium carbonate filler. A major objective will be achieved if the natural filler reinforced composites show superior specific modulus and strength to the common calcium carbonate reinforced composites. Hence the UP resin is going to be used for the experiments conducted to prove the BMC optimization model [2]. Table 2.5 shows the changes in mechanical properties when olive stone and almond shell is reinforced in different matrices.

Filler	Matrix	Remarks
Olive Stone	PVC	Increase in flexural and tensile modulus, decrease in flexural and tensile strength [100]
	UPR	Increase in flexural modulus, slight increase in flexural strength upto maximum loading [40]
	PP	Increase in tensile and flexural modulus, decrease in strength with untreated fibres [41]
	PLA	Increase in tensile modulus, decrease in tensile strength[101]
Almond Shell	UPR	Increase in flexural modulus and strength [102]
	PP	Increase in tensile and flexural modulus. Initial decrease followed by increase in tensile strength [38]
	PLA	Increase in tensile and flexural properties [103]
	PBS	Increase in tensile properties [104]

Table 2.5: Influence of Olive Stone and Almond Shell fillers on different matrices

2.2 Rule of Mixtures

Semi-empirical models play an essential role in predicting the mechanical properties of multiphase composites. This is because the equations derived are based partly on theory and partly on a series of experiments, which aid in predicting approximate if not accurate mechanical properties. Common properties determined using analytical models are stiffness, strength, thermal and electrical conductivities of a composite, a few of which will be calculated in later chapters. Multiple analytical models have been designed to predict the stiffness of various composites. The use of a particular model depends on the characteristics of fillers and fibres. A few essential reinforcements properties for selecting a model are its length, aspect ratio, orientation and shape. Short fibre or filler reinforced filler composites use models like Halpin-Tsai, Cox, Mori Tanaka, Lewis-Nielsen, Reuss and Voigt for determining their elasticity modulus. These models calculate properties for spherical as well as non-spherical fillers. The above-stated Halpin-Tsai and Lewis-Nielsen models are the most successful models for random non-uniform oriented fibre systems.

Lewis Nielsen Model: The Lewis-Nielsen model (modified Halpin-Tsai model) is similar to the Halpin-Tsai model with the addition of packing fraction ($_f$) of the filler. This model considers the

Einstein coefficient (k_E), altered for both slip and no-slip conditions. This helps improve the accuracy of the model concerning the experimental results. The drawback of the model, is the reduced flexibility to determine the elastic stiffness[105]. The equation for the elastic modulus of composite is as shown below:

$$E_C = E_M[\frac{1 + A\nu_N V_f}{1 - \psi\nu_N V_f}] \tag{2.1}$$

Where,

$$A = k_E - 1 \tag{2.2}$$

$$\nu_N = [\frac{E_f/E_m - 1}{E_f/E_m + A}] \tag{2.3}$$

$$\psi = 1 + [\frac{1 - \phi_{max}}{\phi_{max}^2}]V_f \tag{2.4}$$

Filler Type	**Distribution**	**Aspect Ratio**	**A**
Cubes	-	1	2
Spheres	-	1	1.5
Fibres	Random	2	1.58
Fibres	Random	4	2.08
Fibres	Random	6	2.80
Fibres	Random	10	4.93
Fibres	Random	15	8.38
Fibres	Uniaxial Orientation	-	2(l/d)

Table 2.6: : Aspect Ratio Table [106]

Filler Shape	Packing type	Maximum Packing fraction
Spheres	Hexagonal Close	0.7405
Spheres	Face Centred Cubic	0.7405
Spheres	Body Centred Cubic	0.6
Spheres	Simple Cubic	0.524
Spheres	Random loose	0.601
Spheres	Random Close	0.637
Irregular	Random Close	0.637
Fibres	3 Dimensional	0.52
Fibres	Uniaxial Hexagonal Close	0.907
Fibres	Uniaxial Simple Cubic	0.785
Fibres	Uniaxial Random	0.82

Table 2.7: : Packing Fraction Table [106]

The model has been experimentally proven and extensively used for polymer nano-composites [105, 106, 107]. However, not much study on the relation of the model with respect to micro-composites has been done and the application of this model for the micro-composites remains limited.

Faud et al. [108] have compared analytical and experimental results of PP/white rice husk ash composites and found both model to be applicable at lower filler aspect ratios. An assumption they made for their analysis is the spherical shape of the fillers. The experimental points obtained lie between the trend lines with A=1 and 1.5 as shown in Figure 2.4(a). It can be observed that the experimental values are in agreement with the theoretical curves. Similarly, the experimental points obtained lie between the trend lines with A=2 and 2.5 for black rice husk ash as shown in Figure 2.4(b). This again shows a good agreement between both the theoretical and experimental results.

A similar study on the relation of micro-composites with analytical models like Lewis Nielsen has been done, where a comparison of storage modulus of bisphenol-A/aniline based polybenzoxazine (PBA-a) and alumina particle micro-composites at glassy region is analyzed. The dough was compression moulded and tested for mechanical properties. These properties were then compared with

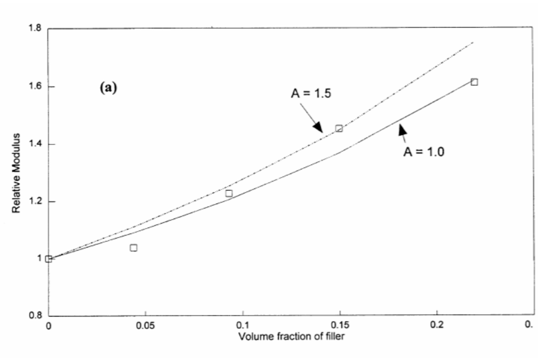

(a) PP/White Rice Husk Ash (A=1.0, 1.5)

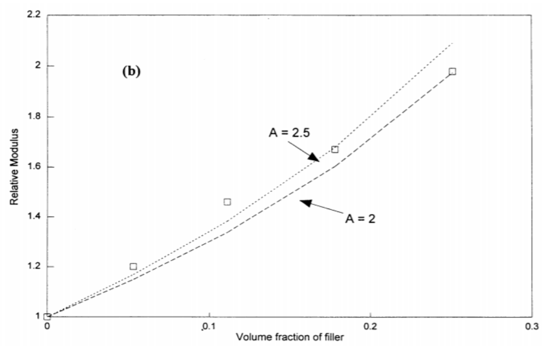

(b) PP/Black Rice Husk Ash (A=2.0, 2.5)

Figure 2.4: PP/ Rice Husk Ash Experimental vs Analytical results[108]

multiple analytical models to check which model provides better agreement with the experimental results [109].

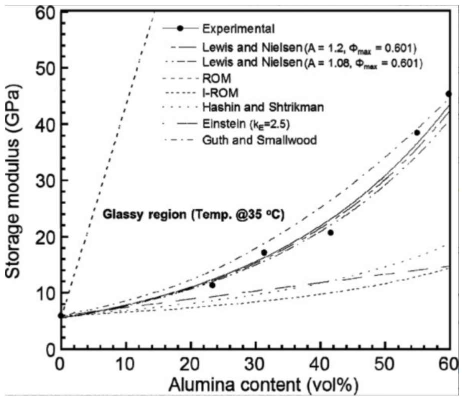

Figure 2.5: Comparison of experimental and theoretical storage modulus of the PBA-a/Al2O3 composites at glassy region [109]

Figure 2.5 shows the comparison of various analytical models with the experimental results. It can be observed that Einstein and Guth underestimated the results due to their consideration of a spherical particle and that the equations assume particles to be rigid compared to the matrix. Although the Hashin Shrikman curve provides better results than the former two, it still underestimates the results due to the assumption of stiffer particles than the matrix. Finally, the Lewis Nielsen model predicts better results and a good fit as it involves the reduced concentration term, which involves the maximum packing fraction of the filler in the matrix. It can be observed from the graph that different aspect ratios are considered to check which one would give a better fit to the experimental values. Alumina particles used for the experiments are irregular in shape, affecting their aspect ratio and maximum packing fraction, which are not considered in other models—incorporating these leads to improved prediction in results. Apart from the A value, the maximum packing fraction can also be tweaked to check for the correct value to obtain a good fit of results.

There is also a comparison done between nano and micro silica particles and a combination of both [110]. The tensile tests showed a good arrangement with the Halpin-Tsai and Lewis Nielsen models. The Lewis Nielsen was slightly better than the Halpin-Tsai model's absence of maximum packing density. The experimental data points trend between the Lewis Nielsen slippage and non-slip conditions suggesting an intermediate level of adhesion.

Additionally, Fredi et al. [111] in their study performed a detailed investigation of the thermo-mechanical properties of paraffin microcapsules incorporated epoxy composites. The theoretical and experimental results comparison is shown in Figure 2.6. After comparing the experimental results to theoretical models (Halpin-Tsai and Lewis Nielsen), it can be observed that the Halpin-Tsai model succeeds in predicting the modulus at low microcapsule content at about 20 vol% and overestimates the modulus above that content. The Lewis Nielsen model accounts for the adhesion between the matrix and the filler as it incorporates the maximum packing fraction in its equation. This helps the model give a better fit than the other models. Another factor to look out for is Einstein's coefficient k_E, which, as reported, depends on the filler-matrix adhesion. The slip factor influences it. The results show that the model considering the slippage hypothesis slightly underestimates the experimental results, while the one with no interfacial slippage perfectly fits the results. This suggests that the matrix-filler interfacial interaction is better at low deformations.

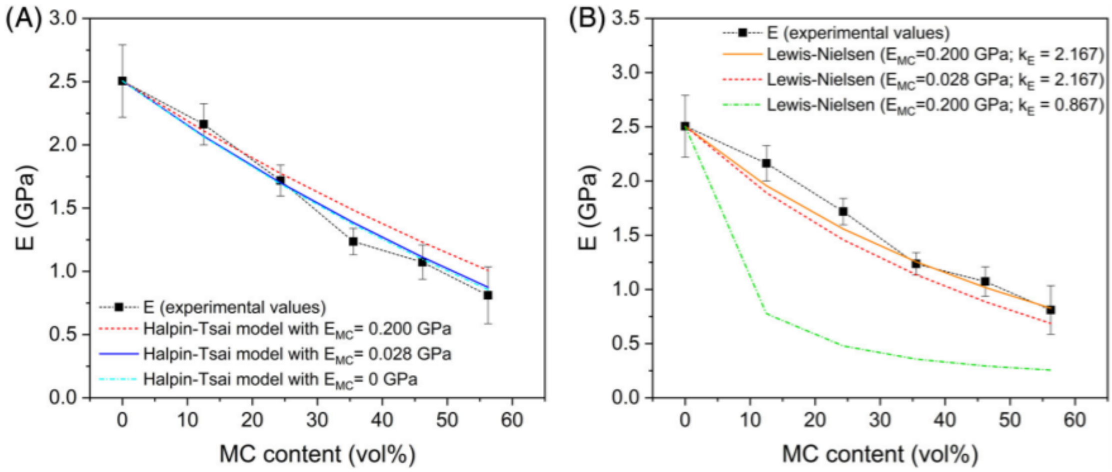

Figure 2.6: Theoretical vs Experimental comparison of tensile modulus of paraffin microcapsules incorporated Epoxy resin A) Halpin-Tsai B) Lewis Nielsen model [111]

A study on the micromechanical models for alumina trihydrate (ATH) reinforced poly (methyl methacrylate) (PMMA) compares elastic modulus based on various analytical models like Generalised self-consistent (GSC) model, Lielens model, Mori-Tananka model, Halpin-Tsai and Lewis Nielsen model[112]. The Lewis Nielsen model and Halpin-Tsai model predicted closer results as compared to GSC or Mori Tanaka models as observed in Figure 2.7. When the elastic modulus is compared at different temperatures, Lielens and Lewis Nielsen models provide better agreement with the results as compared to other models. However, Lielens model is presented as the superior model as it is based on constitutive equations which predict all elastic constants at once unlike Lewis Nielsen model which relies heavily on empiricism.

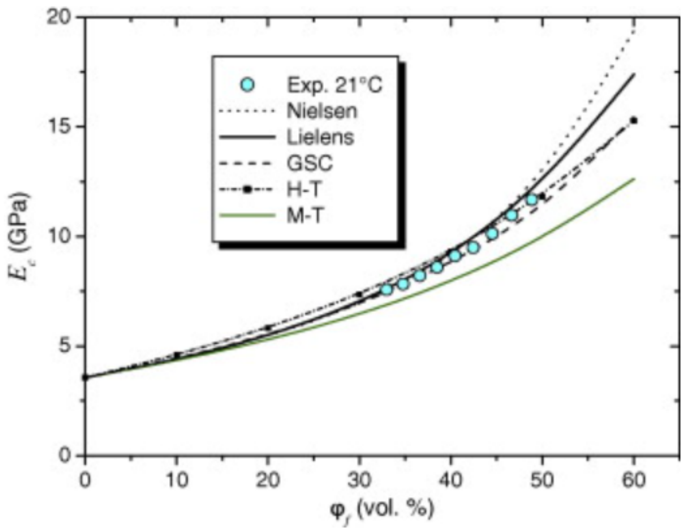

Figure 2.7: Prediction comparison of elastic modulus vs volume fraction of various analytical models for ATH reinforced PMMA [112]

As mentioned earlier, the drawback of model is the reduced flexibility to determine stiffness of the composite. In fibre reinforced composites, the short or long fibres generally have aspect ratio more than 100 or even 1000. Unfortunately, the model only has the capability to determine composite modulus reinforced with fillers having an aspect ratio up to 15. Beyond that, the model predictions fail. Not much literature could be found for Halpin-Tsai model too which could work at much higher aspect ratios. Fuchs et al. [113] briefly talks about the good fitting of Halpin-Tsai model to microfibril reinforced polypropylene/ poly(ethylene terephthalate) composites at aspect ratios over 100. A study about carbon nanotubes (CNTs) show a good fitting of the Halpin-Tsai equations above 100 to the experimental data but this however is only upto 2 vol% of CNTs in the matrix [114]. In theory, Halpin-Tsai model predicts a linear increase in mechanical properties on increasing the aspect ratio, but unfortunately could not find experimental evidence to support this. Hence, studies have to be conducted on other models which can predict accurate modulus results at higher aspect ratios. Several models have been derived for predicting fibre reinforced composites.

Some common mechanical models include the series and parallel models.

Series model:

$$\frac{1}{E_c} = \frac{V_f}{E_f} + \frac{1 - V_f}{E_m} \tag{2.5}$$

Parallel model:

$$E_c = V_f E_f + (1 - V_f) E_m \tag{2.6}$$

On adding efficiency factor η_0

$$E_c = \eta_0 V_f E_f + (1 - V_f) E_m \tag{2.7}$$

When η_0 =1/5 for 3D isotropic
η_0=3/8 for 2D isotropic
η_0=1 (//) and 0 ($\perp$)

The Cox and Krenchel theory is also one of the widely used models for in plane:

$$E_c = \eta_L \eta_0 V_f E_f + (1 - V_f) E_m \tag{2.8}$$

Where,

$$\eta_L = 1 - \frac{\tanh(\beta L/2)}{\beta L/2} \tag{2.9}$$

and

$$\beta = \frac{2}{d} \sqrt{\frac{2G_m}{E_f ln(\sqrt{\pi}/X_i V_f}} \tag{2.10}$$

d, L and G_m are the fibre diameter, the fibre length and the shear modulus of the matrix respectively. The value of X_i and π_0 is determined by the packing orientation of fibres.

Flax fibres of 20-50 mm length are reinforced with polypropylene resin and the theoretical values are approximately similar to those of the experimental values [75]. The Cox model seemed ineffective for smaller fibre lengths and underutilized due to fibre disorientation.

The 2D and 3D isotropic micromechanical models have an efficiency factor/fibre orientation factor of 3/8 and 1/5 respectively. For thin samples, the fibres have 2 orientation directions, while for thicker samples; they have 3 orientation directions[115, 116].

2.3 BMC Optimization Model

Following the master thesis work of Martin Van Der Schelling who had chosen Bayesian Optimization as the heuristic for optimizing the bio-based composites, the focus of this thesis directs towards validating accuracy of the model.

The Bayesian Optimization is based on the Bayes theorem and is highly efficient for expensive to evaluate objective functions[117, 118]. The Bayes theorem describes the probability of an event based on prior information of situations or conditions which might be related to that event. It states that the posterior probability of an event A given event B is proportional to the probability of B given A multiplied by the prior probability A. This is written as:

$$P(A|B) = \frac{P(B|A)P(A)}{P(B)} \tag{2.11}$$

This principle can be applied to the case of predictions of optimized bio-based composite recipes. Event B can be thought of as the stored data inputs (fibre and filler weight fraction and mechanical properties). We can consider an unknown objective function ‘f’ for example. As the number of data inputs increase (more information is accumulated), the posterior distribution improves and the algorithm is able to predict which area of the search space is worth exploring and which is not. The surrogate model A uses this prior information to finally estimate the objective functions.

The Bayesian Optimization algorithm consists of the following steps:
1) Optimizing the acquisition function and finding the next sampling point over the surrogate model.
2) Obtaining and testing recommendations based on the parametrized loss functions.
3) Updating the surrogate model and further optimizing the acquisition function for the evaluation of the next point.

Surrogate model:

Out of the popular surrogate models, Gaussian process (GP) is used as the surrogate model for this case. Gaussian process (GP) directly captures the model uncertainty. Also, when using GP, you are able to add prior knowledge and specifications about the shape of the model by selecting different kernel functions, also known as covariance function [119].

Acquisition Function:

Out of the several acquisition functions proposed in literature, the perfect balance between exploitation and exploration behaviour has to be found. Acquisition functions like maximum probability of improvement’ (MPI) and ’Lower Confidence Bound’ (LBC) searches for parameters where surrogate mean value is the highest, while ’Upper Confidence Bound’ (UCB) searches for parameters where surrogate covariance is the greatest. The former is purely exploitative, while the latter is purely explorative. Hence, ’Expectation of Improvement’ (EI) acquisition function is chosen as it finds the balance between exploitation and exploration behaviour [120]. The acquisition function is created for the surrogate model based on the prior data inputs, recipe ($\vec{x_t}$) and mechanical properties (f($\vec{x_t}$)), which then predicts the next data point recipe ($\bar{x}_{t+1}$) for which mechanical properties (f($\bar{x}_{t+1}$)) are calculated.

Bayesian Optimization as a suitable heuristic

Martin’s thesis dived deep into the literature to state the reasons for choosing Bayesian Optimization as a suitable for heuristic for optimizing bio-based composites. Comparing with other optimizers like CMA-ES or Particle Swarm Optimization, the Bayesian optimization can be efficient as no boundary condition is needed. CMA-ES although reducing the computational time to a great extent, often discards most of the information. This is because it uses only the current population to recommend next data point and does not update and apply the past evaluations like the Bayesian Optimization. It also has a high space and time complexity problem while dealing with large scale optimization problems[121]. ADAM on the other hand is dependent on gradient information of the of the response surface. Hence it cannot be applied to the case of natural composites which is noisy due to variations in its mechanical properties. In addition there is no direct access to the gradient information it.

Bayesian Optimization has been deemed as a potential heuristic due to its ability to handle noisy dataset, efficiently using prior information for prediction of the next data point and its effective search scan capability. It has a good agreement with box constrained boundaries as well as unknown constraints [122, 123].

One of the drawbacks of the Bayesian optimization is the time complexity when dealing with high number of iterations. The time complexity $\mathcal{O}(\mathrm{n}^3)$ due to inversion of an n×n matrix, where n is the number of iterations[124, 125]. The optimization is computationally expensive with 10^4 iterations. Additionally increasing the number of iterations beyond 10^4 iterations further increases the computational time for hyperparameter optimization, making it a less suitable approach [126]. However, with the thesis perspective, the number of iterations more than 10^4 is not possible. This is because the production and testing of the composites takes multiple days. This shows that time complexity is not a drawback from the thesis point of view.

Another drawback is selecting the appropriate kernel for the Gaussian process. Not selecting the right kernel leads to inaccurate model. Hence, choosing a relatively uninformed kernel which covers all types of function is a better approach. For this thesis, a Radial basis function (RBF) kernel is chosen that helps covering all types of function characteristics [127].

Finally, the inability of the optimizer to handle higher dimensionality is considered to be major challenge although recent studies are attempting to counter the curse of dimensionality [126, 128]. The efficiency is pretty high while fine tuning a few hyper parameters but it significantly degrades the moment dimensionality increases. However, since the implementation of Bayesian optimization in the field of bio-based composites is a novel concept, the scope of the thesis is set to experimentally confirm the model for lower dimensionality optimization. Finally, after briefly diving into strengths and limitations of various types optimizations and analysing the results obtained by Martin during his thesis, Bayesian Optimization is considered to be the best match for the optimization of the bio-based composites and the design of experiments carried out in chapter 3 will be primarily focused on experimentally validating the model using natural fillers and natural fibres.

Chapter 3

Design Of Experiments

This chapter discusses bio-based composite production in collaboration with NPSP B.V. in Amsterdam. NPSP B.V. provides the production of the BMC doughs and plates for this thesis, and characterization of the reinforcements is done at TU Delft. The design of experiments is divided into two sections. The first section covers a set of experiments that serve as the BMC Optimizer's training set before the model is tested. This training set consists of multiple data parameters (mechanical properties of composites-flexural modulus, strength and density) of varying filler and fibre concentrations which serve as data inputs for predicting optimized recipes based on the objective function. The second section covers a designed set of experiments, the mechanical properties of which are to be compared with the theoretical rule of mixtures models (Lewis-Nielsen and Cox-Krenchel models). The objective is to obtain a good agreement between the theoretical and experimental properties of the binary phase system followed by that of the ternary and quaternary phase systems of the same fillers and fibres.

Methodology
Bulk Moulding compounds (BMC) involve mixing the reinforcements in a matrix to form a BMC dough, followed by curing this dough into a plate by compression at high temperature and pressure. These plates are then tested to determine their mechanical properties. Section 3.1 and section 3.2 cover the experimental procedure from the BMC dough mixing to plate production to testing those plates in detail. This thesis involves using thermosetting resin as the matrix, four fillers and two fibres as reinforcements, used in different ratios with respect to each other. The materials used for BMC composite production in both the sections are same.

Materials
The bio-based dough consists of three components: a) Matrix b) Fillers c) Fibres. NPSP B.V. has provided all three components. The matrix is the wet part of the dough, while the fillers and fibres constitute the dry part. The constituents of each section are as follows:

Matrix: Unsaturated polyester resin is used as the thermosetting resin. A peroxide initiator is used that acts as the hardener for the thermosetting resin. The hardener added to the resin initiates the curing process of the reaction by cross-linking to the resin. To uniform and better flow the dry parts in the matrix, a plasticizer has to be used. A thickening agent is added that helps increase the dough's viscosity. This is helpful while curing the dough using compression moulding. Finally, a releasing agent is used to prevent the dough from sticking to any surfaces. The name of the chemicals cannot be revealed for confidential purposes.

Filler: Reference (Inorganic filler) - Calcite derived from waste streams is used as reference filler since it is the conventional filler used at NPSP, which it ultimately aims to replace with lignocellulosic fillers. The reasons for replacing them have been mentioned in section 2.1.1.

Lignocellulosic (Bio-filler)- Lignocellulosic 1 and Lignocellulosic 2 are chosen as potential filler options to replace calcite based on studies gathered in chapter 2.

Waste based filler (Bio-filler)- The waste based filer is produced by pyrolysis of waste streams. These waste streams consists of agricultural and forest wastes.

The fillers' size distribution ranges from 50µm-250µm. Figure 3.1 shows different fillers used for BMC Plates.

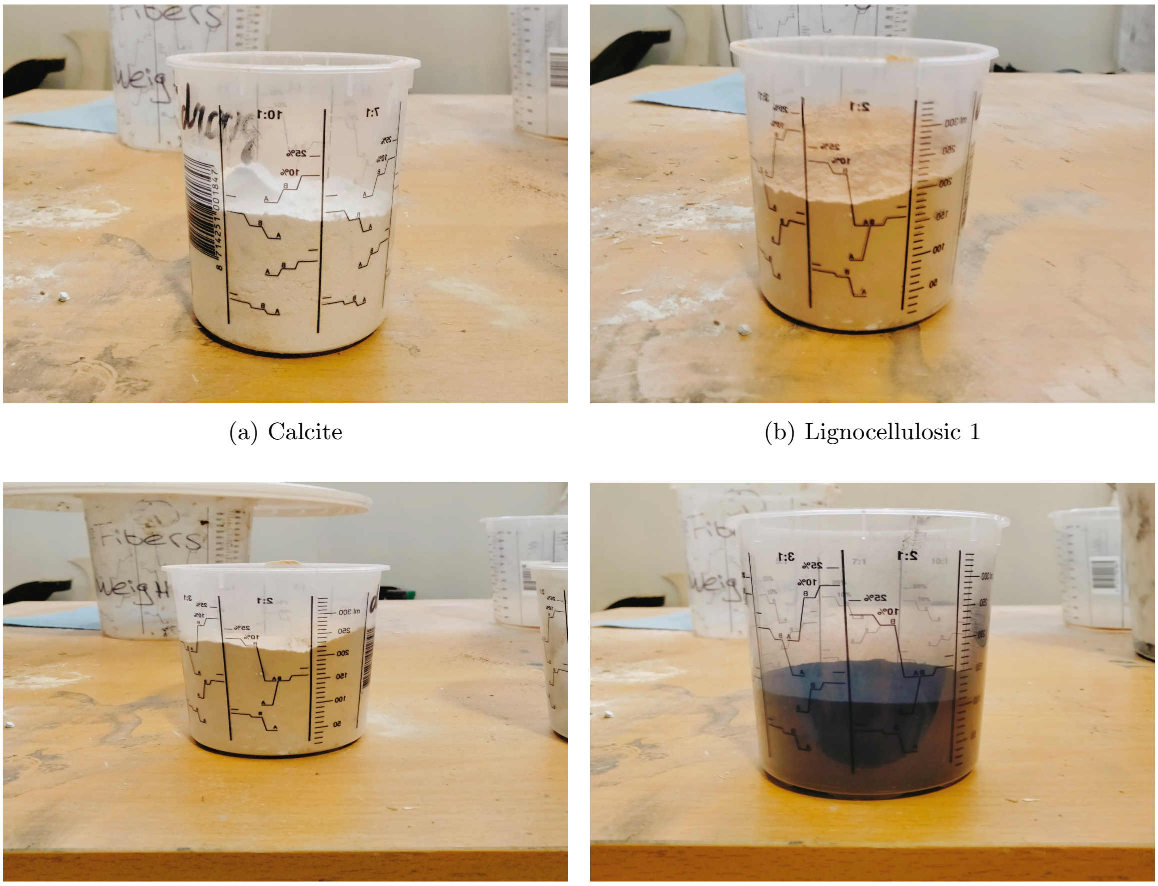

(a) Calcite

(b) Lignocellulosic 1

(c) Lignocellulosic 2

(d) Watse based filler

Figure 3.1: Different fillers used for BMC Plates

Fibre: Flax (6mm) and Bamboo (5mm) are the two fibres used for the production of the bio-composite plates. Figure 3.2 shows the flax and bamboo short fibres. It can be observed that flax appears to be a more curvy/wavy fibre as compared to bamboo which seems to be straight and stiff.

Sections 3.1 and 3.2 covers the experimental procedure used for dough production and plate production for BMC Optimizer and Analytical models.

(a) Flax fibres

(b) Bamboo fibre

Figure 3.2: Flax (6mm) and Bamboo (5mm) fibres used for BMC Production

3.1 BMC Optimizer

The experiments have been designed with varying ratios of fillers and fibres with respect to each other in order to set a diverse, well-designed database that will help reduce the search space and improve the accuracy of the optimizer. Table 3.1 depicts the design of experiments carried out to create a database with the desired filler and fibre combinations.

The filler ratios mentioned in table 3.1 are the ratios of co-fillers with respect to each other. For example, Lignocellulosic 1/Calcite (75/25) is the ratio of lignocellulosic 1 and calcite where 75 and 25 represent the weight ratios of both the reinforcements with respect to each other. This means, if the total filler loading in the dough is 50 weight % , then 75% of that total filler loading (37.5 weight%) comprises lignocellulosic 1, while the remaining 12.5 weight% is calcite. The total filler and fibre fraction in the dough is the maximum that can be added before the dough is dry and becomes more like solid clumps instead of viscous dough.

The ratio of calcite to natural filler is varied as shown in the Table 3.1 to get varying results of stiffness. Calcite is known to have a higher modulus than the natural fillers; hence calcite reinforced composites will have higher modulus, strength and density comparable to that of natural filler reinforced composites. The selected DOE provides a set of data inputs with a wide range of mechanical properties, which helps the model map out optimized recipes according to the desired objective functions. The fibre content in the composite varies from flax to bamboo. Flax fibres are hydrophilic and curvy and absorb more resin than bamboo, making the dough drier and a lower amount of fibre. On the other hand, bamboo fibres have more fat content on their surface, making

Flax Based (6mm) **9%Fibre content**	**Bamboo Based (5mm)** **14%Fibre content**
Calcite	Calcite
Calcite/ Lignocellulosic 1 (75/25)	Calcite/Lignocellulosic 1 (75/25)
Calcite/ Lignocellulosic 1 (50/50)	Calcite/Lignocellulosic 1 (50/50)
Calcite/ Lignocellulosic 1 (25/75)	Calcite/Lignocellulosic 1 (25/75)
Calcite/ Lignocellulosic 1 (0/100)	Calcite/Lignocellulosic 1 (0/100)
Calcite/ Lignocellulosic 2 (75/25)	Calcite/Lignocellulosic 2 (75/25)
Calcite/Lignocellulosic 2 (50/50)	Calcite/Lignocellulosic 2 (50/50)
Calcite/Lignocellulosic 2 (25/75)	Calcite/Lignocellulosic 2 (25/75)
Calcite/Lignocellulosic 2 (0/100)	Calcite/Lignocellulosic 2 (0/100)
Calcite+Waste based filler (75/25)	Calcite+Waste based filler (75/25)
Calcite+Waste based filler (50/50)	Calcite+Waste based filler (50/50)
Calcite+Waste based filler(25/75)	Calcite+Waste based filler(25/75)
Calcite/Waste based filler (0/100)	Calcite/Waste based filler (0/100)
Flax Based (6mm) **14%Fibre content**	**Bamboo Based (5mm)** **18-19%Fibre content**
Calcite/Lignocellulosic 1 (88/12)	Calcite/Lignocellulosic 1 (88/12)
Calcite/Lignocellulosic 1 (71/29)	Calcite/Lignocellulosic 1 (71/29)
Calcite/Lignocellulosic 1 (45/55)	Calcite/Lignocellulosic 1 (45/55)
Calcite/Lignocellulosic 1 (0/100)	Calcite/Lignocellulosic 1 (0/100)
Calcite/Lignocellulosic 2 (86/14)	Calcite/Lignocellulosic 2 (86/14)
Calcite/Lignocellulosic 2 (68/32)	Calcite/Lignocellulosic 2 (68/32)
Calcite/Lignocellulosic 2 (41/59)	Calcite/Lignocellulosic 2 (41/59)
Calcite/Lignocellulosic 2 (0/100)	Calcite/Lignocellulosic 2 (0/100)

Table 3.1: Design of Experiments for BMC Optimizer Validation

them hydrophobic and improving interfacial adhesion. This allows for more loading of bamboo fibres as compared to flax fibres. The fibre weight percentages in Table 3.1 show the loading range for each fibre. The recommended flax fibre range is 9-14 weight%, while that of bamboo is 14-19 weight%. The addition of fibres lower than the limit reduces its viscosity and strength and lowers its modulus. Going above the limit makes the dough dry and clumpy, which does not give a uniform mixture, further reducing the strength and modulus of the composite.

Dough Preparation

The procedure followed to make the dough is as follows:
1) The fillers and the fibres are dried in the oven at about 100°C and kept for about 2 hours to remove any moisture.

2) The hardener, plasticizer, thickening agent and releasing agent are added to unsaturated polyester resin (UP) and mixed thoroughly to form a uniform mixture/ matrix.

3) Next, this matrix is added to the sigma (Z) blade mixer shown in figure 3.3 where the fillers are added in batches of two and mixed for about 8 and 12 minutes, respectively, so that the fillers uniformly mixes with the matrix. This time can vary depending on the type of filler.

4) After uniformly mixing the filler, the fibres are divided and mixed in 3 batches for 3-4 minutes (depending on the type of fibre). Mixing the fibres in smaller batches facilitates better mixing than a single large batch of fibres.

5) After thoroughly mixing the fibres, the final dough is stored in vacuum bags and stored at cooler

temperatures until they are taken out for compression moulding. The reason for keeping them in vacuum bags is to prevent the evaporation of styrene present in the unsaturated polyester resin.

Figure 3.3: Sigma (Z) blade mixer for BMC dough mixing

Table 3.2 shows an example recipe. The recipe is an example of filler and fibre reinforced polymer. The actual recipes are confidential, hence are not included in the report.

Number	Ingredient	Name	Weight %	Weight (g)
1	Thermosetting Resin	Unsaturated polyester resin	50	1500
2	Hardener	Peroxide initiator	2.5	75
3	Releasing Agent	Stearate based compound	10	300
4	Plasticiser	-	4	120
5	Thickening Agent	-	0.5	15
6	Filler	Bio/waste based fillers	25	750
7	Fibre	Natural fibres	8	240
Total	N.A	N.A	100	3000

Table 3.2: Example recipe of BMC Dough recipe

Plate Production

The dough prepared is now cured using compression moulding to a composite plate. A common fluid behaviour is the decrease of viscosity with the increase in temperature. This results in free flow of resin in the dough, uniformly mixing with fibres and fillers until the cross-linking starts occurring and forming gelation. Around this temperature (145°C for unsaturated polyester resin), the resin starts curing into solid plate slowly preventing the viscous flow. Figure 3.4 shows the hot press machine for curing the dough. The procedure for compression moulding is as follows:

Figure 3.4: Hot Press Machine

1) The pressure and temperature of the hot press machine is set to 100 bar and 145°C.
2) The dough is divided into 4-5 equal parts (usually around 500-600 g each).
3) The upper and lower moulds of the hot press machine are layered with stearate compound to facilitate easy removal of the composite plate from the lower mould.
4) The standard time for curing the dough is 6-7 minutes, after which the plate is pulled out from the lower mould. Figure 3.5 shows four different cured plates.

Post Production

After the bio composite doughs are cured into plates, they are cut into smaller test samples using water jet cutting. The dimensions of the cut samples are in accordance with ISO 14125 (1998), which is also the standard used to conduct flexural tests of fibre reinforced plastics and BMC specifically. The test samples are tested for their flexural properties according to ISO 14125 (1998), using a 3 point bend test and an average of five values are calculated. The stress strain curves and results of samples are shown in Appendix A.

3.2 Rule of Mixtures

Experimental Procedure

(a) Calcite plate

(b) Lignocellulosic 1 plate

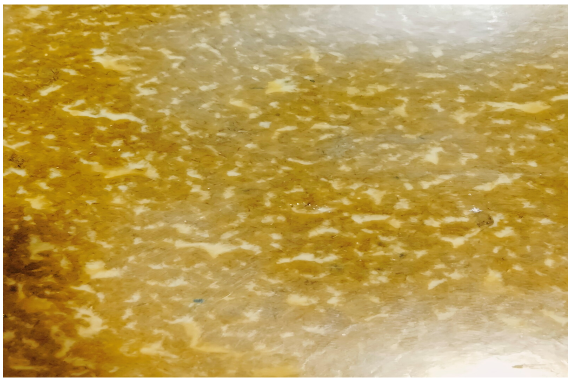

(c) Lignocellulosic 2 plate

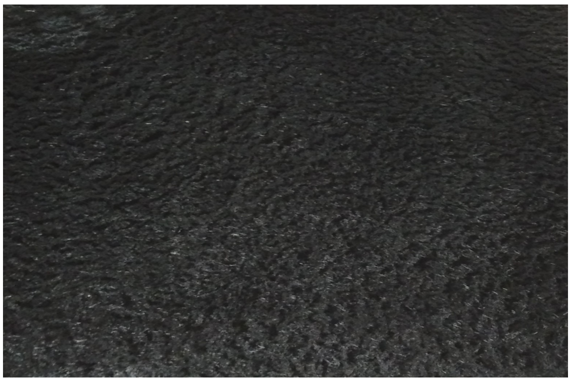

(d) Waste based filler plate

Figure 3.5: BMC plates post curing in the hot press machine

The experiments have been designed to test the agreement between the values obtained from the rule of mixtures model and the experimental values. To determine the predictions of filler/fibre reinforced system or a multi-filler/fibre reinforced system which are ternary and quaternary phased system, a binary phase system has to be designed initially which has to be in agreement with the theoretical values as the rule of mixtures models deals with only a binary phase system, involving a matrix and a reinforcement (filler or a fibre). There is no single model which deals with matrix, filler and randomly arranged short fibre together. Hence, the binary phase composites are made first followed by cascading of the binary models to form a multiphase component system.

The binary phase system consists of:

a) The matrix and the filler
b) The matrix and the fibre

A different approach is taken in the production of the binary phase system as compared to section 3.1 due to two challenges.

1) The matrix/filler or matrix/fibre system is not mixed in the Z blade mixer. This is due to the fact that the low viscosity of the matrix and filler causes difficulties in getting the dough out of the

mixer and cleaning it.
2) The hot press machine at 100 bar used for ternary and quaternary system cannot be used for the binary system. This is due to the fact that at such high pressure, the low viscosity dough will flow out of the mould, contaminate the lab and causing unnecessary delays in the experiments.

Figure 3.6: Low Pressure Hot Press Machine

Hence, a different approach has to be taken in the production of the binary dough system which is as follows-

1) Table 3.3 shows recipes of filler (calcite) reinforced and a fibre (flax) reinforced polymer. Multiple ratios of calcite with respect to the matrix are mixed. This process is carried out for all fillers (calcite, lignocellulosic 1, lignocellulosic 2 and waste based filler). The same goes for both the fibres (flax, bamboo) as well. The mixing is done in a beaker with a spiral blade drill. The fillers/fibres are added in multiple batches in the beaker and mixed thoroughly till it is uniformly mixed.
2) Following this, the binary mixtures are cured in a lower pressure hot press machine figure 3.6 at lower pressure (50 bar).
3) The pressure and temperature for curing the mixtures are kept at 50 bar and 145°C for 6-7 minutes. To compare the theoretical and experimental values, a reference point is needed which is that of a matrix with no fillers/fibres. Hence, the matrix is cured at the same conditions to get a cured plate.
4) Since the mould provides a smaller plate, equivalent to the size of a test sample, there is no need to cut the plates into smaller samples but rather use the cured plate extracted from the mould to test for its flexural properties.
5) The flexural test standards are in accordance with ISO 14125 (1998), which is the similar to the conditions mentioned in section 3.1.

Table 3.3 provides an example recipe used for making the binary filler/fibre plates.

Ingredient	**Weight (g)**	**Weight fraction**
Unsaturated Polyester Resin	177.3	0.349
Hardener	2.7	0.005
Releasing Agent	12.8	0.025
Plasticizer	12.8	0.025
Thickening agent	1.73	0.003
Calcite	300	0.591

Ingredient	**Weight (g)**	**Weight fraction**
Unsaturated Polyester Resin	177.3	0.716
Hardener	2.7	0.011
Releasing Agent	12.8	0.052
Plasticizer	12.8	0.052
Thickening agent	1.73	0.006
Flax	40	0.162

Table 3.3: Example Recipes of Filler/Fibre reinforced polymer

Chapter 4

Rule of Mixtures Model Validation

This chapter deals with the comparison of theoretical model values of the binary, ternary and quaternary phase composites with its experimental results. For filler reinforced binary composites, the Lewis Nielsen model is selected as a potential model and is used compare the theoretical and experimental results. On the contrary, the Cox-Krenchel model is used to compare the results for fibre reinforced binary composites. The reason for this change in modelling is explained in section 2.2. The codes for both the models have been written in Matlab.

4.1 Binary Phase System

As explained in the previous paragraph, two separate models have been used to compare the results to filler reinforced and fibre reinforced composites respectively.

4.1.1 Filler Reinforced Composites

The Lewis Nielsen model 2.1 requires specific parameters to be characterized before the modulus of the composite (E_c) can be calculated. The characterization of the particles can determine the aspect ratio of the filler reinforcements. This has been done using a tabletop Scanning Electron Microscope (SEM). Figure 4.1 shows the microscopic images of the filler reinforcements. These images provide an approximate aspect ratio of the filler reinforcements.

The images of particles under observation are of irregular sizes and shapes, as seen in figure 4.1. Apart from this, since a small sample size of the fillers is characterized, the aspect ratio obtained from these microscopy images cannot be considered accurate. Therefore, an approximate value has to be considered initially by comparing the figures and table 2.6, followed by tweaking this approximate value to fit the theoretical curve. For example, the microstructure of calcite shown in figure 4.1 a is irregular in shape but more spherical than a fibrillar structure. On the other hand, lignocellulosic 1 and lignocellulosic 2 are shown in figure 4.1 b and c have similar microstructures, probably slightly higher aspect ratio. Hence, the value of 'A' is kept somewhat in a similar range for all the fillers. Also, waste based filler particles have irregular sizes and shapes with varying aspect ratios (shown in figure 4.1 d).

It is difficult to determine the modulus of a filler particle (E_f) experimentally because of the irregular particle size and shape distribution. Hence, their bulk modulus can be determined and used to

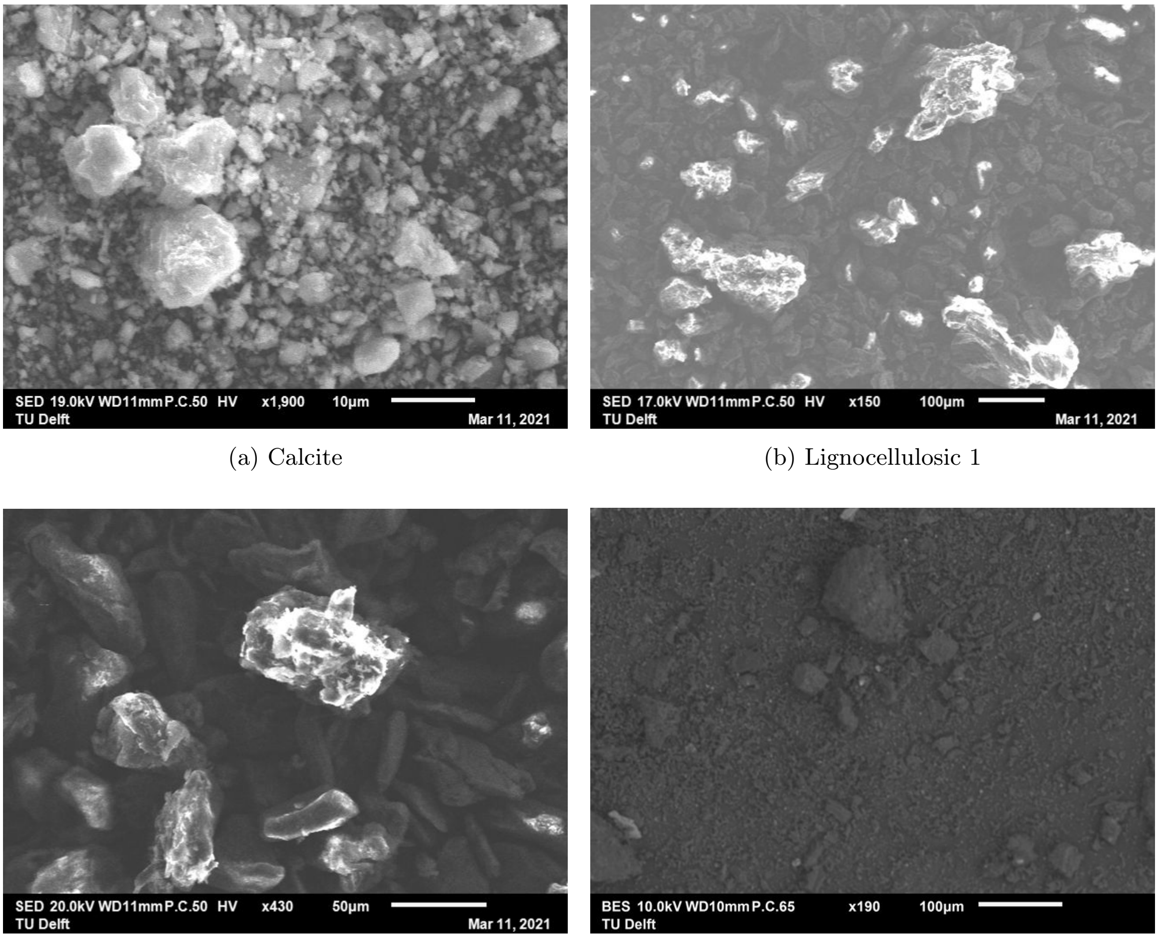

(a) Calcite

(b) Lignocellulosic 1

(c) Lignocellulosic 2

(d) Waste based filler

Figure 4.1: SEM images of the filler reinforcements

get an approximate value of E_f, for example, determining the modulus of a piece of calcite rock, lignocellulosic 1 or lignocellulosic 2. A detailed literature study can also provide an approximate value of the mechanical properties of these inorganic and lignocellulosic fillers. The approach taken in this thesis is to vary the filler modulus to fit the experimental points in combination with the literature study, thus eliminating the possibility of unrealistic values. Waste based filler is a relatively novel particle reinforcement because it has only been used as fertilizer until now. Only in the past few years have there been attempts to use waste based filler as a composite reinforcement. Its mechanical properties, such as modulus, strength porosity, etc., depend on its source (agricultural/forestry waste) before pyrolysis, the temperature at which it is pyrolyzed, and other processing conditions. The waste based filler provided by Torrgas has different source and processing conditions compared to the studies done earlier, leaving the properties incomparable. Hence, the E_f for waste based filler has to be assumed and altered based on fitting and agreement with the experimental points.

The matrix modulus (E_m) constituting unsaturated polyester resin, hardener, releasing agent, and

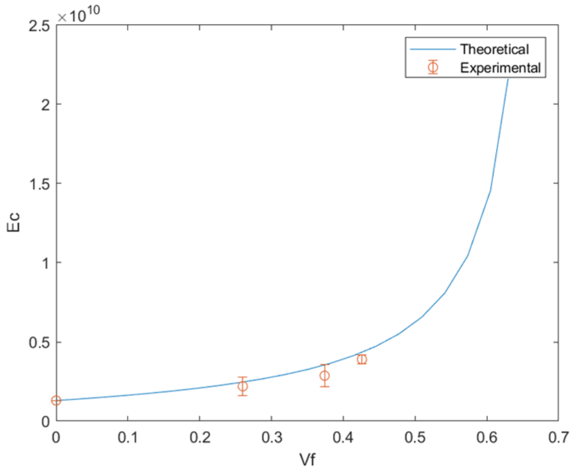

(a) Calcite

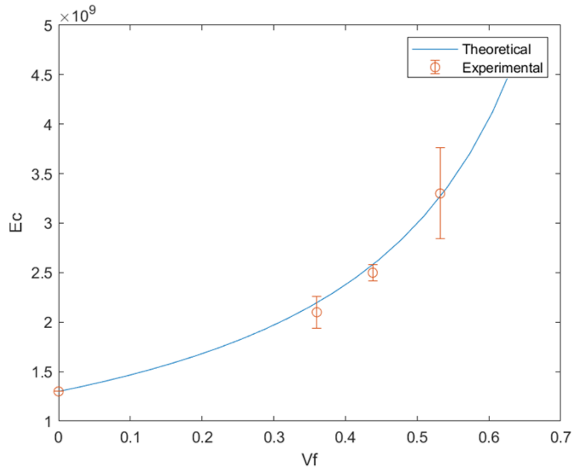

(b) Lignocellulosic 1

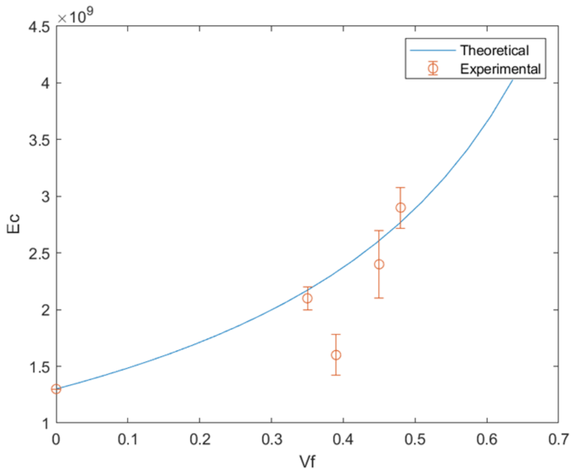

(c) Lignocellulosic 2

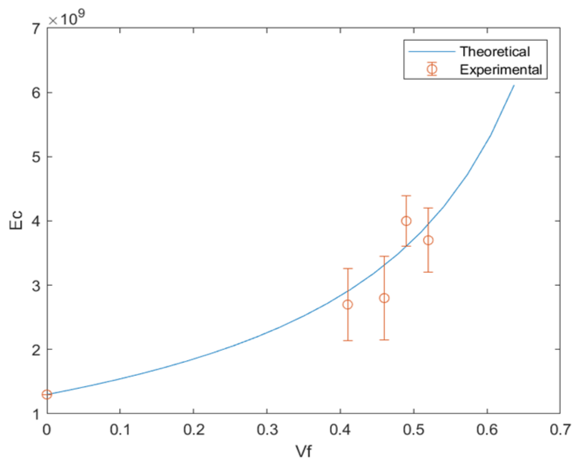

(d) Waste based filler

Figure 4.2: Theoretical vs Experimental data comparison of the fibre reinforced composites (binary phase)

the additive is experimentally tested and determined in chapter 3. The maximum packing fraction depends on the type of filler reinforcements added, and its value can be obtained from Table 2.6.

Theoretical vs Experimental Comparison

For accurate comparison, the chemical constituents of the composite which are measured using weight fraction have to be converted to volume fraction. Table 4.1 shows an example of the weight to volume fraction conversion procedure.

Ingredient	Weight (g)	Density (g/cc)	Volume (cc)	Volume Fraction (V_f)
Unsaturated Polyester Resin	177.3	1.1	161.18	0.64
Hardener	2.7	1.04	2.59	0.01
Releasing Agent	12.8	1.1	11.64	0.04
Plasticizer	12.8	1.26	10.16	0.04
Thickening Agent	1.73	3.58	0.48	0.01
Filler	175	2.7	64.81	0.26
Total	382.33		250.86	

Table 4.1: Weight to Volume fraction conversion

The experimental results are compared with the theoretical curve for each binary system as shown in the figure 4.2.
Figure 4.2 provides a theoretical curve that is in excellent and impressive agreement with the experimental values. The graph represents the modulus of the composite (E_c) with respect to the volume fraction. As mentioned in the earlier paragraphs, the filler modulus and aspect ratio and hence 'A' have been varied to provide a realistic value and fit the experimental points. About 3-4 experimental points have been considered for each case. The last point in each case is the maximum loading possible for that particular filler in the premix. Beyond this point, the dough becomes dry and clumpy.

Filler	Filler Modulus E_f (GPa)	A	Maximum Packing Fraction (ϕ_f)
Calcite	30	1.58	0.637
Lignocellulosic 1	5.3	1.8	0.637
Lignocellulosic 2	4.8	1.6	0.637
Waste based filler	7.5	1.6	0.637

Table 4.2: Parameters for individual fillers in binary phase system

Table 4.2 above shows the parameters considered for fillers in each binary system.The aspect ratio and filler modulus chosen for each system is the value which best fits the experimental line. The maximum packing fraction is the taken from table 2.6 after observing its size and shape obtained by SEM analysis.

To analyze which filler has the best fitting, a linear regression analysis is run and the R^2 value is compared as shown in table 4.3.

Analysis and comparison of different filler based composites shown in table 4.3 shows that calcite based composite has the best curve fitting as compared to lignocellulosic 1, lignocellulosic 2 or waste based filler. With a R^2 value of 0.99, the regression analysis states that 99% of the variance of the dependent variable being studied is explained by the variance of the independent variable. As for the other fillers, lignocellulosic 1 and waste based filler have good curve fitting too. Lignocellulosic

Filler reinforced composite	**Coefficient of determination (R^2)**
Calcite reinforced composite	0.99
Lignocellulosic 1 reinforced composite	0.98
Lignocellulosic 2 reinforced composite	0.76
Waste based filler reinforced composite	0.97

Table 4.3: Liner Regression analysis of filler reinforced composites. Comparison of R^2 values of different filler reinforced composites to compare and analyze which filler based composite provides best fitting

2, on the other hand, although having a good fit, does not perform well as compared to the other three fillers. The reason for this is due to the outlier experimental point observed in figure 4.2 (c). The R^2 value can be improved by performing the repeating the experiment or taking a larger data set. Nevertheless, the current regression analysis performed implies calcite based composite is the best fitted model.

4.1.2 Fibre Reinforced Composites

The Cox-Krenchel theory (2D and 3D isotropic) equation 2.7 is used to obtain the theoretical curve for fibre reinforced composites. The unknown variable in the isotropic equations is the efficiency factor or the fibre orientation factor, which has to be varied to fit the curve with the experimental results. Due to the comparable values of fibre length (5-6 mm) and plate thickness (4-5 mm) and the randomly arranged fibres in the plate having different fibre orientations, the efficiency factor can be varied between ($1/5 \leq \eta_0 \leq 3/8$). Since the fibre length is around 5mm (flax) to 6mm (bamboo) and the thickness plate is around 4-5mm (varies from plate to plate), a lot of the fibres are going to be around the 2D plane, whereas a lot around the 3D. Hence, the efficiency factor must be varied accordingly to fit the curve to the experimental data points. The value of fibre modulus has been determined by a literature review and slight tweaking of the values to fit the experimental points.

An approach similar to the filler reinforced composite has been taken to convert weight fraction to volume fraction. The theoretical versus experimental graph comparison for flax and bamboo fibre can be observed in figure 4.3. Similar to the filler reinforced composites, a good fitting can be obtained between the theoretical curve and experimental points for fibre reinforced composites. The efficiency factor used for fitting the flax-based composite is 0.24, while that for bamboo fibre reinforced composite is 0.31. These values lie between the 2D and 3D efficiency values shown in the equation. The standard deviation observed in fibre reinforced composites is higher than filler reinforced composites. This can be due to the improper mixing of the fibres in the matrix. The sudden drop in the modulus of bamboo reinforced composite, as observed in figure 4.3 d) can be attributed to the fibre overloading in the matrix.

Analysis and comparison of the fibre reinforced composites in table 4.4 shows us that flax reinforced composite has better curve fitting than bamboo reinforced composites based on the regression analysis. A score of 0.97 in regression analysis means 97% of the data is accounted for and is explained by the model. Bamboo reinforced composite on the other hand has a R^2 of 0.84 which implies 84% of the variability of the dependent variable in the data set is accounted for and is fitted by the model. Although this is a good score, the curve fitting of flax fibre reinforced composite is better than the bamboo reinforced composite.

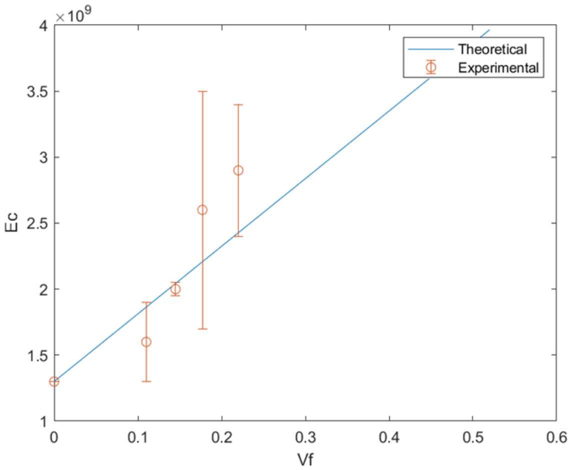

(a) Flax Fibre

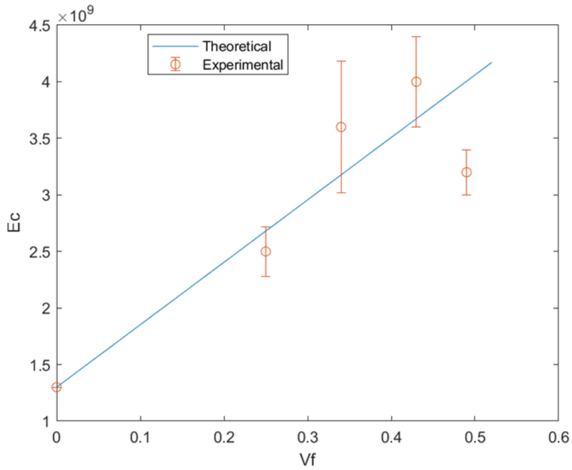

(b) Bamboo Fibre

Figure 4.3: Theoretical vs Experimental data comparison of the fibre reinforced composites (binary phase)

Filler reinforced composite	**Coefficient of determination (R^2)**
Flax reinforced composite	0.97
Bamboo reinforced composite	0.84

Table 4.4: Liner Regression analysis of fibre reinforced composites. Comparison of R^2 values of different fibre reinforced composites to compare and analyze which fibre based composite provides best fitting

4.2 Ternary and quaternary phase system

Following the excellent fitting of the theoretical curve with the experimental graph for the binary system, a combination of models (Lewis Nielsen + Cox-Krenchel) is then tested to determine the accuracy of a multiphase system involving mono/bi filler and a fibre system. The Lewis Nielsen model is applied to calculate and determine the filler-reinforced polymer, followed by using the obtained modulus as the matrix modulus for the Cox-Krenchel model. For example, in the case of an equal weight fraction of calcite and waste based filler written as Calcite/Waste based filler (50/50) and flax as the fibre reinforcement, the weight fraction is converted into volume fraction as shown in Table 4.5

Combination of the Lewis Nielsen and Cox-Krenchel models

Considering the example of Calcite/Waste based filler (50/50) Bamboo shown in table 4.5, figure 4.4 shows the sequence adopted to combine the models and obtain the final composite modulus value (E_c) which consists of two fillers and a fibre.This is done in three stages, using equation 2.1 and 2.7:

Composition	Weight (g))	Density (g/cc)	Volume (cc)	Volume fraction (V_f)
Unsaturated Polyester Resin	886.5	1.1	805.91	0.352
Hardener	13.5	1.04	12.98	0.006
Releasing Agent	64	1.1	58.18	0.025
Plasticizer	64	1.26	50.79	0.022
Thickening Agent	9	3.58	2.51	0.001
Waste based filler	650	1.1	590.91	0.258
Calcite	650	2.7	240.74	0.105
Bamboo	525	1	525	0.229
Total	2862		2287.03	

Table 4.5: Weight to Volume fraction conversion

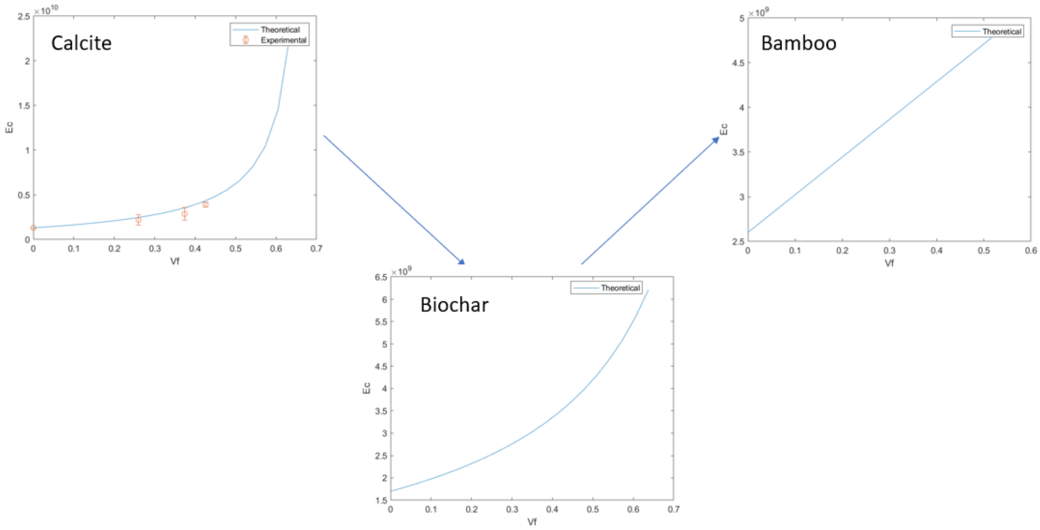

Figure 4.4: Analytical models addition sequence

Stage 1
The parameter values determined for calcite and the matrix shown below are substituted in Lewis Nielsen equation 2.1:
Matrix modulus (E_m) = 1.3 GPa
Derived from aspect ratio (A) = 1.58
Calcite modulus (E_f) = 30 GPa
Maximum packing fraction (ϕ_{max}) = 0.637
Volume Fraction (V_f) = 0.105
The composite modulus (E_{c1}) determined after substitution is 1.7 GPa.

Stage 2
The composite modulus (E_{c1}) determined in stage 1, now becomes the matrix modulus for stage 2.

The matrix modulus for stage 2 is hence matrix + calcite. The filler used for stage 2 is waste based filler.
The parameter values determined for waste based filler and the matrix shown below are substituted in Lewis Nielsen equation 2.1:
Matrix modulus $(E_m) = 1.7$ GPa
Derived from aspect ratio $(A) = 1.6$
Waste based filler modulus $(E_f) = 7.5$ GPa
Maximum packing fraction $(\phi_{max}) = 0.637$
Volume Fraction $(V_f) = 0.258$
The composite modulus (E_{c2}) determined after substitution is 2.56 GPa.

Stage 3
The composite modulus (E_{c2}) determined in stage 2, finally becomes the matrix modulus for stage 3. The matrix modulus for stage 2 is hence matrix + calcite + waste based filler. The fibre used for stage 3 is bamboo.
The parameter values determined for calcite and the matrix shown below are substituted in Cox Krenchel equation 2.7:
Matrix modulus $(E_m) = 1.7$ GPa
Efficiency factor $(\eta_0) = 0.31$ Calcite modulus $(E_f) = 22$ GPa
Volume Fraction $(V_f) = 0.229$
The composite modulus (E_c) determined after substitution is 3.6 GPa.

The experimental modulus obtained for this composite is 3.8 GPa, which denotes approximately a 5% difference compared to the theoretical value. This shows a great and impressive agreement between both the results.

A similar approach has been taken for several composites made with different ratios of fibres and fillers with respect to each other. Table 4.6 shows a comparison between theoretical and experimental values for several composites made.

Composite	Theoretical (GPa)	Experimental-50 bar (GPa)	Experimental-100 bar (GPa)	Theoretical-100 bar (GPa)
Calcite/Waste based filler(50/50) Flax	3.6	3.8	6.2	5.7
Calcite/Waste based filler(50/50) Flax	4.2	4.6	7.2	5.9
Calcite (100) Bamboo	4.3	5.2	8.1	7.8
Lignocellulosic 1 (100) Flax	3.7	4.5	4.1	4.6
Calcite/Waste based filler(25/75) Flax	3.3	3.2	4.9	5.6
Calcite/Lignocellulosic 2(75/25) Bamboo	3.8	4.1	7.1	5.1
Calcite/Lignocellulosic 1 (53/47) Flax	3.21	3.45	6.5	5.6
Calcite/Lignocellulosic 1 (23/77) Flax	2.78	3.1	5.4	5.5
Calcite/Lignocellulosic 1 (25/75) Bamboo	3.1	3.25	5.2	5.3
Calcite/Lignocellulosic 1 (78/22) Bamboo	3.7	4.5	7.8	6.1
Calcite/Lignocellulosic 2(75/25) Flax	2.9	3.12	6.2	5.6
Calcite/Lignocellulosic 2(12/88) Flax	2.55	2.45	4.4	4.4
Calcite/Lignocellulosic 2(35/65) Bamboo	3.04	2.71	5.4	5.1
Calcite/Lignocellulosic 2(89/11) Bamboo	2.85	3.06	6.9	5.4
Calcite/Waste based filler(35/65) Flax	3.1	3.25	5.3	5.3
Calcite/Waste based filler(69/31) Bamboo	3.3	3.05	8	6.1

Table 4.6: Theoretical and Experimental Modulus comparison

Calcite/Waste based filler (50/50) Bamboo states that equal ratios of Calcite and Waste based filler are added to the matrix and the fibre used is bamboo. Hence, this becomes a quaternary phase system with two fillers and one fibre. The other composites have to be interpreted in the same way.

For reasons mentioned in chapter 3, the experiments for the analytical models have been carried out at 50 bar pressure. This, however, is half of the conventional pressure used for a filler/multi-filler fibre system at NPSP but carried out to maintain the same uniform pressure as was used for the binary phase system. This, however, leads to the modulus values at 50 bar being lower than the matters at 100 bar pressure because the fibres and fillers are not pressed to form a closed packing system, leading to the inadequate consolidation of the fibres and fillers with the matrix and formation voids.
To compare the theoretical and experimental results from a linear regression perspective, a scatter graph is plotted.

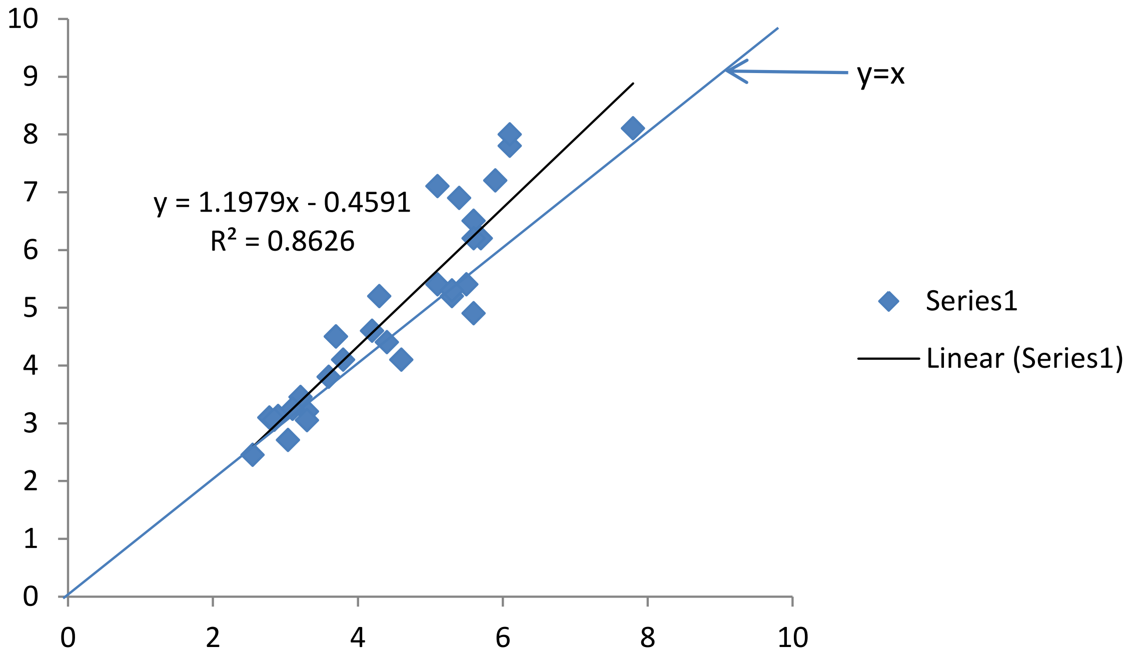

Figure 4.5: Scatter Plot for Theoretical vs Experimental Comparison

Figure 4.5 provides a comparison of theoretical and experimental results obtained from table 4.6. A simple linear regression analysis of the plot can be done on MS Excel as shown in figure 4.6. The graph shows cumulative 50 and 100 bar experimental data points on the x-axis and theoretical data on the y axis data points on the x-axis. The blue line represents the linear graph y=x and while the black trendline represents the equation of scatter plot y = 1.1979x - 0.4591. The ideal case scenario requires the black trendline to be y = x too, which agrees with theoretical and experimental results. But this is not the case as there is a deviation between the results. The linear regression analysis provides us with the R^2 (coefficient of determination) value which comes up to roughly 0.87 which is a good score stating that the model fits the data well. A score of 0.87 means that 87% of the variability of the dependent variable in the data set is explained by the regression model and is accounted for. The rest 13% of the variability cannot be explained by the model and is unaccounted for. The standard deviation obtained is within the 95% confidence level, as it can be observed from figure 4.6. The y=x is in the 2 σ bounds within the boundary, but scarcely. Thus, it is fair to say that the theory works well but slightly underestimates the experimental data, presumably due to synergistic effects (uniform interactions between resin, fillers and fibres combined, result in higher modulus values than individually calculated via cascading of the models). It can also be due to minor inaccuracies while performing the experiments themselves. But overall, the theory works well and provides approximate results.

SUMMARY OUTPUT

Regression Statistics	
Multiple R	0.9284065
R Square	0.8619387
Adjusted R Square	0.8573366
Standard Error	0.631861
Observations	32

ANOVA

	df	*SS*	*MS*	*F*	*Significance F*
Regression	1	74.77710219	74.7771	187.2947	1.95413E-14
Residual	30	11.97744781	0.399248		
Total	31	86.75455			

	Coefficients	*Standard Error*	*t Stat*	*P-value*	*Lower 95%*	*Upper 95%*	*Lower 95.0%*	*Upper 95.0%*
Intercept	-0.461425	0.405701614	-1.13735	0.264395	-1.28997779	0.367129	-1.28997779	0.36712867
X Variable 1	1.1994774	0.087645431	13.68557	1.95E-14	1.020481579	1.378473	1.02048158	1.37847328

Figure 4.6: Linear Regression Analysis of the Scatter Plot

Although the model provided good results for stiffness calculation, strength is a difficult parameter to model in general. On one hand, stiffness within reasonable limits, has more or less uniform behaviour. Strength on the other hand, is sensitive to the process of mixing, wetting or the lack of wetting, slight differences in surface chemistry. Other than mixing process, minor changes in the curing conditions (pressure conditions, temperature and curing time) too, affects strength values incredibly. Also, addition of minor amounts of additives can vary the strength by a considerable amount. Additionally, no universal theories exist because materials strength in case of composites is determined by the onset of fracture and not via a yielding mechanism. Hence, strength modelling usually only has a chance within a well defined, limited, formulation space.

4.3 Recommendations

As mentioned earlier, the model, although pretty approximate, still slightly underestimates the experimental results. A major challenge faced is the cascading of the Lewis Nielsen model twice, causing problems in calculating the maximum packing fraction of the fillers. The maximum packing fraction is a parameter that is not tweaked in the Lewis Nielsen equation and is cumulative. For the case of (matrix + filler A + filler B) + fibre, if the maximum packing fraction is 0.64 and hypothetically add 0.33 fraction of filler A in the matrix, it's not possible to add 0.63 fractions of filler B in the new matrix (resin + A), causing complications at higher volume fractions. The cumulative addition of both the fillers should give a maximum packing fraction of 0.64. Neglecting this theory is what causes the model to underestimate the experimental results. A way to tackle this challenge is to use the Lewis Nielsen model once by combining the parameters of both the fillers. In this scenario, a common aspect ratio can be chosen as they are more or less similar for all the fillers. The maximum packing fraction is taken as 0.64. The challenge faced here is to find a way to add or extrapolate the modulus values for the two fillers. Another way is to nest the Lewis Nielsen and Halpin-Tsai model together to get multi-component systems. Halpin-Tsai model does not include a maximum packing fraction, so combining these models and finding a solution to fit the theoretical curve with the experimental results in a better way can be possible. The way of doing it is still unclear as cascading of analytical models has never been done before, and hence the problems arising from it are novel. Therefore, it seems like a good recommendation to be studied in the future.

Chapter 5

BMC Optimizer Model Validation

The BMC Optimizer model which is a proof-of-concept optimization model is based on Bayesian Optimization. This model is tested in this chapter. After designing the training set for the model as discussed in chapter 3, the next step is to create a database consisting of the recipes of the composites made and their mechanical properties (flexural modulus, flexural strength and density).

5.1 Model Explanation

Figure 5.1 covers the process applied to determine optimized predictions from the model. The steps below are a brief description of the process:

1) The first step is to manufacture and test bio-based composite plates of different ratios of fillers and fibres, as discussed in chapter 3.

2) The next step is to create a database of recipes and properties discussed in step 1 in an Excel file, as shown in table 5.1. This database essentially acts as a training set used as input for the model divided into input (bio-based composite recipes) and output (flexural modulus, flexural strength and density) columns.

3) It is essential to set the weight and polarization values for each output parameter/mechanical property. The weight value controls the importance of each individual property for the weighted sum of single objective loss function while the polarity value controls if the property has to be maximized or minimized. Both these values will be explained in detail later.

4) Next, the desired fibre and filler are selected from the database, followed by the desired number of recipes. The model can generate up to 6 recipes based on the output score calculated. The parametrized loss function or the output score is essentially the difference between the expected output and the current output of the algorithm. The optimization problem in this study seeks to minimize this expected loss. The process of defining the loss function for this study will be discussed later in this chapter.

5) Finally, the Bayesian optimization process begins. Initially, a Gaussian Process surrogate model is constructed with an RBF kernel, including the input data and output scores. An 'Expected Improvement' (EI) acquisition function is then prepared and optimized. Following this, the model provides the recommended recipe/recipes for the next set of experiments. The entire model is coded in Python.

6) Once the recommended composites are made and tested, the results are analyzed, the database is updated for performing the next iteration.

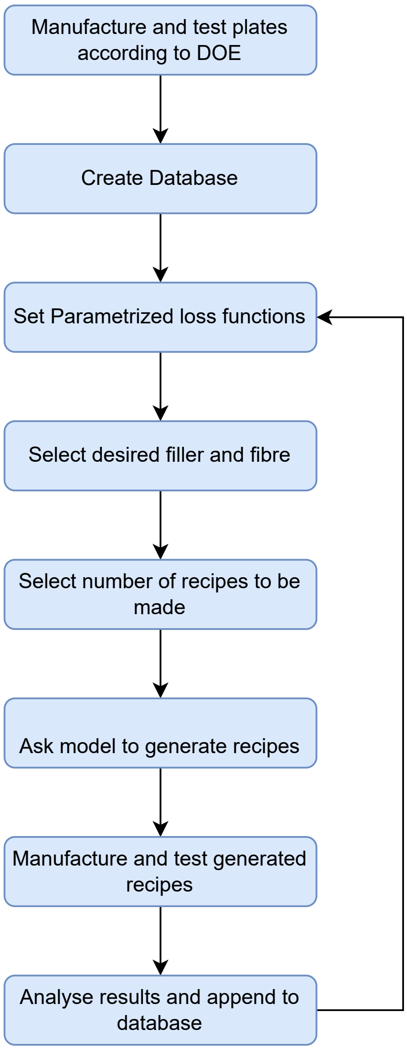

Figure 5.1: BMC Optimization model Flowchart

A	B	C	D	E	F	G
name	**type fiber**	**type filler**	**fiber ratio**	**filler ratio**	**dry ratio**	**plasticizer**
Calcite100%-Flax	Flax	Calcite	0.0925	0	0.5671	0
CalWas(75/25)-Flax	Flax	Waste based filler	0.0925	0.25	0.7141	0
CalWas(50/50)-Flax	Flax	Waste based filler	0.15	0.5	0.5673	0
CalWas(40/60)-Flax	Flax	Waste based filler	0.15	0.6	0.5673	0
CalWas(25/75)-Flax	Flax	Waste based filler	0.1075	0.75	0.6678	0
CalWas(14/86)-Flax	Flax	Waste based filler	0.0995	0.86	0.6926	0
Was100%-Flax (44wt%)	Flax	Waste based filler	0.1169	1	0.6387	0
Was100%-Flax (40wt%)	Flax	Waste based filler	0.1515	1	0.7272	0
CalLig1(88/12)-Flax	Flax	Lignocellulosic 1	0.1111	0.12	0.7272	0
CalLig1(75/25)-Flax	Flax	Lignocellulosic 1	0.0925	0.25	0.7141	0
CalLig1(71/29)-Flax	Flax	Lignocellulosic 1	0.0808	0.29	0.7272	0
CalLig1(57/43)-Flax	Flax	Lignocellulosic 1	0.1111	0.43	0.7272	0
CalLig1(50/50)-Flax	Flax	Lignocellulosic 1	0.0889	0.5	0.6866	0
CalLig1(45/55)-Flax	Flax	Lignocellulosic 1	0.15	0.55	0.5673	0
CalLig1(39/62)-Flax	Flax	Lignocellulosic 1	0.1026	0.62	0.683	0
CalLig1(23/72)-Flax	Flax	Lignocellulosic 1	0.1151	0.72	0.6444	0
CalLig1(25/75)-Flax	Flax	Lignocellulosic 1	0.131	0.75	0.595	0
Lig1(100%)-Flaxvol	Flax	Lignocellulosic 1	0.0925	1	0.5671	0
Lig1(100%)-Flax	Flax	Lignocellulosic 1	0.0925	1	0.5674	0
CalLig2(86/14)-Flax	Flax	Lignocellulosic 2	0.0925	0.14	0.7141	0
CalLig2(75/25)-Flax	Flax	Lignocellulosic 2	0.0925	0.25	0.7141	0
CalLig2(68/32)-Flax	Flax	Lignocellulosic 2	0.1492	0.32	0.5155	0
CalLig2(50/50)-Flax	Flax	Lignocellulosic 2	0.202	0.5	0.7272	0
CalLig2(47/53)-Flax	Flax	Lignocellulosic 2	0.0808	0.53	0.7272	0

Table 5.1: An Excel database example of the input (weight ratios of different components of the composite) parameters.

H	I	J	K
testable?	density	stiffness	flex. Strength
yes	1.43	1800	40.6
yes	2	2800	39.6
yes	1.63	3800	36.9
yes	1.63	4800	40.3
yes	1.78	5800	31.8
yes	1.98	6800	36.6
yes	1.64	7800	29
yes	2.11	8800	33.1
yes	1.97	6600	40.7
yes	2.15	7600	43.9
yes	2.18	9800	45.14
yes	2.15	9400	40
yes	1.96	10400	48
yes	1.02	11400	37.4
yes	2.09	12400	45.2
yes	2.02	13400	44.5
yes	1.43	14400	36.6
yes	2	15400	35.3
yes	1.63	16400	31.9
yes	1.63	17400	40.8
yes	1.78	18400	39.2
yes	1.98	19400	37.6
yes	1.64	8500	36.3
yes	2.11	7600	44.4

Table 5.2: An Excel database example of the output parameters (mechanical properties of the bio-based composites.

Tables 5.1 and 5.2 show an example of a database used for the model as the actual recipes are not being shared for confidential purposes. Columns B to G are the input columns that describe the composites' composition. Columns B and C store the types of fibre and filler used. Columns D, E and F store the input parameter values as a three-dimensional search space. For this study, the dimensionality and search space boundaries is determined to express the bio-based composite recipes as an optimization problem. The search space scales up exponentially with respect to the dimensionality of the problem, which is referred to as the curse of dimensionality [129]. This dimension increase is a disadvantage since manufacturing bio-based composites is extremely expensive; hence, a massive search space is not favourable. Many input parameters have thus been clustered together to reduce the total number of parameters/dimensions and, in turn, reduce the search space. They are the fibre ratio, filler ratio and dry ratio of the composite. Figure 5.2 is a visual representation of how the three input parameters are set up.

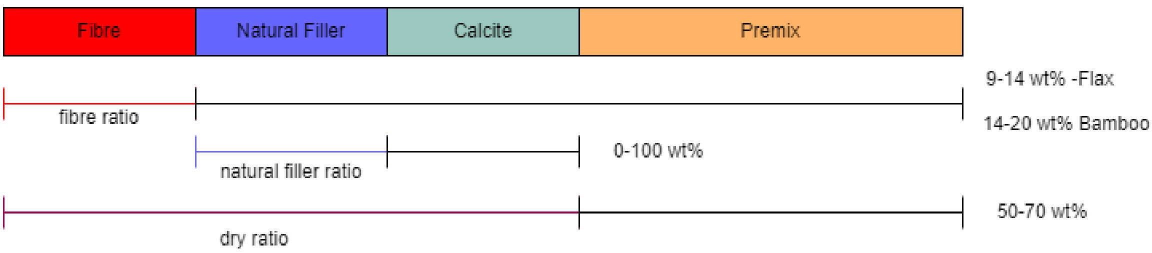

Figure 5.2:
A visual representation of how the three input parameters of the bio-based composites set up. The premix composition remains constant.

Column D stores the weight fraction of the fibre. The recommended upper and lower bounds for flax and bamboo fibres are different for reasons mentioned earlier (related to the physical and chemical characteristics of the fibre). For flax fibres the recommended range is around 9-14 wt% and that for bamboo is around 14-19 wt% as it can be observed in figure 5.2. These ranges are determined by the initial set of experiments performed and the company's previous experience and knowledge. Column E stores the ratio of the filler concerning calcite. This ratio will vary from 0 (no natural filler) to 1 (only natural filler). As mentioned earlier, calcite is strong and inexpensive but heavy and brittle, hence aimed to be reduced if not replaced. Finally, column F stores the dry ratio, the total weight fraction of all the fillers and fibres added. The dry ratio's range is kept from 50 - 70 wt%. Lower than this range makes the dough wet and less viscous and vice versa.

If the plate has not formed correctly and cannot be tested, it is treated as an outlier, and column G is filled accordingly. Adding outliers aids the elimination of any search done by the model in that region. Columns H to K are the output columns that describe the mechanical properties of the bio-based composites and act as the output parameters while calculating the single objective output score. For this thesis, NPSP focuses on the flexural properties and the density of the composite. So the impact properties and the elastic modulus are ignored.

Single Objective Output Score

The BMC Optimizer is created for single objective optimization. The multiple output parameters (in this case the objective scores) are reduced to a single objective output score by constructing a weighted objective score. The parameters of the loss functions in this case the output scores are the weight and polarization values given to the output parameters. Polarization value determines whether to maximize or minimize that parameter, and weight value determines the influence a parameter has on the overall output and the recommended recipe. Higher weight values dominate and have a greater influence than lower weight. If, for example, a stiff, strong and lightweight plate is considered with more emphasis given to the stiffness followed by strength and density, table 5.3 shows an example of the parameters defined for the output score. Density has to be minimized; hence a polarization value of 0 is given to it, whereas modulus and strength are maximized; thus, polarization value is 1. Weight values, as mentioned earlier, more weightage/priority has been shown to modulus (1), followed by strength (0.7) and finally density (0.4).

	Density	**Flexural Modulus**	**Flexural Strength**
Weight value (ω)	0.4	1	0.7
Polarization value (a)	0	1	1

Table 5.3: Example of parameters defined for output score. An example which shows the weight and polarity values set for each output parameters. These values will be used in the equation to calculate the output score.

The equation used to calculate this single objective output score is

$$s_i = \frac{\sum_{j=0}^{d} \omega_j \left| a_j - \dfrac{y_i^j - y_i^{\min}}{y_i^{\max} - y_i^{\min}} \right|}{\sum_{j=0}^{d} \omega_j} \tag{5.1}$$

s_i in equation 5.1 denotes the overall output score, which includes output score of flexural modulus, strength and density. $\vec{y}_i = (y_0, ..., y_d)_i$ considered is a vector consisting of 'd' number of mechanical properties of a bio based composite i. Out of the total number of composites in the datasheet, only λ number of composites which have the same fibre and filler combinations are considered. Every element in $\vec{y}_i$ is normalized for the maximum and minimum values as described in equations 13 and 14

$$y_i^{\max} = max(y_i^0, ..., y_i^\lambda) \tag{5.2}$$

$$y_i^{\min} = min(y_i^0, ..., y_i^\lambda) \tag{5.3}$$

ω_j stores the weight value for each mechanical property $\vec{\omega} = (\omega_0, ..., \omega_d)$, while 'a' stores the polarization value for each mechanical property $\vec{a} = (a_0, ..., a_d)$. The output score of the mechanical properties are added and the final output score is calculated.

5.2 Results and Discussion

After obtaining the single objective output score and entering the number of recipes to be made, the model generates recipes for the desired natural filler and fibre. Similarly, recipes have been generated for every natural filler and a natural fibre combination. Two different sets of loss function parameters have been used for each bio-filler/fibre combination, and one recommended recipe has been made for each loss function parameter. One such filler/fibre combination is explained below, involving calcite and lignocellulosic 2 as the fillers and flax as the fibre. Figure 5.3 depicts the mechanical

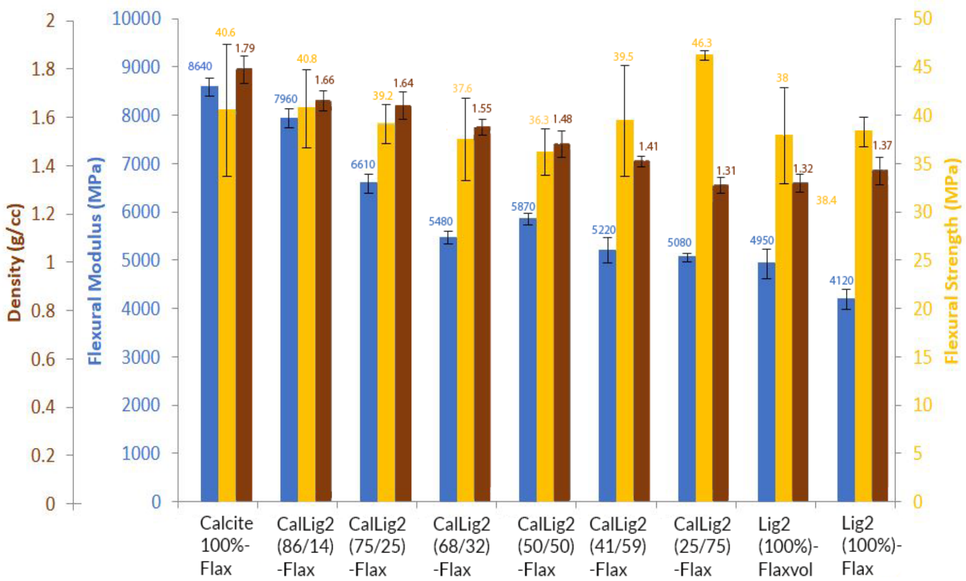

Figure 5.3: Results from Design of Experiments/ Model Training Set. The flexural modulus is shown in blue, flexural strength in yellow and the density in brown. The mechanical properties results obtained along with the error bars for each recipe is denoted as well.

properties of the training set before moving on to the test set. The trend for flexural modulus is as expected from the literature. Composites containing a higher calcite fraction have a higher modulus than those with a higher fraction of bio-filler. Flexural strength depends on a uniform dispersion and mixing of the natural fibres into the matrix. This facilitates a better bonding at the interface and improves bio-based composites' properties. Composites with optimal and better mixing of these fibres in the resin have higher mechanical properties. Calcite/Lig2 (25/75) has the highest flexural strength, which can be attributed to better mixing and dispersion of fibres while curing. Density depends mainly on the type of filler and the weight fraction of the total filler. The chosen fibres have a low density (1 g/cc), and varying the fibre percent between 9 and 14 weight% does not affect the thickness to a significant extent. Calcite has a higher density as compared to lignocellulosic 2, suggesting a decreasing trend in the density of the plates as the fraction of calcite in the plate decreases. Figure 5.3 confirms this, as a decreasing trend in density is observed as the lignocellulosic 2 fraction increases and calcite decreases. Lig2 (100 weight%) tends to have a higher weight fraction than Lig2 (100 volume%) due to a higher dry ratio in the former recipe than the latter.

First Iteration The objective functions chosen for the 1^{st} iteration are as shown in tables 5.4 and 5.5. There are multiple ways to define the single objective loss functions parameters and test the model. Determining the weight and polarity values depends on the application of the model. For the kind of research NPSP does, it is ideal for defining weight values that provide stiff, strong and lightweight composites in lesser iterations. Considering time and resources, the bio-based composites have an extremely expensive sampling process as it takes roughly a month or a bit more for one iteration (from dough making to curing to testing). Hence, trying out all possible weight and polarity values will be both time and resource expensive and beyond the thesis scope. Another part of NPSP is focuses on manufacturing composites according to the clients needs, which may for example, prefer a higher weight value of one parameter over the other and not have any focus on the third one at all. Hence, a better chosen approach for this study is to investigate if the model is robust to using different parameters of the output score. This approach allows us to test if Bayesian Optimization works if the weight and polarity values are altered for lesser iterations. Two sets of different loss function parameters are chosen. The recipes generated by the model for these parameters are analysed and compared to see if the change in mechanical properties is in accordance with the parameters defined. For the first iteration, the aim is to generate recipes providing stiff, strong and lightweight plates. The first recipe's highest priority is the flexural modulus, followed by flexural strength and then density. For the second recipe, the highest priority is the flexural modulus, followed by the density and flexural strength. The modulus weight value is kept constant for both cases, while strength and density are varied. Additionally, we can observe from tables 5.4 and 5.5 that the weight value of density for single objective parametrized loss function-2 is higher than that for single objective parametrized loss function-1. Contrarily, the weight value of strength for parametrized loss function-1 is higher than that of parametrized loss function-2. Ideally, the recommended recipe based on parametrized loss function-1 should have a higher density and strength than the recipe generated based on parametrized loss function-2.

	Density	**Flexural Modulus**	**Flexural Strength**
Weight value (ω)	0.6	1	0.7
Polarization value (a)	0	1	1

Table 5.4: Weight and Polarity values defined for single-objective parametrized loss function - 1

The model first calculates output score using equation 5.1, based on the above stated objective

	Density	Flexural Modulus	Flexural Strength
Weight value (ω)	0.8	1	0.6
Polarization value (a)	0	1	1

Table 5.5: Weight and Polarity values defined for single-objective parametrized loss function - 2

functions. These scores are shown in tables 5.6 and 5.7

Recipe	Output Score
Calcite100%-Flax	0.51
CalLig2(86/14)-Flax	0.48
CalLig2(75/25)-Flax	0.62
CalLig2(68/32)-Flax	0.72
CalLig2(50/50)-Flax	0.71
CalLig2(41/59)-Flax	0.58
CalLig2(25/75)-Flax	0.24
Lig2 (100%)-Flaxvol	0.61
Lig2 (100%)-Flax	0.68

Table 5.6: Output Score - 1 combining the cumulative loss functions of flexural modulus, flexural strength and density. The recipe marked red has the least output score indicating it is the most optimized in the training set for loss function parameters in table 5.4

Recipe	Output Score
Calcite100%-Flax	0.57
CalLig2(86/14)-Flax	0.51
CalLig2(75/25)-Flax	0.64
CalLig2(68/32)-Flax	0.70
CalLig2(50/50)-Flax	0.69
CalLig2(41/59)-Flax	0.54
CalLig2(25/75)-Flax	0.20
Lig2 (100%)-Flaxvol	0.56
Lig2 (100%)-Flax	0.62

Table 5.7: Output Score - 2 combining the cumulative loss functions of flexural modulus, flexural strength and density. The recipe marked red has the least output score indicating it is the most optimized in the training set for loss function parameters in table 5.5

From both the tables, we observe that calcite and lignocellulosic 2, with the ratio of 25:75 (Calcite/Lig2(25/75)-Flax), marked in red, has the lowest output score. This recipe is the most optimized in the given training set for the weight and polarity values mentioned in 5.4 and 5.5. The output scores shown in these tables are the final output scores (adding the output scores of flexural modulus, strength and density). By observing figure 5.3, it is evident that Calcite/Lig2(25/75)-Flax performs best in terms of flexural strength, good in terms of density and average in terms of flexural modulus. Therefore, this recipe receives the lowest cumulative score for particular loss parameter functions by calculating the output scores. CalLig2(68/32)-Flax has the highest output score indicating that it is the least optimized recipe. The reason for this is also evident from figure 5.3, where the recipe has low modulus and a high density, opposite of what the expected optimal recipe requires. However, these scores can change if we vary the weight and polarity values further. The model can recommend recipes anywhere in the search space for the first iteration that may or may not be near this recipe. It is still very early with a small training set for the optimizer to recommend highly optimized recipes. Ideally, the model requires a a more extensive training set of a few hundred iterations to recommend highly optimized recipes. The results after the first iteration are nonetheless impressive.

For every loss function parameter, 2-3 recipes are generated from which only one recipe is made. The reason for generating two or three recipes is that the model based on the weight and polarity values can sometimes generate recipes with higher calcite loading. One of the goals NPSP plans to achieve is to replace calcite with a lignocellulosic filler. So, testing out recipes with higher calcite content is not the right approach from the company's perspective if calcite is to be replaced soon. Also the current model is not equipped with boundary conditions for filler ratio with which it is possible to set upper and lower bounds of calcite. Hence, human interference is currently essential in the model to choose a recommended recipe. However, Bayesian optimization is a single-objective optimization. The optimization algorithm recommends a single optimized recipe. The accuracy will be affected by multiple recipes to be generated as the acquisition function is not updated until the current iteration is performed and tested. The approach taken to generate multiple recipes is using the 'constant liar' strategy. The constant liar strategy duplicates the surrogate model and documents the first generated recipe with a fake loss function with the lowest loss function within a 95% confidence interval. The updated model is rerun to develop the second recipe. This process is repeated for the number of additional recipes to be generated, which in our case is 2-3. The first recommended recipe might have a higher calcite loading out of the generated recipes. In contrast, the next one, which might be a less optimized recipe, has a higher natural filler loading, which the company needs. To reduce the human interference in choosing the recommended recipes in future, the model needs to be modified and improved in such a way that the natural filler to calcite ratio in the recipe can be set. Table 5.8 shows the human chosen recommended recipes given by the model for both the loss function parameters.

Objective Function	**Fibre Ratio**	**Filler Ratio**	**Dry Ratio**
Parametrized loss function - 1	0.1043	0.5306	0.5150
Parametrized loss function - 2	0.0771	0.8963	0.4976

Table 5.8: Recommended recipe for each set of loss function parameters

The recipes are chosen from the recommended list such that the natural filler loading is higher than calcite.

The recommended recipes are manufactured and tested for their mechanical properties, and the results are obtained as shown in figure 5.4. Using the same terms as the earlier experiments to denote

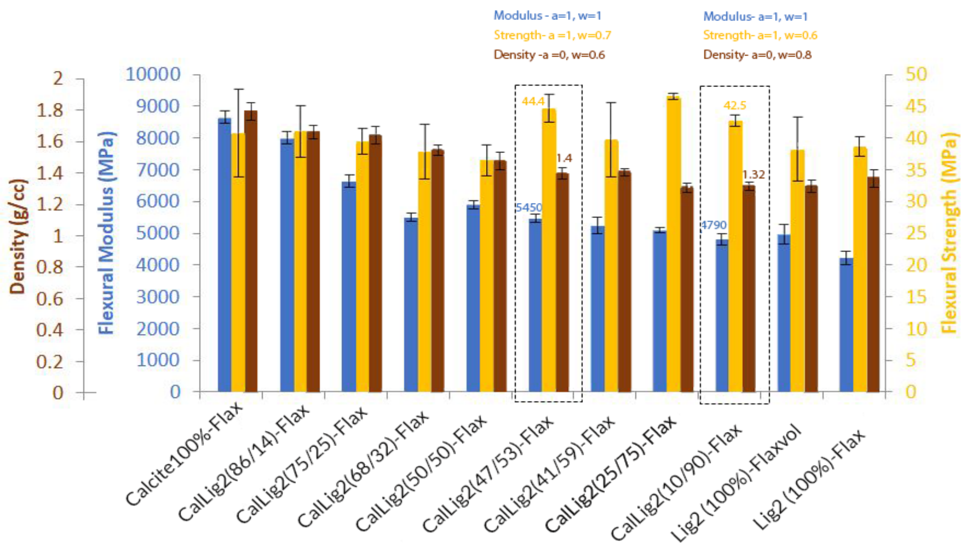

Figure 5.4:
Output Parameters results from training set and first iteration. The graphs for modulus, strength and density are plotted together. The columns in blue, yellow and brown denotes flexural modulus, strength and density respectively.

the composites, the composite derived from objective function 1 is Calcite/Lig2 (47/53)- Flax. The one derived from objective function 2 is Calcite/Lig2 (10/90)-Flax.

The graphs for modulus, strength and density are plotted together. The columns in blue, yellow and brown denotes flexural modulus, strength and density respectively. The results obtained from the first iteration are highlighted by dotted columns. In this graph, analyzing the strength and density values is of more interest than the modulus because the weight values of the former are varied while that of the latter is kept constant.

The flexural strength of Calcite/Lig2 (47/53) is observed to be higher than that of Calcite/Lig2 (10/90)-Flax. These results are impressive given it is the first iteration, showing that the model recommends recipes according to the weight and polarity values. It also shows that the broad and diverse data points/recipes created as the initial set of experiments helped the model get an initial idea about the search space's more promising and less promising regions. An increase in the weight value of flexural strength allows the model to recommend recipes somewhere around the lowest output score. Since this is the first iteration, this may not be the most optimized solution, but the goal is to see how the model reacts to varying objective functions and if it is in the right direction. The test values ultimately show that by increasing the weight/priority values of the flexural strength, the model recommended recipes that improved the flexural strength (For weight value 0.6 $\rightarrow$ 42.5 MPa and for weight value 0.7 $\rightarrow$ 44.4 MPa).

Similar results are observed for density columns as well. Density, however, is minimized. A higher weight value should recommend a plate with lower density and vice versa, which is exactly what is observed from the graphs. The model recommended the recipe Calcite/Lig2 (47/53) for a weight value of 0.6 (density - 1.4 g/cc) while Calcite/Lig2 (10/90)-Flax is recommended for a weight value of 0.8 (density - 1.32 g/cc). This again shows that the model reacts well to the varying loss parameter values and the model's recommendations in the first iteration are in the right direction towards getting a highly optimized recipe.

Regarding the bio-based composite's composition, 'Calcite/Lig2 (47/53)' has a higher fibre and calcite ratio (Table 5.8). Fibres aid in binding the composite and improving its strength and modulus, implying a higher fibre ratio (within reasonable bounds) offering to higher strength and modulus of the composite. A higher calcite ratio improves the modulus but increases the density of the composite. On the other hand, 'Calcite/Lig2 (10/90)' has a lower calcite and fibre ratio contributing to its lower modulus, strength, and density. Therefore, although the fibre ratio and the calcite: lignocellulosic 2 of 'Calcite/Lig2 (47/53)' is much higher than 'Calcite/Lig2 (10/90)', the difference in mechanical properties is not that high. A significant reason and an important parameter to observe here is the dry ratio of both the composites. Natural fillers like lignocellulosic 2 absorb more resin and make the composite dry at lower filler percentages than calcite, where more filler loading is possible. Hence doughs with higher calcite have a higher dry ratio than those with higher natural filler. Looking at table 5.8, the dry ratio of both the composites is similar, although the difference in calcite loading in both the composites is relatively high. From past knowledge and experience of making composites involving different ratios of calcite and lignocellulosic 2, it is evident that the dry ratio of 'Calcite/Lig2 (47/53)' is relatively less and more filler, in theory, can be loaded to improve its mechanical properties. This can be a significant reason for a low difference in mechanical properties between the two recipes.

Second iteration

The background study explains that choosing Expected Improvement (EI) as an acquisition function balances exploration and exploitation. Currently, the goal is to sample the regions where the surrogate model predicts a low loss function, meaning regions that provide recipes mechanical properties better in choice of loss function parameters. There are multiple applications of the BMC Optimization model, and multiple approaches can be taken to prove if the model works for a particular application. In one approach, the weight and polarity values are similar to the first iteration, and the goal is to observe how many iterations it takes to reach an optimized recipe for those values. Another approach is the one-shot learning approach. The weight and polarity values are varied at every iteration, meaning the model has one shot at getting an optimized recipe. As explained earlier in the first iteration, the approach taken for this study is to test how the model works and reacts if the objective functions are altered. This approach will help NPSP cater to clients' needs with different goals. The objective functions chosen for this iteration are not similar to the previous iteration because the modulus between the two objective functions was not varied; hence, it was unclear how the model reacted to varying weight values of modulus.

After appending the input and output parameters to the current database, the objective functions for the second iteration are entered into the model. Tables 5.9 and 5.10 show the objective functions. A different approach is taken for this iteration. Instead of varying two output parameters like the previous iteration, just one of them is varied now. For the same filler/fibre combination (Calcite/Lig2 - Flax), density and strength are constant, while the modulus is varied for comparing different weight values. In the second iteration, flexural strength is given the highest priority. As a result, modulus and density are slightly lower in weight values than strength. The polarity values are kept the same as the first iteration as the goal is to maximize strength and modulus while minimizing density.

After defining the objective functions the output scores are calculated as shown in tables 5.11 and

	Density	Flexural Modulus	Flexural Strength
Weight value (ω)	0.6	0.8	1
Polarization value (a)	0	1	1

Table 5.9: Weight and Polarity values of single-objective parametrized loss function - 1

	Density	Flexural Modulus	Flexural Strength
Weight value (ω)	0.6	0.5	1
Polarization value (a)	0	1	1

Table 5.10: Weight and Polarity values of single-objective parametrized loss function - 2

5.12. The recipes obtained from the first iteration, CalLig2(41/59)-Flax and CalLig2(10/90)-Flax are appended to the database. It can be observed that once again, CalLig2(25/75)-Flax, which is marked in red has the lowest output score recorded for both the cases, followed by CalLig2(86/14)-Flax and Calcite100%-Flax. The highest output score is calculated for Lig2 (100%)-Flax. This can be attributed to the fact that it has the low modulus and strength, while those are the parameters given a higher priority.

Recipe	Output Score
Calcite100%-Flax	0.44
CalLig2(86/14)-Flax	0.43
CalLig2(75/25)-Flax	0.56
CalLig2(68/32)-Flax	0.70
CalLig2(50/50)-Flax	0.68
CalLig2(47/53)-Flax	0.40
CalLig2(41/59)-Flax	0.59
CalLig2(25/75)-Flax	0.33
CalLig2(10/90)-Flax	0.49
Lig2 (100%)-Flaxvol	0.62
Lig2 (100%)-Flax	0.71

Table 5.11: Output Score - 1 for iteration 2. The recipe marked red has the the least output score indicating it is the most optimized in the training set for loss function parameters in table 5.9

Recipe	Output Score
Calcite100%-Flax	0.42
CalLig2(86/14)-Flax	0.41
CalLig2(75/25)-Flax	0.58
CalLig2(68/32)-Flax	0.68
CalLig2(50/50)-Flax	0.63
CalLig2(47/53)-Flax	0.43
CalLig2(41/59)-Flax	0.58
CalLig2(25/75)-Flax	0.38
CalLig2(10/90)-Flax	0.50
Lig2 (100%)-Flaxvol	0.59
Lig2 (100%)-Flax	0.70

Table 5.12: Output Score - 2 for iteration 2. The recipe marked red has the the least output score indicating it is the most optimized in the training set for loss function parameters in table 5.10

The recipes recommended by the model after calculating the output are shown in table 5.13. The recipes names are almost similar to some of the previous recipes but the composition of input parameters are different. They can be called as 'CalLig2(11/89)-Flax' and 'CalLig2(25/75)-Flax IT2' where IT2 refers to second iteration. Similar to the previous iteration, these plates are manufactured and tested for their mechanical properties and appended to the database for the next iteration.

Objective Function	Fibre Ratio	Filler Ratio	Dry Ratio
Parametrized loss function - 1	0.0951	0.7511	0.5854
Parametrized loss function - 2	0.0729	0.8911	0.4453

Table 5.13: Recommended recipe for each set of loss function parameters

The mechanical properties obtained after the second iteration are shown in figure 5.5. The results obtained from the second iteration and highlighted by dotted columns. Once again, the results obtained are impressive. The flexural modulus columns are of importance here since that is the parameter which was varied. The flexural modulus of the generated recipes are proportional to the defined weight values. The recipe recommended for a higher weight value (CalLig2(25/75)-Flax IT2) has a higher flexural modulus as compared to the recipe recommended for a lower weight value (CalLig2(11/89)-Flax). For weight value 0.8 $\rightarrow$ 6150 MPa and for weight value 0.5 $\rightarrow$ 4350 MPa.

Regarding the bio-based composites' composition, CalLig2(25/75)-Flax IT2 has a higher fibre percentage, higher calcite percentage than the natural filler, and a higher dry ratio. Higher fibre ratio aid in binding the composite, hence improving its strength, while a higher calcite ratio improves the modulus of the composite. 'CalLig2(11/89)-Flax', on the other hand, has a lower calcite and fibre ratio as compared to 'CalLig2(25/75)-Flax IT2', which are the reasons for a lower modulus and strength of 'CalLig2(11/89)-Flax'. Another parameter to be considered here is the dry ratio, which is lower for 'CalLig2(11/89)-Flax'. A higher ratio of natural filler implies a lower dry ratio.

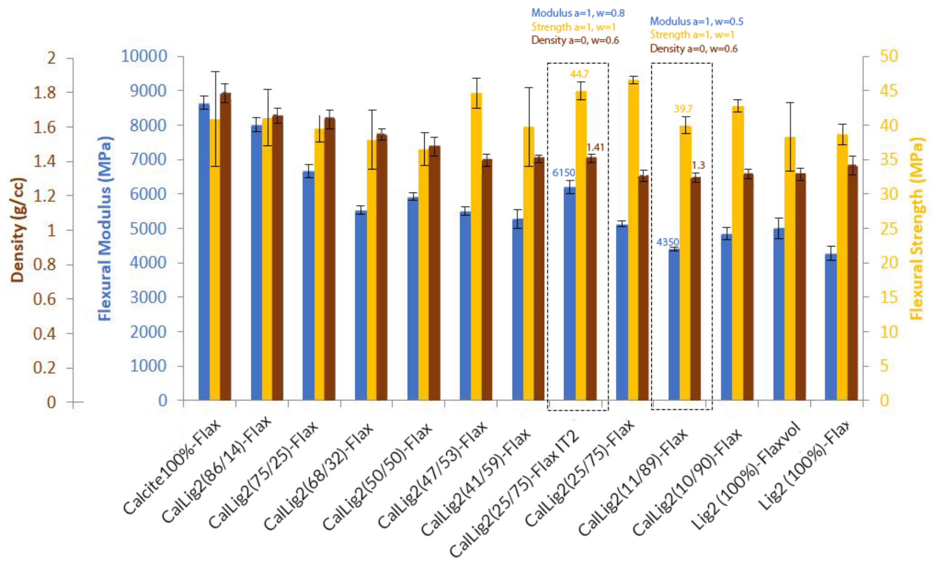

Figure 5.5: Results from training set, first and second iterations for flexural modulus, flexural strength and density along with the error bars. Values obtained for the second iteration are stated on top of them and marked with dotted rectangles. The weight 'w' and 'a' values for each output parameters are mentioned on top of their respective recipe

From previous experience and knowledge, the dry ratio for both the composites seem reasonable and realistic. This is because natural fillers absorb more resin than calcite and make the composite dry at a lower weight percentage than calcite.

The results obtained from the two iterations show that the recommendations given by the model is moving towards the right direction. It shows that the Bayesian optimization works if the objective function is altered, as we are finding lower output scores also known as optimization step improvements in the first two iterations. Similar iterations are carried out for Calcite/Lig2 with bamboo fibre. Separate objective functions are defined, output scores is calculated and results are analyzed for both iterations of (Calcite/Lig1) and (Calcite/Was) each with flax and bamboo. The results are shown in appendix B.

5.3 Recommendations

Few shot learning approach

The results obtained from the two iterations show that the model recommendations for one-shot learning where the objective functions are altered at every iteration has shown true potential. Furthermore, the model shows significant progress within two iterations from an improved mechanical properties point of view. Keeping the objective functions constant and carrying out iterations till an optimized recipe is reached is another approach which can be tried. Having higher weight values for the output parameters and iterating at these values is something which should also be tried to improve the mechanical properties and getting highly optimized recipes for a particular set of loss function parameters.

Incorporating Rule of Mixtures model with the Bayesian Optimization model

The previous recommendation is a time and cost expensive process, but the recommended recipes eventually give highly optimized and accurate recipes. On the other hand, the rule of mixtures approach is a quick and inexpensive method, which requires minimal or no training but provides a rough approximation of the mechanical properties of bio-based composites. A combination of the current Bayesian Optimization model with the analytical Rule of Mixtures models discussed in chapter 4 can significantly reduce the number of iterations to be performed to reach a highly optimized recipe. The Rule of Mixtures model provides a theoretical trend for the mechanical properties and if it is nested with the Bayesian Optimization model, it can supporting prompt instantiation of the Bayesian Optimization model. This can reduce the current cost and time expensive sampling process as it is more likely to attain better mechanical properties in a few iterations. The correct approach towards combining these models is yet to be explored and hence is fit to be a recommendation. An added advantage of this process is the incorporation of newer fillers and fibres. The Bayesian Optimization model by itself assume functional forms that is it assumes the data is sampled from a Gaussian process. However, it cannot associate variables to physical properties i.e. it does not know the physical meaning of the continuous variables. Adding a new filler or a fibre will mean creating another training set altogether, which is a tedious process and training the model with new iterations, which is a long and expensive procedure, not realistic from a company's point of view. Incorporating it with analytical models that can differentiate between different properties and parameters and adapt quickly to a change or addition of materials can prove helpful and a much easier and more practical approach than going over the entire exploration and exploitation of the model.

Production of composite production using a high throughput system

Although the experimental process has been optimized slightly, which involves making four doughs a day (initially 2 per day), it is still quite far from expected compared to a high throughput system. This challenge of collecting experimental data points can be solved by employing a high throughput system. Although the current training set is quite a diverse set of recipes, having a high throughput system that makes at least a few hundred doughs per week/few weeks is best suited for generating optimized recipes in the least number of iterations.

Setting boundary conditions for filler ratio

As mentioned earlier, human interference is required to choose a recipe recommended by the model. The model aims to eliminate human interference in selecting an optimised recipe and let the model generate highly optimised recipes. Unlike the fibre and dry ratios, the filler ratio currently does not have any set boundary conditions. A way to tackle the problem of human interference is to define the permissible upper and lower bounds of calcite allowed in the recommended recipe. The filler ratio currently recognised by the model is the ratio of natural filler to calcite. For example, on setting the maximum calcite loading hypothetically to 30 wt%, the filler ratio recommended by the model will range from 70 wt% to 100wt%. This boundary setting will help the model recommend recipes with more natural fillers than calcite. In addition to the fibre and dry ratio, boundary settings will aid reducing the 3-dimensional search space boundary towards obtaining a highly optimised recipe.

Chapter 6

Conclusion

In conclusion, this thesis divided into potential ways to apply machine learning algorithms and the rule of mixtures theory to the upcoming novel research of bio-based composites.

The rule of mixtures models has been started from the binary phase system involving a filler (calcite, lignocellulosic 1, lignocellulosic 2, waste based filler), the matrix, a fibre (flax, bamboo), and the matrix. After tweaking the unknown parameters using literature review and random numbering, the theoretical curves are successfully fitted to all the experimental data points, thus concluding that the parameter values chosen are approximate values if not accurate. The challenges faced were the uniform mixing of the filler/fibre in the matrix. Using the sigma blade mixer did not make sense as the minimum quantity it mixes is 2 kg, and from a purely experimental and testing point of view, there is no need for such a huge amount of dough to be prepared. Also, mixing just a filler and matrix system was impossible in this mixer as the viscosity is low. It was difficult to extract it then and clean the mixer regularly as it leads to both time costs expensive. Hence, a small drill-based hand mixer was the only option available, leading to minor non-uniformities in mixing. Also, curing the binary phase plates at the conventional 100 bar pressure was not possible due low viscosity of the system leading to contamination of the machines. Hence it had to be done at 50 bar. Nevertheless, the experimental results obtained were within reasonable limits and not unrealistically off.

The cascading of binary models to determine the stiffness of the ternary phase (matrix + filler + fibre) and quaternary phase (matrix + filler 1 + filler 2 + fibre) provides approximate values in most cases compared to the experimental data points. The linear regression of experiments vs theory gives a standard deviation of 2 sigma bounds in the acceptance range.

From an industry's perspective, if any filler or fibre has to be substituted, the binary curve fitting for that particular reinforcement must be performed, followed by the cascading of the models. As mentioned in chapter 4, strength modelling is slightly complicated due to reasons discussed in the aforementioned chapter and is possible only in a well defined, limited, formulation space.

On the other hand, the machine learning approach used for generating optimized recipes uses Bayesian optimization. Using a weighted single-objective output score, the optimization of multiple output parameters is combined into a single objective. Not having a high throughput system was one of the challenges faced to obtain a bigger and more extensive training set and perform more iterations quickly. Nevertheless, with the current training set and iterations performed, it is evident that the model is progressing in the right direction and generates recipes according to the objective function. The recipes generated within the current two iterations following the one-shot learning system already generate promising recipes that are better in specific mechanical properties than the training set.

From an industry's perspective, adding newer parameters like chemical modifiers and additives will increase the dimensionality and search space that can be tackled by performing more iterations and employing a high throughput system.

It will take many more iterations to generate a highly optimized recipe which is why combining it with the current rule of mixtures model is a potential approach toward generating an optimized recipe within an extremely low number of iterations, as the rule of mixtures model can predict the trendline based on varying ratios of fillers and fibres. This nesting process can significantly reduce both time and cost of the sampling process.

Acknowledgements

First and foremost, I would sincerely like to thank NPSP B.V., especially Zoya and Willem, for giving me this wonderful opportunity. During my time at the company, I learned a lot from Zoya about the exciting and potential world of bio-based composites. Her friendly attitude encouraged me to ask more questions and try out newer approaches to any challenges, even if they were silly or did not work out. Furthermore, her suggestions and comments helped me improve my work and knowledge on the subject during my thesis. Thank you so much for your support Zoya!

I would also like to thank my main supervisor Stephen for his contributions to my thesis from the first day. The online meetings with him were informative and helped push my thesis to the next level. I have great admiration for his knowledge and critical thinking. His patience during explanations and helping me figure out different approaches is highly appreciated. Thank you for your endless support, Stephen!

I would sincerely like to thank Miguel for his contributions to my thesis and interest in composites. His course on 'Mechanical Behaviour of Materials' was what rekindled my interest in composite materials. Furthermore, I am grateful to him for being my supervisor. Even though the meetings with him were only a few, his comments and suggestions helped improve my thesis work. In addition, his quick and relatable explanations helped enhance my understanding and approach to data-driven optimization. Thank you so much, Miguel, for your support!

I would also like to thank Martin for his support in understanding his model and his valuable comments and suggestions in improving my report and thesis. His thesis work inspired me to understand more about machine learning. In addition, his subject knowledge and quick explanations towards the end of my thesis enhanced my learning process, which would have otherwise taken a lot of time individually. Thank you for your help Martin!

I would also like to thank Ian from NPSP B.V., who showed and helped me make bio-based composites from the first day of my internship. In addition, he helped me with any technical difficulties I faced in the lab throughout my time at NPSP. In addition, I would like to thank everyone at NPSP for their constant support and feedback about my work. I would also like to thank my friends in Delft for their continuous support and memorable moments and for being there for me through thick and thin.

Last and most important, I would like to thank my parents for their constant support, for helping me through all the tough times during this phase, and for always encouraging and motivating me to be the best version of myself. Thank You!

References

[1] S Richard, J Selwin Rajadurai, and V Manikandan. “Influence of particle size and particle loading on mechanical and dielectric properties of biochar particulate-reinforced polymer nanocomposites”. In: *International journal of polymer analysis and characterization* 21.6 (2016), pp. 462–477.

[2] W. Böttger M. Lepelaar and R. Groot. *NPSP Composieten*. Accessed: 2021-11-15. 2009.

[3] F.C. Campbell. “Commercial Composite Processes: These Commercial Processes Produce Far More Parts than the High-performance Processes”. In: *Manufacturing Processes for Advanced Composites*. Elsevier Science, 2004, pp. 399–438.

[4] CH Park and WI Lee. “Compression molding in polymer matrix composites”. In: *Manufacturing techniques for polymer matrix composites (PMCs)*. Elsevier, 2012, pp. 47–94.

[5] P.K. Mallick. “Particulate Filled and Short Fiber Reinforced Polymer Composites”. In: 2016, pp. 360–400.

[6] R. Brooks. “6.16 - Composites in Automotive Applications: Design”. In: *Comprehensive Composite Materials*. Ed. by Anthony Kelly and Carl Zweben. 2000, pp. 341–363.

[7] Dominick V. Rosato, Donald V. Rosato, and Matthew V. Rosato. In: *Plastic Product Material and Process Selection Handbook*. Ed. by Dominick V. Rosato, Donald V. Rosato, and Matthew V. Rosato. Elsevier, 2004, pp. 455–496.

[8] Jonas Mockus. *Bayesian approach to global optimization: theory and applications*. Vol. 37. Springer Science & Business Media, 2012.

[9] Martin van der Schelling. *A data-driven heuristic decision strategy for data-scarce optimization*. TU Delft Repositories. 2021.

[10] Kim L Pickering, MG Aruan Efendy, and Tan Minh Le. “A review of recent developments in natural fibre composites and their mechanical performance”. In: *Composites Part A: Applied Science and Manufacturing* 83 (2016), pp. 98–112.

[11] Lisa Wikström, Juha Hakala, Elina Saarivuori, Ulla Forsström, and Janne Keränen. “Utilization of side streams from paper industry as fillers in polypropylene composites”. In: *Polymer Composites* 39.11 (2018), pp. 4000–4009.

[12] V Fombuena, L Bernardi, O Fenollar, T Boronat, and R Balart. “Characterization of green composites from biobased epoxy matrices and bio-fillers derived from seashell wastes”. In: *Materials & Design* 57 (2014), pp. 168–174.

[13] Rajendran Baskaran, Muthusamy Sarojadevi, and Chinnaswamy Thangavel Vijayakumar. “Mechanical and thermal properties of unsaturated polyester/calcium carbonate nanocomposites”. In: *Journal of reinforced plastics and composites* 30.18 (2011), pp. 1549–1556.

[14] Susan Wong, Robert Shanks, and Alma Hodzic. "Properties of poly (3-hydroxybutyric acid) composites with flax fibres modified by plasticiser absorption". In: *Macromolecular Materials and Engineering* 287.10 (2002), pp. 647–655.

[15] Elsadig Mahdi and Aamir Dean. "The effect of filler content on the tensile behavior of polypropylene/cotton fiber and poly (vinyl chloride)/cotton fiber composites". In: *Materials* 13.3 (2020), p. 753.

[16] A. Nair, N.B. Ithnin, H.L. Sim, and D.R. Appleton. "Energy Crops". In: *Encyclopedia of Applied Plant Sciences (Second Edition)*. Ed. by Brian Thomas, Brian G Murray, and Denis J Murphy. Second Edition. Oxford: Academic Press, 2017, pp. 164–176.

[17] Badal Saha, Rodney Bothast, and Douglas Jordan. "Enzymes, Industrial". In: *Encyclopedia of microbiology* (2009), pp. 281–294.

[18] Christopher Brigham. "Biopolymers: biodegradable alternatives to traditional plastics". In: *Green chemistry*. Elsevier, 2018, pp. 753–770.

[19] I. Kögel-Knabner and W. Amelung. "12.7 - Dynamics, Chemistry, and Preservation of Organic Matter in Soils". In: *Treatise on Geochemistry (Second Edition)*. Ed. by Heinrich D. Holland and Karl K. Turekian. Second Edition. Oxford: Elsevier, 2014, pp. 157–215.

[20] Xiaowei Zhou, Linda J Broadbelt, and Ravikrishnan Vinu. "Mechanistic understanding of thermochemical conversion of polymers and lignocellulosic biomass". In: *Advances in chemical engineering* 49 (2016), pp. 95–198.

[21] Guillermo Rodrıguez, Antonio Lama, Rocıo Rodrıguez, Ana Jiménez, Rafael Guillén, and Juan Fernández-Bolaños. "Olive stone an attractive source of bioactive and valuable compounds". In: *Bioresource technology* 99.13 (2008), pp. 5261–5269.

[22] *Olive Pit Powder, www.bio-powder.com/en/olive-pit/*. `www.bio-powder.com/en/olive-pit/`. Accessed: 2021-09-30.

[23] Xuemin Li, Yinan Liu, Jianxiu Hao, and Weihong Wang. "Study of almond shell characteristics". In: *Materials* 11.9 (2018), p. 1782.

[24] J.A. Caballero, R Font, and A Marcilla. "Comparative study of the pyrolysis of almond shells and their fractions, holocellulose and lignin. Product yields and kinetics". In: *Thermochimica Acta* 276 (1996), pp. 57–77.

[25] Eduardo Robles, Nagore Izaguirre, Ander Martin, Dimitra Moschou, and Jalel Labidi. "Assessment of Bleached and Unbleached Nanofibers from Pistachio Shells for Nanopaper Making". In: *Molecules* 26.5 (2021), p. 1371.

[26] Yue Gao, Xinbo Guo, Yu Liu, Zhiqiang Fang, Mingwei Zhang, Ruifen Zhang, Lijun You, Tong Li, and Rui Hai Liu. "A full utilization of rice husk to evaluate phytochemical bioactivities and prepare cellulose nanocrystals". In: *Scientific reports* 8.1 (2018), pp. 1–8.

[27] Anwar Ma'ruf, Bambang Pramudono, and Nita Aryanti. "Lignin isolation process from rice husk by alkaline hydrogen peroxide: Lignin and silica extracted". In: *AIP Conference Proceedings*. Vol. 1823. 1. AIP Publishing LLC. 2017, p. 020013.

[28] Elena Husanu, Angelica Mero, Jose Gonzalez Rivera, Andrea Mezzetta, Julian Cabrera Ruiz, Felicia D'Andrea, Christian Silvio Pomelli, and Lorenzo Guazzelli. "Exploiting Deep Eutectic Solvents and Ionic Liquids for the Valorization of Chestnut Shell Waste". In: *ACS Sustainable Chemistry & Engineering* 8.50 (2020), pp. 18386–18399.

[29] Fabiano Avelino Gonçalves, Héctor A Ruiz, Everaldo Silvino dos Santos, José A Teixeira, and Gorete Ribeiro de Macedo. “Valorization, comparison and characterization of coconuts waste and cactus in a biorefinery context using NaClO 2–C 2 H 4 O 2 and sequential NaClO 2–C 2 H 4 O 2/autohydrolysis pretreatment”. In: *Waste and Biomass Valorization* 10.8 (2019), pp. 2249–2262.

[30] Fei Lu, Julia Rodriguez-Garcia, Isabella Van Damme, Nicholas J Westwood, Liz Shaw, James S Robinson, Geoff Warren, Afroditi Chatzifragkou, Simon McQueen Mason, Leonardo Gomez, et al. “Valorisation strategies for cocoa pod husk and its fractions”. In: *Current Opinion in Green and Sustainable Chemistry* 14 (2018), pp. 80–88.

[31] Poulomi Sannigrahi, Arthur J Ragauskas, and Gerald A Tuskan. “Poplar as a feedstock for biofuels: a review of compositional characteristics”. In: *Biofuels, Bioproducts and Biorefining* 4.2 (2010), pp. 209–226.

[32] Nannan Xiao, Peter Bock, Sebastian J Antreich, Yannick Marc Staedler, Jürg Schönenberger, and Notburga Gierlinger. “From the soft to the hard: changes in microchemistry during cell wall maturation of walnut shells”. In: *Frontiers in Plant Science* 11 (2020), p. 466.

[33] Aleksander Lisowski, Małgorzata Pajor, Adam Świętochowski, Magdalena Dąbrowska, Jacek Klonowski, Leszek Mieszkalski, Adam Ekielski, Mateusz Stasiak, and Michał Piątek. “Effects of moisture content, temperature, and die thickness on the compaction process, and the density and strength of walnut shell pellets”. In: *Renewable Energy* 141 (2019), pp. 770–781.

[34] Hanieh Bamdad, Kelly Hawboldt, and Stephanie MacQuarrie. “A review on common adsorbents for acid gases removal: Focus on biochar”. In: *Renewable and Sustainable Energy Reviews* 81 (2018), pp. 1705–1720.

[35] Vikas Dhawan, Sehijpal Singh, and Inderdeep Singh. “Effect of natural fillers on mechanical properties of GFRP composites”. In: *Journal of Composites* 2013 (2013).

[36] Abouelkacem Qaiss, Rachid Bouhfid, and Hamid Essabir. “Characterization and use of coir, almond, apricot, argan, shells, and wood as reinforcement in the polymeric matrix in order to valorize these products”. In: *Agricultural biomass based potential materials*. Springer, 2015, pp. 305–339.

[37] S.C. Nwanonenyi, MU Obidiegwu, and GC Onuegbu. “Effects of particle sizes, filler contents and compatibilization on the properties of linear low density polyethylene filled periwinkle shell powder”. In: *The International Journal of Engineering and Science* 2.2 (2013), pp. 1–8.

[38] H Essabir, S Nekhlaoui, M Malha, MO Bensalah, FZ Arrakhiz, A Qaiss, and R Bouhfid. “Bio-composites based on polypropylene reinforced with Almond Shells particles: Mechanical and thermal properties”. In: *Materials & Design* 51 (2013), pp. 225–230.

[39] Sara Valvez, Alberto Maceiras, Paulo Santos, and Paulo NB Reis. “Olive stones as filler for polymer-based composites: a review”. In: *Materials* 14.4 (2021), p. 845.

[40] Asma Gharbi, Ramzi Bel Hassen, and Sami Boufi. “Composite materials from unsaturated polyester resin and olive nuts residue: The effect of silane treatment”. In: *Industrial Crops and Products* 62 (2014), pp. 491–498.

[41] Munir Tasdemir. “Effects of olive pit and almond shell powder on polypropylene”. In: *Key Engineering Materials*. Vol. 733. Trans Tech Publ. 2017, pp. 65–68.

[42] Koay Seong Chun and Salmah Husseinsyah. “Agrowaste-based composites from cocoa pod husk and polypropylene: effect of filler content and chemical treatment”. In: *Journal of thermoplastic composite materials* 29.10 (2016), pp. 1332–1351.

[43] ML Sanyang, SM Sapuan, and M Haron. "Effect of cocoa pod husk filler loading on tensile properties of cocoa pod husk/polylactic acid green biocomposite films". In: *AIP Conference Proceedings*. Vol. 1891. 1. AIP Publishing LLC. 2017, p. 020126.

[44] Shakuntala Ojha, G Raghavendra, and SK Acharya. "A comparative investigation of bio waste filler (wood apple-coconut) reinforced polymer composites". In: *Polymer composites* 35.1 (2014), pp. 180–185.

[45] Yang Ding, Yunguo Liu, Shaobo Liu, Zhongwu Li, Xiaofei Tan, Xixian Huang, Guangming Zeng, Lu Zhou, and Bohong Zheng. "Biochar to improve soil fertility. A review". In: *Agronomy for sustainable development* 36.2 (2016), pp. 1–18.

[46] Rizwan Tareq, Nahida Akter, and Md Shafiul Azam. "Biochars and biochar composites: low-cost adsorbents for environmental remediation". In: *Biochar from biomass and waste*. Elsevier, 2019, pp. 169–209.

[47] Shi-Xiang Zhao, Na Ta, and Xu-Dong Wang. "Effect of temperature on the structural and physicochemical properties of biochar with apple tree branches as feedstock material". In: *Energies* 10.9 (2017), p. 1293.

[48] Sergio Neves Monteiro, Verônica Calado, Rubén JS Rodriguez, and Frederico M Margem. "Thermogravimetric stability of polymer composites reinforced with less common lignocellulosic fibers–an Overview". In: *Journal of Materials Research and Technology* 1.2 (2012), pp. 117–126.

[49] Xuqin Pan, Zhepei Gu, Weiming Chen, and Qibin Li. "Preparation of biochar and biochar composites and their application in a Fenton-like process for wastewater decontamination: A review". In: *Science of The Total Environment* 754 (2021), p. 142104.

[50] Kyle Crombie, Ondřej Mašek, Saran P Sohi, Peter Brownsort, and Andrew Cross. "The effect of pyrolysis conditions on biochar stability as determined by three methods". In: *Gcb Bioenergy* 5.2 (2013), pp. 122–131.

[51] Wan Azlina Wan Abdul Karim Ghani, Ayaz Mohd, Gabriel da Silva, Robert T Bachmann, Yun H Taufiq-Yap, Umer Rashid, and H Ala'a. "Biochar production from waste rubber-wood-sawdust and its potential use in C sequestration: chemical and physical characterization". In: *Industrial Crops and Products* 44 (2013), pp. 18–24.

[52] Oisik Das, Ajit K Sarmah, Zoran Zujovic, and Debes Bhattacharyya. "Characterisation of waste derived biochar added biocomposites: chemical and thermal modifications". In: *Science of the Total EnvironmentScience of the Total Environment* 550 (2016), pp. 133–142.

[53] Vidhya Nagarajan, Amar K Mohanty, and Manjusri Misra. "Biocomposites with size-fractionated biocarbon: influence of the microstructure on macroscopic properties". In: *ACS omega* 1.4 (2016), pp. 636–647.

[54] Xiao-Lin Xie, Yiu-Wing Mai, and Xing-Ping Zhou. "Dispersion and alignment of carbon nanotubes in polymer matrix: a review". In: *Materials science and engineering: R: Reports* 49.4 (2005), pp. 89–112.

[55] Rossella Arrigo, Mattia Bartoli, and Giulio Malucelli. "Poly (lactic acid)–biochar biocomposites: Effect of processing and filler content on rheological, thermal, and mechanical properties". In: *Polymers* 12.4 (2020), p. 892.

[56] Qingfa Zhang, Weiming Yi, Zhihe Li, Lihong Wang, and Hongzhen Cai. "Mechanical properties of rice husk biochar reinforced high density polyethylene composites". In: *Polymers* 10.3 (2018), p. 286.

[57] Raj Kumar Dahal, Bishnu Acharya, Gobinda Saha, Rabin Bissessur, Animesh Dutta, and Aitazaz Farooque. "Biochar as a filler in glassfiber reinforced composites: Experimental study of thermal and mechanical properties". In: *Composites Part B: Engineering* 175 (2019), p. 107169.

[58] R Sundarakannan, V Arumugaprabu, V Manikandan, and S Vigneshwaran. "Mechanical property analysis of biochar derived from cashew nut shell waste reinforced polymer matrix". In: *Materials Research Express* 6.12 (2020), p. 125349.

[59] Anesh Manjaly Poulose, Ahmed Yagoub Elnour, Arfat Anis, Hamid Shaikh, SM Al-Zahrani, Justin George, Mohammad I Al-Wabel, Adel R Usman, Yong Sik Ok, Daniel CW Tsang, et al. "Date palm biochar-polymer composites: An investigation of electrical, mechanical, thermal and rheological characteristics". In: *Science of the total environment* 619 (2018), pp. 311–318.

[60] S Arunavathi, RD Eithiraj, and K Veluraja. "Physical and mechanical properties of jute fiber and jute fiber reinforced paper bag with tamarind seed gum as a binder-An eco-friendly material". In: *AIP Conference Proceedings*. Vol. 1832. 1. AIP Publishing LLC. 2017, p. 040026.

[61] SCO Ugbolue. "Structure/property relationships in textile fibres". In: *Textile progress* 20.4 (1990), pp. 1–43.

[62] AK Bledzki and Jochen Gassan. "Composites reinforced with cellulose based fibres". In: *Progress in polymer science* 24.2 (1999), pp. 221–274.

[63] Xue Li, Lope G Tabil, and Satyanarayan Panigrahi. "Chemical treatments of natural fiber for use in natural fiber-reinforced composites: a review". In: *Journal of Polymers and the Environment* 15.1 (2007), pp. 25–33.

[64] HL Bos, MJA Van Den Oever, and OCJJ Peters. "Tensile and compressive properties of flax fibres for natural fibre reinforced composites". In: *Journal of Materials Science* 37.8 (2002), pp. 1683–1692.

[65] S.Haig Zeronian. "Mechanical properties of cotton fibers". In: *Journal of Applied Polymer Science: Applied Polymer Symposium* 47 (1991), pp. 445–461.

[66] ETN Bisanda and Martin P Ansell. "Properties of sisal-CNSL composites". In: *Journal of Materials Science* 27.6 (1992), pp. 1690–1700.

[67] Yinhang Zhang, Jang Rak Choi, and Soo-Jin Park. "Enhancing the heat and load transfer efficiency by optimizing the interface of hexagonal boron nitride/elastomer nanocomposites for thermal management applications". In: *Polymers* 143 (2018), pp. 1–9.

[68] Pooja Bhatt and Alka Goe. "Carbon fibres: production, properties and potential use". In: *Material Science Research India* 14.1 (2017), pp. 52–57.

[69] Anshuman Shrivastava. "4 - Additives for Plastics". In: *Introduction to Plastics Engineering*. Ed. by Anshuman Shrivastava. Plastics Design Library. William Andrew Publishing, 2018, pp. 111–141.

[70] Teijn Aramid. *Twaron – a versatile high-performance fiber*. Brochure. 2012. URL: https://pdf.directindustry.com/pdf/teijin-aramid/twaron-product-brochure/18087-309129-_4.html.

[71] Kin-tak Lau, Pui-yan Hung, Min-Hao Zhu, and David Hui. "Properties of natural fibre composites for structural engineering applications". In: *Composites Part B: Engineering* 136 (2018), pp. 222–233.

[72] Muthukumar Chandrasekar, MR Ishak, Mohammad Jawaid, SM Sapuan, and Z Leman. "Low velocity impact properties of natural fiber-reinforced composite materials for aeronautical applications". In: *Sustainable Composites for Aerospace Applications*. Elsevier, 2018, pp. 293–313.

[73] Libo Yan, Nawawi Chouw, and Krishnan Jayaraman. "Flax fibre and its composites–A review". In: *Composites Part B: Engineering* 56 (2014), pp. 296–317.

[74] Kristiina Oksman. "High quality flax fibre composites manufactured by the resin transfer moulding process". In: *Journal of reinforced plastics and composites* 20.7 (2001), pp. 621–627.

[75] MJA Van den Oever, HL Bos, and MJJM Van Kemenade. "Influence of the physical structure of flax fibres on the mechanical properties of flax fibre reinforced polypropylene composites". In: *Applied Composite Materials* 7.5 (2000), pp. 387–402.

[76] Christophe Baley, Moussa Gomina, Joel Breard, Alain Bourmaud, and Peter Davies. "Variability of mechanical properties of flax fibres for composite reinforcement. A review". In: *Industrial Crops and Products* 145 (2020), p. 111984.

[77] Marco Morreale, Maria Chiara Mistretta, and Vincenzo Fiore. "Creep behavior of poly (lactic acid) based biocomposites". In: *Materials* 10.4 (2017), p. 395.

[78] Kai Zhang, Fangxin Wang, Wenyan Liang, Zhenqing Wang, Zhiwei Duan, and Bin Yang. "Thermal and mechanical properties of bamboo fiber reinforced epoxy composites". In: *Polymers* 10.6 (2018), p. 608.

[79] Idowu D Ibrahim, Tamba Jamiru, Rotimi E Sadiku, Williams K Kupolati, Stephen C Agwuncha, and Gbenga Ekundayo. "The use of polypropylene in bamboo fibre composites and their mechanical properties–A review". In: *Journal of reinforced plastics and composites* 34.16 (2015), pp. 1347–1356.

[80] Hanafi Ismail, S Shuhelmy, and MR Edyham. "The effects of a silane coupling agent on curing characteristics and mechanical properties of bamboo fibre filled natural rubber composites". In: *European Polymer Journal* 38.1 (2002), pp. 39–47.

[81] Siew Choo Chin, Kong Fah Tee, Foo Sheng Tong, Huei Ruey Ong, and Jolius Gimbun. "Thermal and mechanical properties of bamboo fiber reinforced composites". In: *Materials Today Communications* 23 (2020), p. 100876.

[82] BF Yousif, A Shalwan, Chee Wen Chin, and KC Ming. "Flexural properties of treated and untreated kenaf/epoxy composites". In: *Materials & Design* 40 (2012), pp. 378–385.

[83] Makki Abdelmouleh, Sami Boufi, Mohamed Naceur Belgacem, Alain Dufresne, and Alessandro Gandini. "Modification of cellulose fibers with functionalized silanes: effect of the fiber treatment on the mechanical performances of cellulose–thermoset composites". In: *Journal of applied polymer science* 98.3 (2005), pp. 974–984.

[84] Moyeenuddin A Sawpan, Kim L Pickering, and Alan Fernyhough. "Flexural properties of hemp fibre reinforced polylactide and unsaturated polyester composites". In: *Composites Part A: Applied Science and Manufacturing* 43.3 (2012), pp. 519–526.

[85] Anggit Murdani, Syamsul Hadi, and Utsman Syah Amrullah. "Flexural properties and vibration behavior of jute/glass/carbon fiber reinforced unsaturated polyester hybrid composites for wind turbine blade". In: *Key Engineering Materials*. Vol. 748. Trans Tech Publ. 2017, pp. 62–68.

[86] HPS Abdul Khalil, IUH Bhat, M Jawaid, A Zaidon, D Hermawan, and YS Hadi. "Bamboo fibre reinforced biocomposites: A review". In: *Materials & Design* 42 (2012), pp. 353–368.

[87] PJ Roe and Martin P Ansell. “Jute-reinforced polyester composites”. In: *Journal of Materials Science* 20.11 (1985), pp. 4015–4020.

[88] AK Bledzki, AA Mamun, and O Faruk. “Abaca fibre reinforced PP composites and comparison with jute and flax fibre PP composites”. In: *eXPRESS polymer letters* 1.11 (2007), pp. 755–762.

[89] P Lokesh, TSA Surya Kumari, R Gopi, and Ganesh Babu Loganathan. “A study on mechanical properties of bamboo fiber reinforced polymer composite”. In: *Materials Today: Proceedings* 22 (2020), pp. 897–903.

[90] Ragab Abou-zeid, NA El-Wakil, and Y Fahmy. “Thermoplastic composites from natural reed fibers”. In: *Egyptian Journal of Chemistry* 58.3 (2015), pp. 287–298.

[91] T Scalici, V Fiore, and A Valenza. “Effect of plasma treatment on the properties of Arundo Donax L. leaf fibres and its bio-based epoxy composites: A preliminary study”. In: *Composites Part B: Engineering* 94 (2016), pp. 167–175.

[92] Ajjima Nopparut and Taweechai Amornsakchai. “Influence of pineapple leaf fiber and it’s surface treatment on molecular orientation in, and mechanical properties of, injection molded nylon composites”. In: *Polymer Testing* 52 (2016), pp. 141–149.

[93] Libo Yan, Nawawi Chouw, Liang Huang, and Bohumil Kasal. “Effect of alkali treatment on microstructure and mechanical properties of coir fibres, coir fibre reinforced-polymer composites and reinforced-cementitious composites”. In: *Construction and Building Materials* 112 (2016), pp. 168–182.

[94] Ramadevi Punyamurthy, Dhanalakshmi Sampathkumar, Raghu Patel G Ranganagowda, Basavaraju Bennehalli, and Chikkol V Srinivasa. “Mechanical properties of abaca fiber reinforced polypropylene composites: Effect of chemical treatment by benzenediazonium chloride”. In: *Journal of King Saud University-Engineering Sciences* 29.3 (2017), pp. 289–294.

[95] TD Ngo, M Nofar, MT Ton-That, and W Hu. “Flax and its thermoplastic biocomposites”. In: *Journal of Composite Materials* 50.22 (2016), pp. 3043–3051.

[96] Young Hun Jang, Seong Ok Han, I Na Sim, and Hyung-Il Kim. “Pretreatment effects of seaweed on the thermal and mechanical properties of seaweed/polypropylene biocomposites”. In: *Composites Part A: Applied Science and Manufacturing* 47 (2013), pp. 83–90.

[97] Allan C Manalo, Evans Wani, Noor Azwa Zukarnain, Warna Karunasena, and Kin-tak Lau. “Effects of alkali treatment and elevated temperature on the mechanical properties of bamboo fibre–polyester composites”. In: *Composites Part B: Engineering* 80 (2015), pp. 73–83.

[98] Georgios Koronis, Arlindo Silva, and Mihail Fontul. “Green composites: A review of adequate materials for automotive applications”. In: *Composites Part B: Engineering* 44.1 (2013), pp. 120–127.

[99] Adriana Ticoalu, Thiru Aravinthan, and Francisco Cardona. “A review on the characteristics of gomuti fibre and its composites with thermoset resins”. In: *Journal of Reinforced Plastics and Composites* 32.2 (2013), pp. 124–136.

[100] Ilhem Naghmouchi, Pere Mutjé, and Sami Boufi. “Polyvinyl chloride composites filled with olive stone flour: Mechanical, thermal, and water absorption properties”. In: *Journal of Applied Polymer Science* 131.22 (2014).

[101] AF Koutsomitopoulou, JC Bénézet, A Bergeret, and GC Papanicolaou. “Preparation and characterization of olive pit powder as a filler to PLA-matrix bio-composites”. In: *Powder technology* 255 (2014), pp. 10–16.

[102] Marina Ramos, Franco Dominici, Francesca Luzi, Alfonso Jiménez, Maria Carmen Garrigós, Luigi Torre, and Debora Puglia. "Effect of almond shell waste on physicochemical properties of polyester-based biocomposites". In: *Polymers* 12.4 (2020), p. 835.

[103] Luis Quiles-Carrillo, Nestor Montanes, D Garcia-Garcia, A Carbonell-Verdu, Rafael Balart, and S Torres-Giner. "Effect of different compatibilizers on injection-molded green composite pieces based on polylactide filled with almond shell flour". In: *Composites Part B: Engineering* 147 (2018), pp. 76–85.

[104] Patricia Liminana, Luis Quiles-Carrillo, Teodomiro Boronat, Rafael Balart, and Nestor Montanes. "The effect of varying almond shell flour (ASF) loading in composites with poly (butylene succinate (PBS) matrix compatibilized with maleinized linseed oil (MLO)". In: *Materials* 11.11 (2018), p. 2179.

[105] Tom Thorvaldsen, Bernt Brønmo Johnsen, Torbjørn Olsen, and Finn Knut Hansen. "Investigation of theoretical models for the elastic stiffness of nanoparticle-modified polymer composites". In: *Journal of Nanomaterials* 2015 (2015).

[106] Marcio Loos. "Fundamentals of Polymer Matrix Composites Containing CNTs". In: Dec. 2015, pp. 125–170.

[107] Vikas Mittal. "Modeling of Tensile Modulus of Polyolefin-Layered Silicate Nanocomposites: Modified Halpin Tsai Models". In: *Advanced Composites Letters* 21.5 (2012), p. 096369351202100501.

[108] MY Ahmad Fuad, Z Ismail, MS Mansor, ZA Mohd Ishak, and AK Mohd Omar. "Mechanical properties of rice husk ash/polypropylene composites". In: *Polymer journal* 27.10 (1995), pp. 1002–1015.

[109] Jirawat Kajohnchaiyagual, Chanchira Jubsilp, Isala Dueramae, and Sarawut Rimdusit. "Thermal and mechanical properties enhancement obtained in highly filled alumina-polybenzoxazine composites". In: *Polymer composites* 35.11 (2014), pp. 2269–2279.

[110] T Rouyre, AC Taylor, M Fu, F Perrot, and I James. "Nano-and micro-silica modification of epoxy polymers". In: *2010 10th IEEE International Conference on Solid Dielectrics*. IEEE. 2010, pp. 1–4.

[111] Giulia Fredi, Andrea Dorigato, Luca Fambri, and Alessandro Pegoretti. "Detailed experimental and theoretical investigation of the thermomechanical properties of epoxy composites containing paraffin microcapsules for thermal management". In: *Polymer Engineering & Science* 60.6 (2020), pp. 1202–1220.

[112] OA Stapountzi, MN Charalambides, and JG Williams. "Micromechanical models for stiffness prediction of alumina trihydrate (ATH) reinforced poly (methyl methacrylate)(PMMA): Effect of filler volume fraction and temperature". In: *Composites science and technologyComposites science and technology* 69.11-12 (2009), pp. 2015–2023.

[113] C. Fuchs, Debes Bhattacharyya, Klaus Friedrich, and Stoyko Fakirov. "Application of Halpin–Tsai equation to microfibril reinforced polypropylene/poly(ethylene terephthalate) composites". In: *Composite Interfaces - COMPOS INTERFACE* 13 (Jan. 2006), pp. 331–344.

[114] Marcio R Loos and Ica Manas-Zloczower. "Reinforcement efficiency of carbon nanotubes–myth and reality". In: *Macromolecular theory and simulations* 21.2 (2012), pp. 130–137.

[115] SK Garkhail, RWH Heijenrath, and T Peijs. "Mechanical properties of natural-fibre-mat-reinforced thermoplastics based on flax fibres and polypropylene". In: *Applied Composite Materials* 7.5 (2000), pp. 351–372.

[116] Stephen Picken. *Lecture 13: Polymer nanocomposites (properties vs structure)*. Dec. 2019.

[117] George A Barnard and Thomas Bayes. "Studies in the history of probability and statistics: IX. Thomas Bayes's essay towards solving a problem in the doctrine of chances". In: *Biometrika* 45.3/4 (1958), pp. 293–315.

[118] Jonas Mockus, Vytautas Tiesis, and Antanas Zilinskas. "The Application of Bayesian Methods for Seeking the Extremum". In: *Towards Global Optimization* 2.117-129 (1978), p. 2.

[119] Ziyu Wang and Nando de Freitas. "Theoretical analysis of Bayesian optimisation with unknown Gaussian process hyper-parameters". In: *arXiv preprint arXiv:1406.7758* (2014).

[120] Eric Brochu, Vlad M Cora, and Nando De Freitas. "A tutorial on Bayesian optimization of expensive cost functions, with application to active user modeling and hierarchical reinforcement learning". In: *arXiv preprint arXiv:1012.2599* (2010).

[121] Jin Jin, Chuan Yang, and Yi Zhang. "An improved CMA-ES for solving large scale optimization problem". In: *International Conference on Swarm Intelligence*. Springer. 2020, pp. 386–396.

[122] Bobak Shahriari, Kevin Swersky, Ziyu Wang, Ryan P Adams, and Nando De Freitas. "Taking the human out of the loop: A review of Bayesian optimization". In: *Proceedings of the IEEE* 104.1 (2015), pp. 148–175.

[123] James Bergstra, Rémi Bardenet, Yoshua Bengio, and Balázs Kégl. "Algorithms for hyper-parameter optimization". In: *Advances in neural information processing systems* 24 (2011).

[124] Carl Edward Rasmussen. "Gaussian processes in machine learning". In: *Summer school on machine learning*. Springer. 2003, pp. 63–71.

[125] Gongjin Lan, Jakub M Tomczak, Diederik M Roijers, and AE Eiben. "Time efficiency in optimization with a bayesian-evolutionary algorithm". In: *Swarm and Evolutionary Computation* (2021), p. 100970.

[126] Lisha Li, Kevin Jamieson, Giulia DeSalvo, Afshin Rostamizadeh, and Ameet Talwalkar. "Hyperband: A novel bandit-based approach to hyperparameter optimization". In: *The Journal of Machine Learning Research* 18.1 (2017), pp. 6765–6816.

[127] Luis Munoz-González. "Bayesian Optimization for Black-Box Evasion of Machine Learning Systems". PhD thesis. Imperial College London, 2017.

[128] Riccardo Moriconi, KS Sesh Kumar, and Marc Peter Deisenroth. "High-dimensional Bayesian optimization with projections using quantile Gaussian processes". In: *Optimization Letters* 14.1 (2020), pp. 51–64.

[129] "A framework for data-driven analysis of materials under uncertainty: Countering the curse of dimensionality". In: *Computer Methods in Applied Mechanics and Engineering* 320 (2017), pp. 633–667. ISSN: 0045-7825.

Appendix A

Flexural Test Results

The 3 point bending test results are obtained for Calcite/Lig1 (50/50)-Flax and Calcite/Lig1 (50/50)-Bamboo from the Instron instrument which is shown in figure A.1.

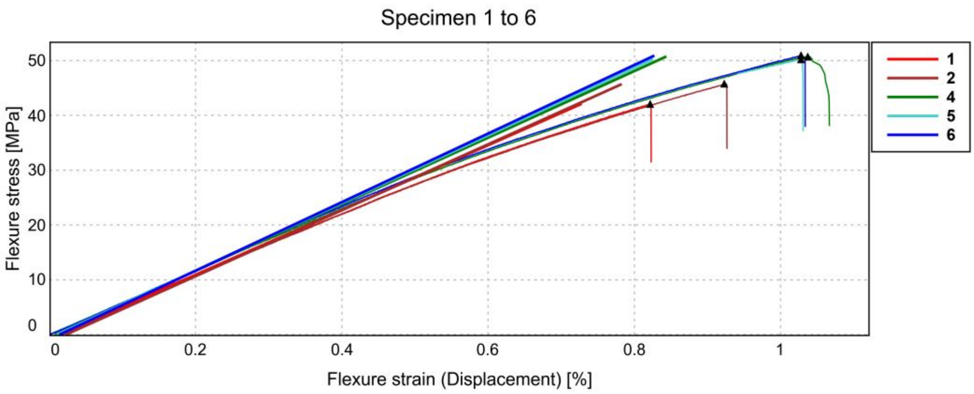

(a) Calcite/Lig1 (50/50)-Flax stress strain curve

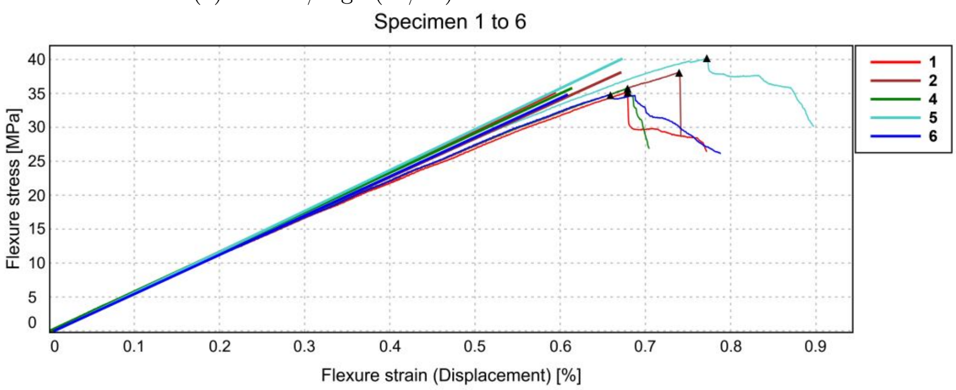

(b) Calcite/Lig1 (50/50)-Bamboo stress strain curve

Figure A.1: 3 point bending test results are obtained for Calcite/Lig1 (50/50)-Flax and Calcite/Lig1 (50/50)-Bamboo

	Flexural Strength (MPa)	Flexural Strain (%)	Flexural Modulus (MPa)	Failure Mode	Force at Maximum Flexure Load (N)
1	42.1	0.82	5910	Tensile fracture at outermost layer	136.22
2	45.7	0.92	6010	Tensile fracture at outermost layer	147.15
3	50.7	1.0	6070	Tensile fracture at outermost layer	167.74
4	50.3	1.0	6160	Tensile fracture at outermost layer	156.90
5	50.9	1.0	6250	Tensile fracture at outermost layer	165.35
Mean	47.9	0.97	6080		154.67
S.D	3.90	0.09	133.91		13.11

	Flexural Strength (MPa)	Flexural Strain (%)	Flexural Modulus (MPa)	Failure Mode	Force at Maximum Flexure Load (N)
1	35.2	0.68	5960	Tensile fracture at outermost layer	109.37
2	38.1	0.74	5700	Tensile fracture at outermost layer	119.09
3	35.8	0.68	5840	Tensile fracture at outermost layer	109.82
4	40.1	0.77	6020	Tensile fracture at outermost layer	122.55
5	34.8	0.66	5780	Tensile fracture at outermost layer	107.34
Mean	36.8	0.71	5860		113.63
S.D	2.26	0.05	131.44		6.74

Table A.1: Flexural test result tables from the Instron testing machine

Figure A.1 and Table A.1 simply compares the same ratio of fillers for 2 different fibres and analyzes their mean properties and standard deviations. It can be observed 5 tests are done per plate and the mean results are used for the BMC Optimizer model.

Some of the flexural stress-strain results obtained from the Instron testing instrument are shown in figure A.2:

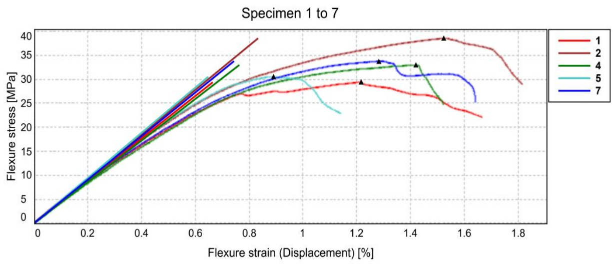

(a) Calcite/Was (0/100) -Flax

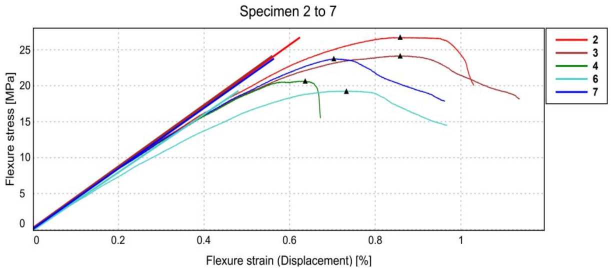

(b) Calcite/Was (0/100) -Bamboo

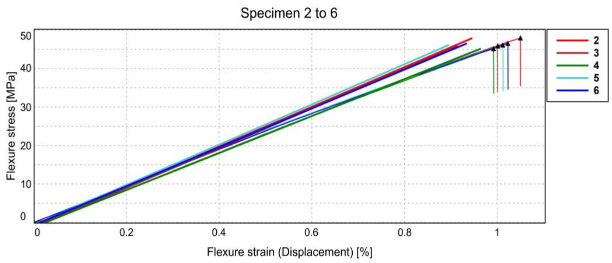

(c) Calcite/Lig2 (25/75) -Flax

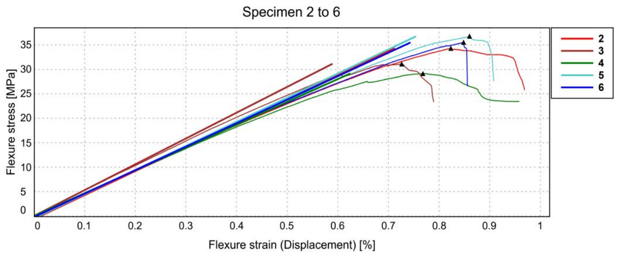

(d) Calcite/Lig2 (25/75) -Bamboo

Figure A.2: Waste based filler and Lignocellulosic 2 based composites stress strain curves

Figure A.3 shows few of the iteration 1 stress strain results obtained for the recipes as recommended by the BMC Optimizer model.

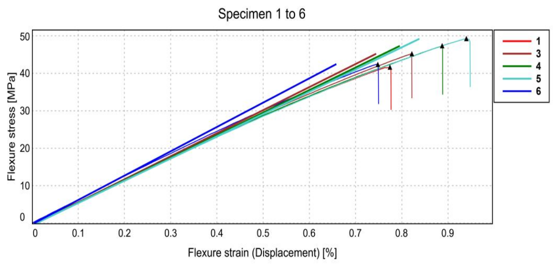

(a) Calcite/Lig1 (61/39) -Flax

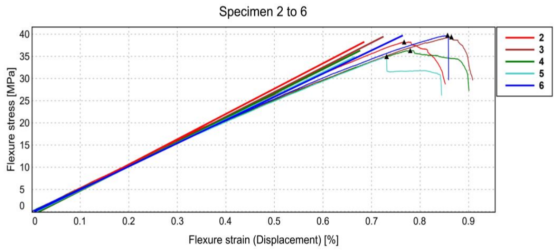

(b) Calcite/Lig1 (82/18) -Bamboo

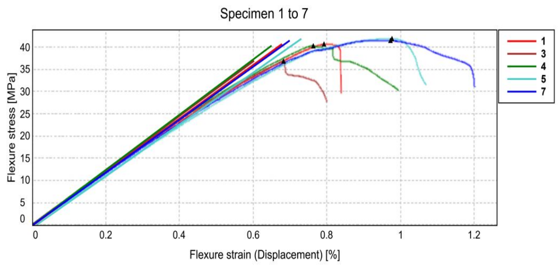

(c) Calcite/Was (60/40) -Flax

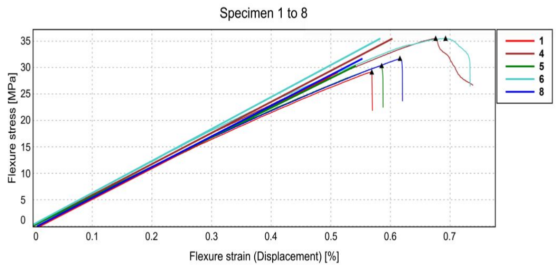

(d) Calcite/Was (20/80) -Bamboo

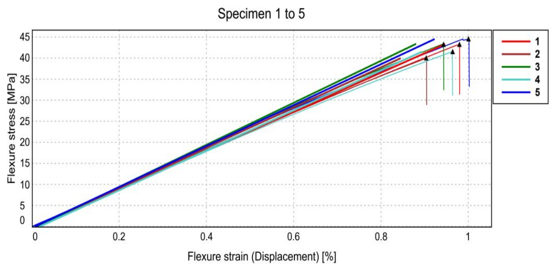

(e) Calcite/Lig2 (10/90) -Flax

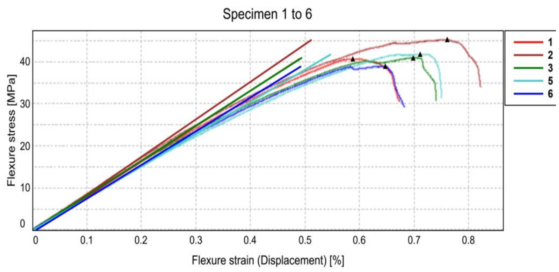

(f) Calcite/Lig2 (81/19) -Bamboo

Figure A.3: Iteration 1 stress strain curves for Lignocellulosic 1, Waste based filler and Lignocellulosic 2 based composites

Figure A.4 shows few of the iteration 1 stress strain results obtained for the recipes as recommended by the BMC Optimizer model.

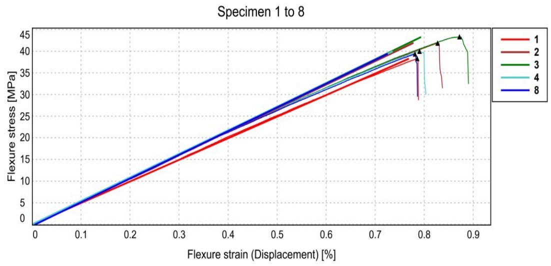

(a) Calcite/Lig1 (25/75) -Flax

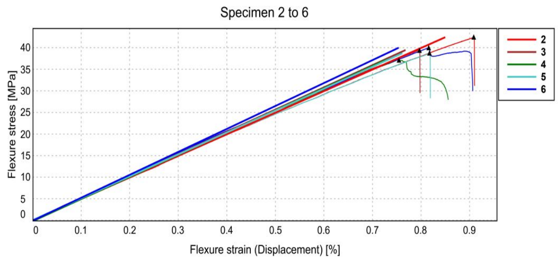

(b) Calcite/Lig1 (25/75) -Bamboo

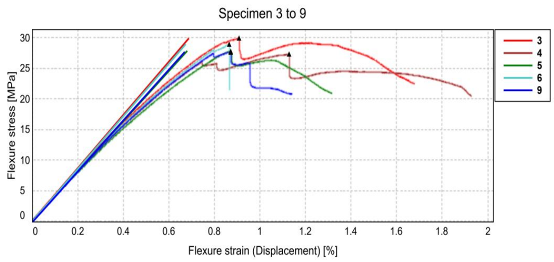

(c) Calcite/Was (08/92) -Flax

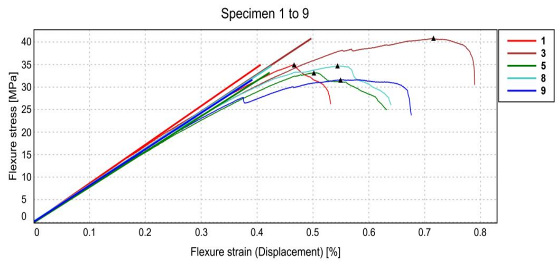

(d) Calcite/Was (69/31) -Bamboo

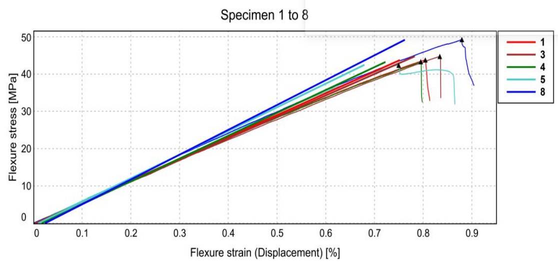

(e) Calcite/Lig2 (25/75) -Flax

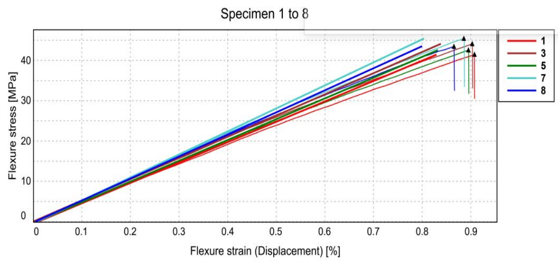

(f) Calcite/Lig2 (11/89) -Bamboo

Figure A.4: Iteration 2 stress strain curves for Lignocellulosic 1, Waste based filler and Lignocellulosic 2 based composites

Appendix B

Mechanical Properties Graphs of Training Set and Iterations 1 and 2

This section covers the mechanical properties of the training set and the two iterations performed. The properties for lignocellulosic 1 and Waste based filler with flax and bamboo and lignocellulosic 2 with bamboo are shown below in figures shown.

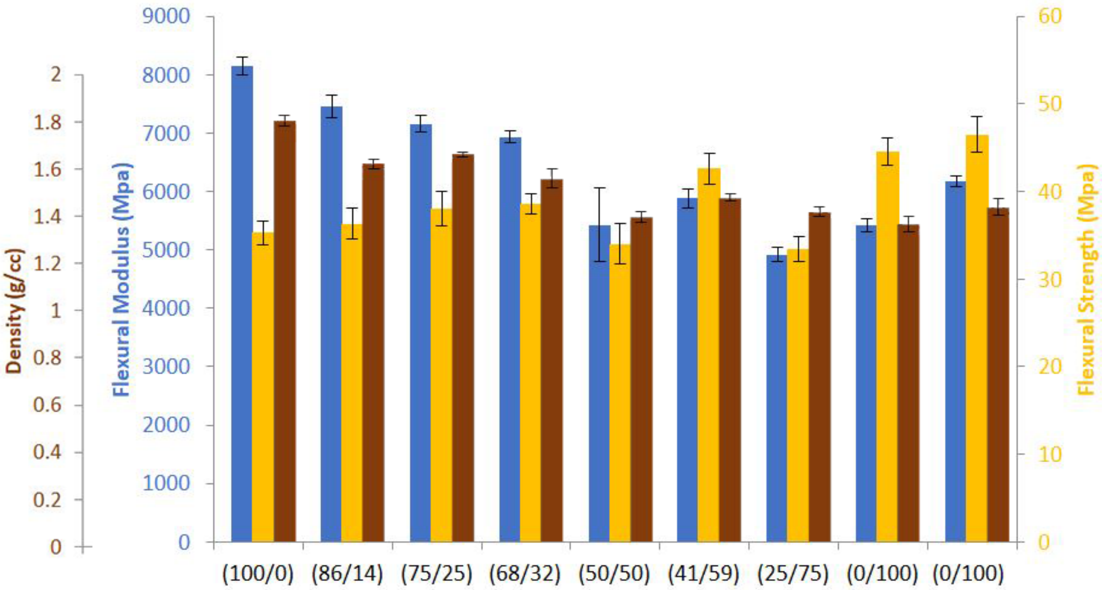

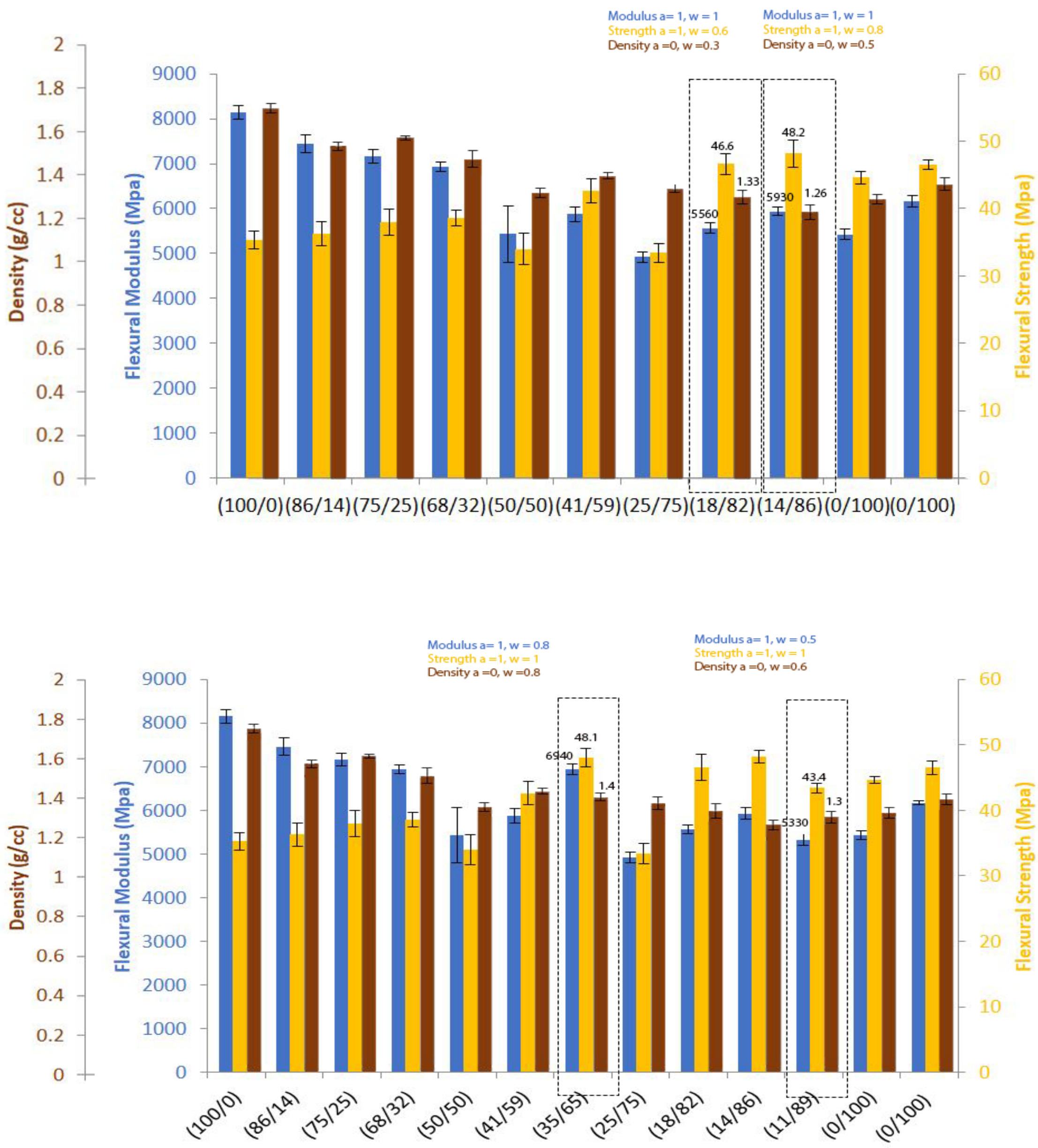

Figure B.1: a) Training set mechanical properties of Calcite/Lig2 with Bamboo fibre. b) Mechanical properties from training set and first iteration for Calcite/Lig2 with Bamboo fibre. c) Mechanical properties from training set, first and second iterations for Calcite/Lig2 with Bamboo fibre

Figure B.1 (a) represents the design of experiments performed which forms the training set and the recommended recipes obtained from it for at the desired objective functions are manufactured and shown in (b) and (c). The results obtained in both the iterations are pretty impressive and similar to what was achieved in chapter 5. The one shot learning approach implemented shows an increase in modulus and strength as the weight value is increased and decrease in density as the function is minimized.

Figure B.2, B.3, B.4, B.5 show similar graphs for other filler and fibre systems.

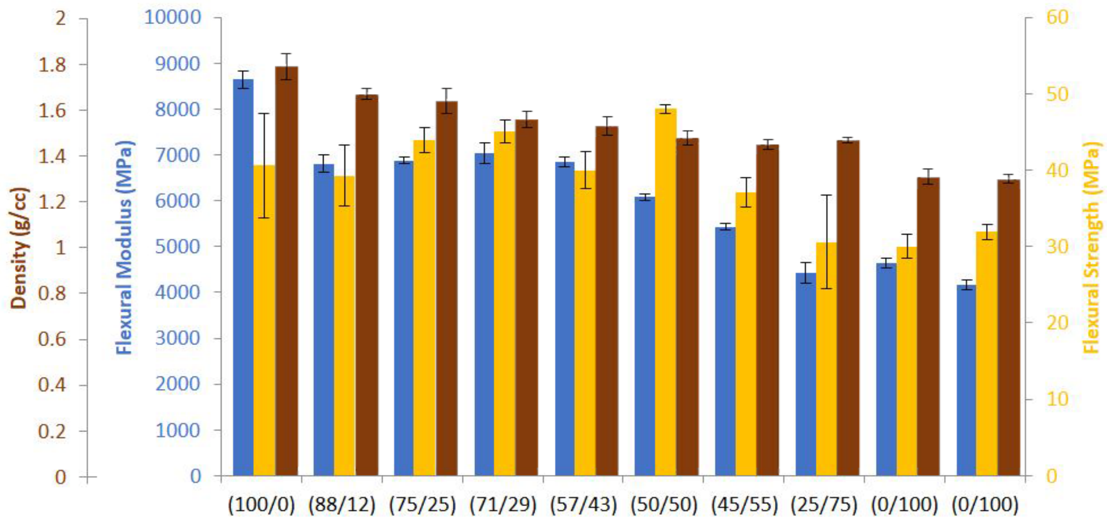

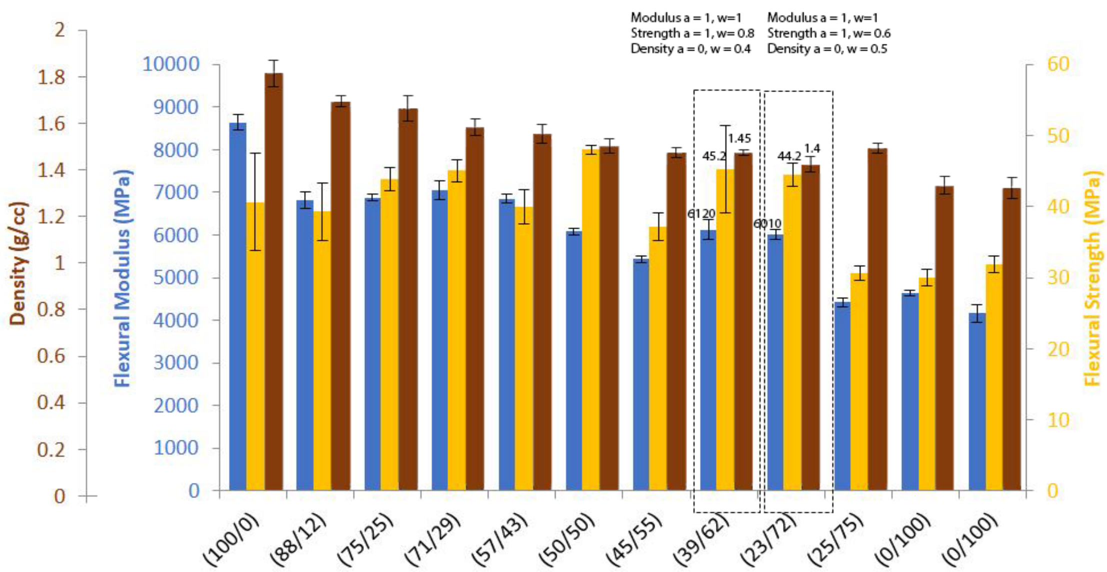

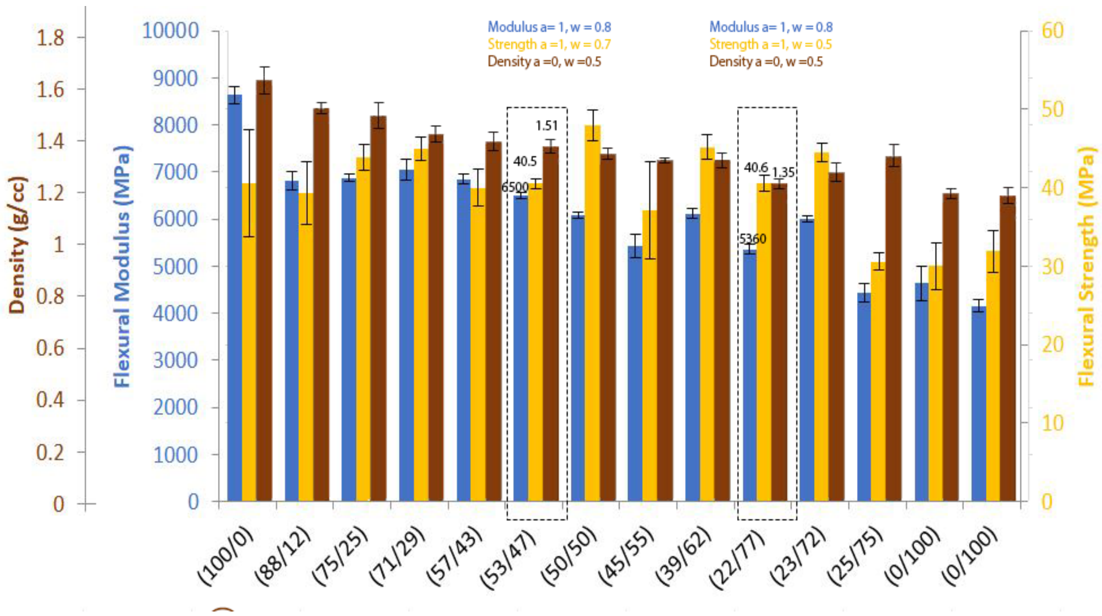

Figure B.2: a) Training set mechanical properties of Calcite/Lig1 with Flax fibre. b) Mechanical properties from training set and first iteration for Calcite/Lig1 with Flax fibre. c)Mechanical properties obtained for training set, first and second iterations for Calcite/Lig1 with Flax fibre

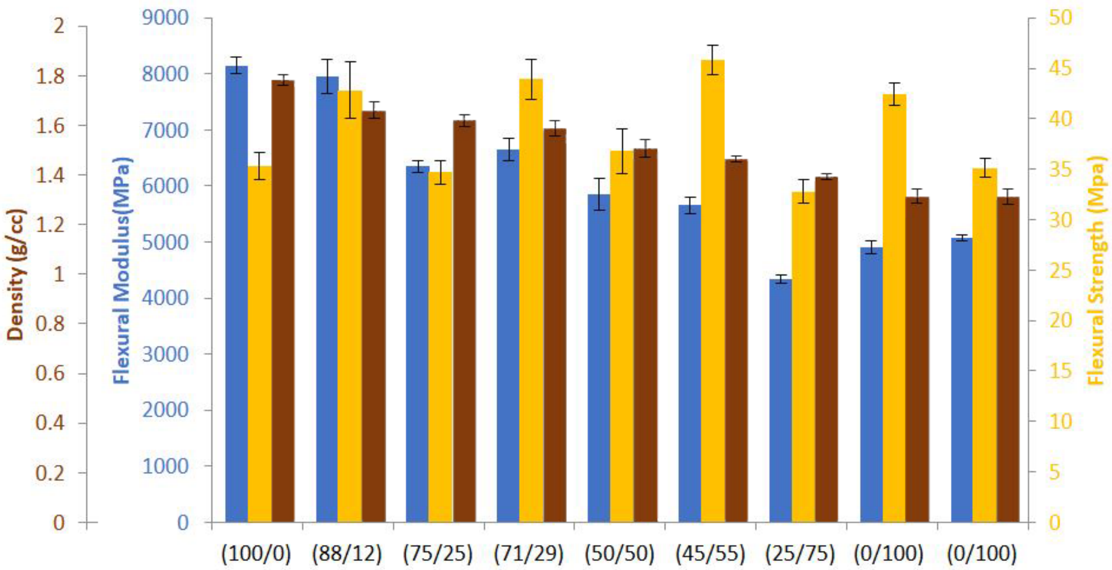

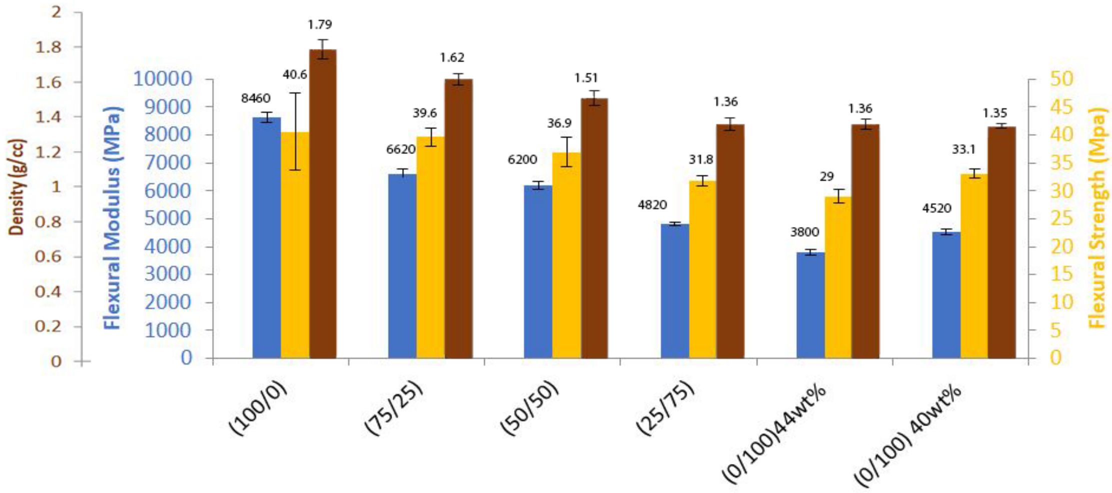

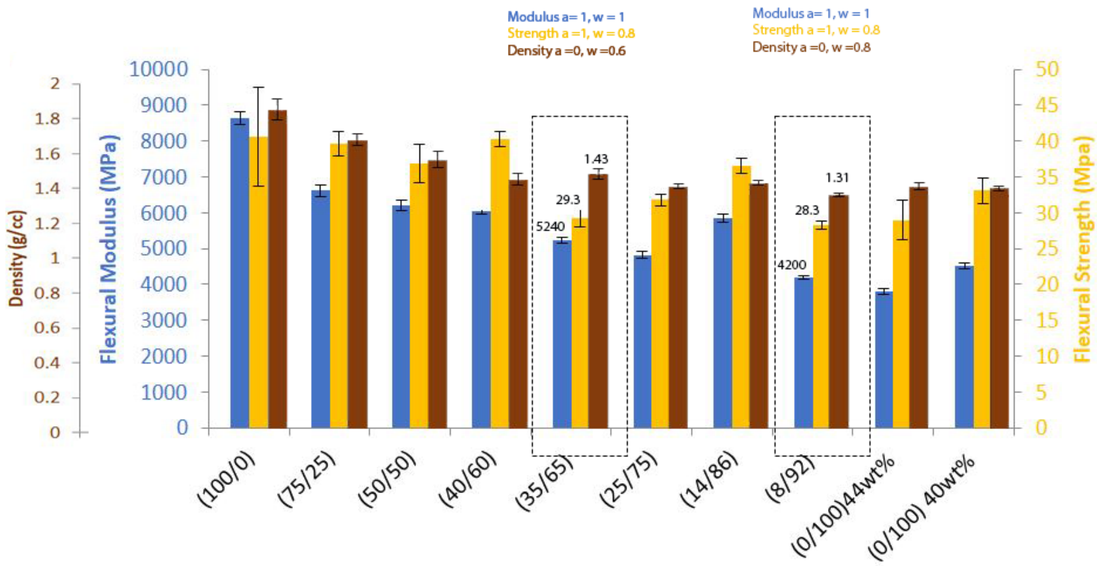

Figure B.4: a) Results from training set and first iteration for Calcite/Waste based filler with Flax fibre. b) Mechanical properties from training set and first iteration for Calcite/Waste based filler with Flax fibre. c) Mechanical properties from training set, first and second iterations for Calcite/Waste based filler with Flax fibre

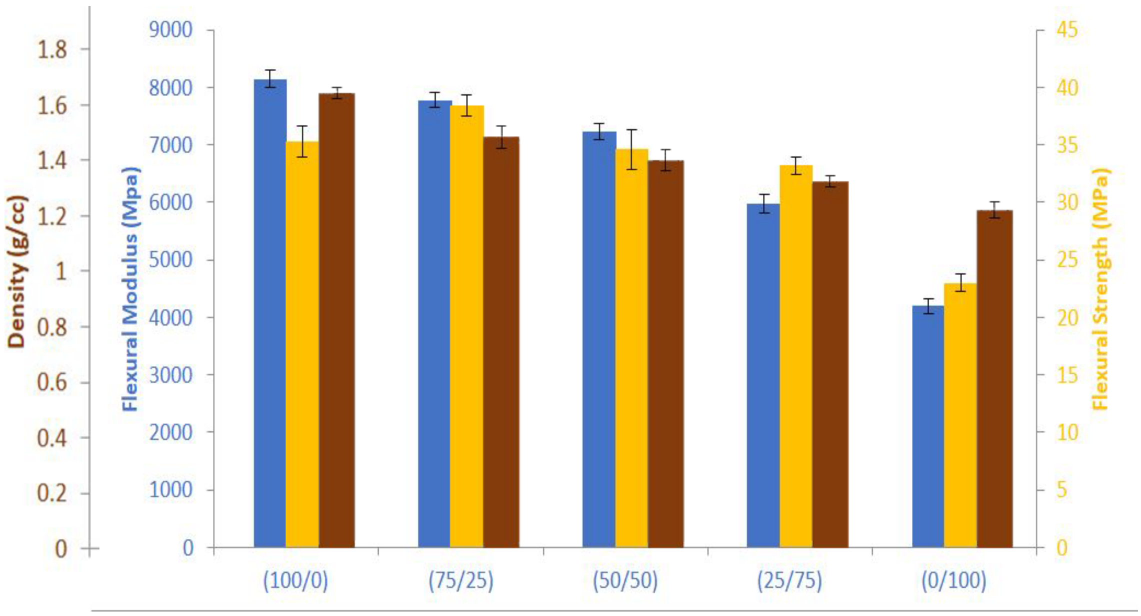
Density (g/cc)
Flexural Modulus (Mpa)
Flexural Strength (MPa)
(100/0)
(75/25)
(50/50)
(25/75)
(0/100)

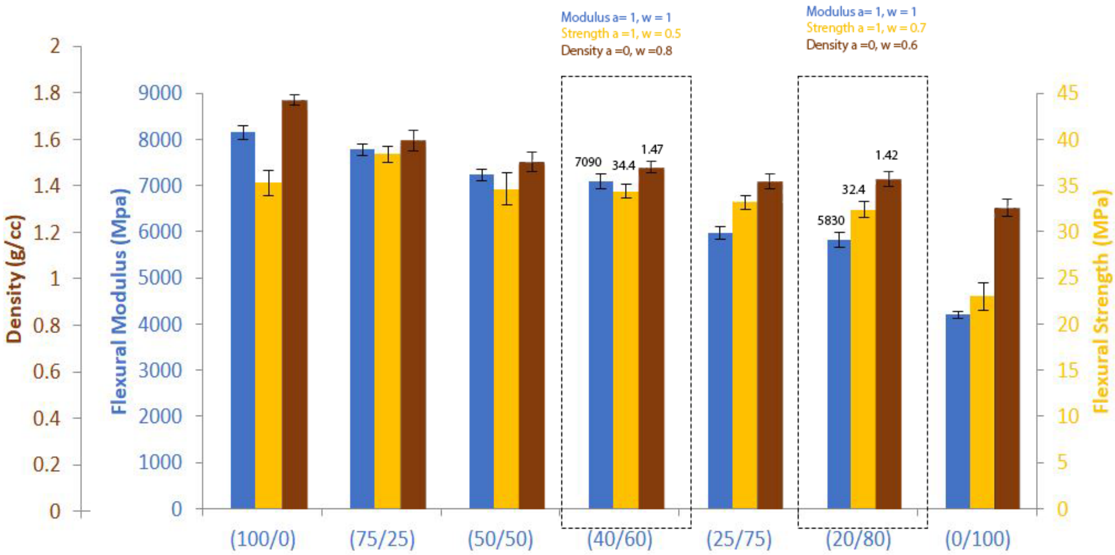
Modulus a= 1, w = 1
Strength a =1, w = 0.5
Density a =0, w =0.8
Modulus a= 1, w = 1
Strength a =1, w = 0.7
Density a =0, w =0.6
7090
34.4
1.47
5830
32.4
1.42
Density (g/cc)
Flexural Modulus (Mpa)
Flexural Strength (MPa)
(100/0)
(75/25)
(50/50)
(40/60)
(25/75)
(20/80)
(0/100)

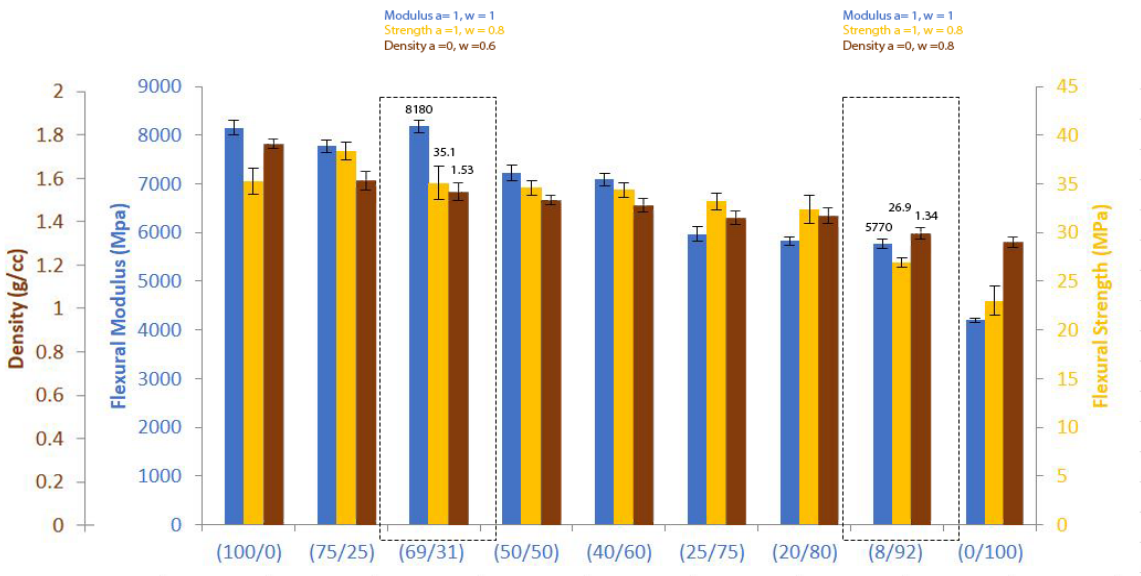

Figure B.5: a) Training set mechanical properties of Calcite/Waste based filler with Bamboo fibre. b) Mechanical properties from training set and first iteration for Calcite/Waste based filler with Bamboo fibre. c) Mechanical properties from training set, first and second iterations for Calcite/Waste based filler with Bamboo fibre

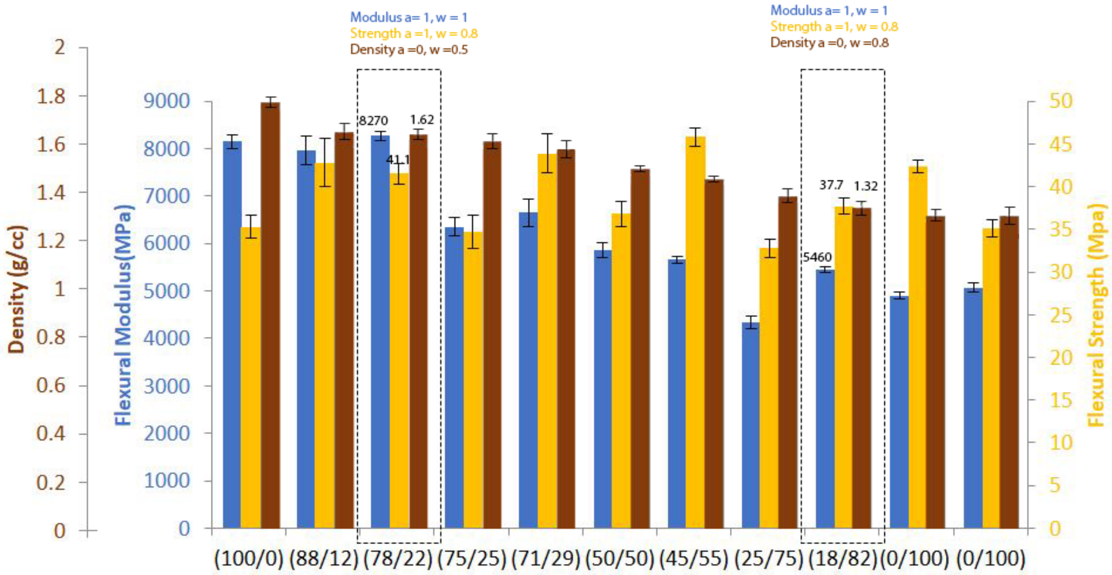

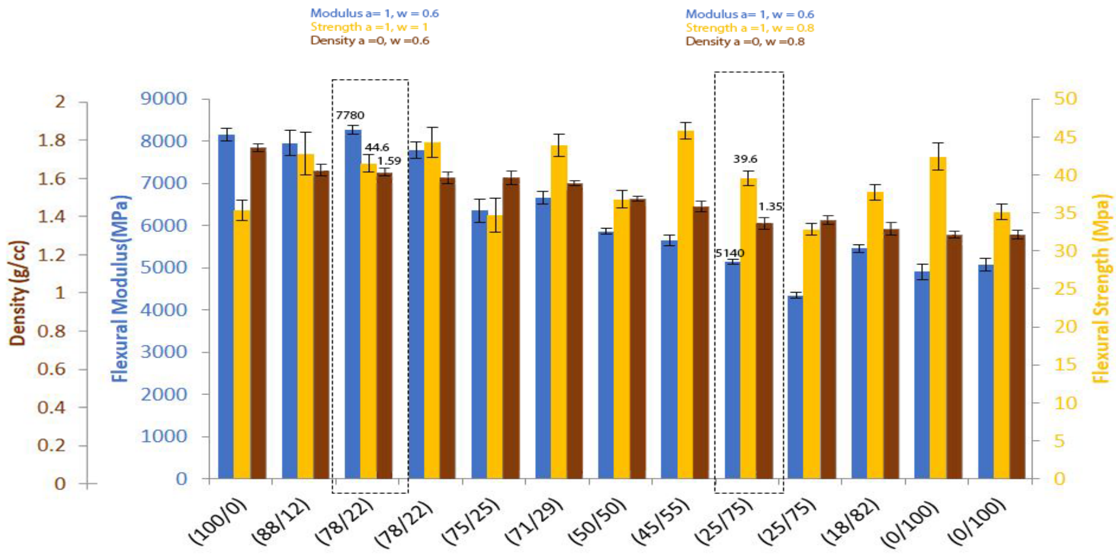

Figure B.3: a) Training set mechanical properties of Calcite/Lig1 with Flax fibre. b) Mechanical properties from training set and first iteration for Calcite/Lig1 with Bamboo fibre. c) Mechanical properties from training set, first and second iterations for Calcite/Lig1 with Bamboo fibre